Diploma thesis

OPTIMIZATION OF CHAIN ELONGATION AND BUTANOL PRODUCTION

Using Syngas- and Electrofermentation Techniques

Submitted in satisfaction of the requirements for the degree of

Diplom-Ingenieurin

Under the supervision of

Privatdoz. Dr. Seiboth Bernhard

(Institute of Chemical, Environmental and Bioscience Engineering, TU Wien)

Ao.Univ.Prof.Dipl.-Ing. Dr.nat.tech. Fuchs Werner

(Institute for Environmental Biotechnology, Boku Wien)

submitted by

DINA MOHAMED

01127132

Vienna, April 2024

I have taken note of the fact that I am only authorized to publish my thesis under the title "Diploma thesis" with the approval of the examination board.

I further declare in lieu of an oath that I have completed my thesis independently in accordance with the recognized principles for scientific papers and that I have cited all the resources used, in particular the literature on which it is based.

Furthermore, I declare that I have not previously submitted this thesis topic in any form as an examination paper either in Austria or abroad (to an assessor for assessment) and that this thesis corresponds to the thesis assessed by the assessor.

Acknowledgement

I would like to take this opportunity to thank Prof. Werner Fuchs for being an amazing supervisor during my master's project and thesis. Without his expertise and dedication, this project would not have been possible. I am truly thankful for his outstanding support and mentorship.

I would like to extend my gratitude to Privatdoz. Dr. Seiboth Bernhard, who accompanied me throughout my master's thesis. His guidance carried me through all the stages and I appreciate the support he provided.

Also thank you to my colleague Clemens Hiebl for his support during the project. Thank you for being a constant source of assistance and encouragement.

Last but not least, I want to express my heartfelt appreciation to my mother and family, who have always been there for me. A special thanks also goes to my friends, who provided unwavering support during challenging times. I extend particular gratitude to Funda Baran for her consistent support throughout my studies. Without all of you, I wouldn't be in this position. Your encouragement has meant the world to me.

Abstract

Research into renewable resources continues to be an actual topic. One of these renewable resources is energy production from biomass, e.g. through ethanol. Given the urgent need to reduce CO_2 emissions, this study looks at the promising route of utilizing carbon dioxide for biofuel production, focusing on butanol production and chain elongation through electrofermentation and syngas fermentation techniques.

Electrofermentation, an emerging field in biotechnology, integrates syngas fermentation processes with electrochemistry, offering a sustainable approach with substantial environmental benefits.

In spite of progress of chain extension, alcohol production in this context faces persistent challenges. This master thesis is dedicated to optimizing chain extension and increasing alcohol production in trickle bed reactors using syngas and electrofermentation techniques with anaerobic bacteria. A crucial aspect of the research involves the intricate interactions between electroactive bacteria and bioelectrochemical systems, which are still not fully understood and need further investigation.

Simultaneously, the study explores the influence of various parameters such as trace elements, pH, and salts on productivity, aiming to investigate their impact on trickle bed reactor optimization. By addressing these key aspects, this research contributes to the advancement of sustainable biofuel production, aligning with the broader goal of using renewable resources for a more environmentally conscious energy landscape.

The utilization of electro-fermentation in trickle bed reactors emerges as a promising avenue for increasing productivity. The integration of electrochemical processes into reactor design presents unique advantages, further exploration is needed to fully understand the implications and potential benefits of this approach in the context of alcohol production.

Moreover, experiments with salt supplementation, particularly potassium chloride (KCl), exhibited a positive effect on alcohol production, underscoring the potential role of salts in enhancing reactor conditions for improved alcohol synthesis.

Zusammenfassung

Die Erforschung nachwachsender Rohstoffe ist nach wie vor ein aktuelles Thema. Eine dieser erneuerbaren Ressourcen ist die Energieerzeugung aus Biomasse, z. B. durch Ethanol. Angesichts der dringenden Notwendigkeit, die CO_2-Emissionen zu verringern, befasst sich diese Studie mit dem vielversprechenden Weg, abgeschiedenes Kohlenstoffdioxid für die Biokraftstoffproduktion zu nutzen, wobei der Schwerpunkt auf der Butanolproduktion und der Kettenverlängerung durch Elektrofermentations- und Syngasfermentationsverfahren liegt.
Die Elektrofermentation, ein aufstrebender Bereich in der Biotechnologie, integriert Syngas-Fermentationsprozesse mit der Elektrochemie und bietet einen nachhaltigen Ansatz mit erheblichen Vorteilen für die Umwelt.

Trotz der Fortschritte bei der Kettenverlängerung steht die Alkoholproduktion in diesem Zusammenhang vor anhaltenden Herausforderungen. Diese Masterarbeit widmet sich der Optimierung der Kettenverlängerung und der Steigerung der Alkoholproduktion in Rieselbettreaktoren unter Verwendung von Syngas- und Elektrofermentationsverfahren mit anaeroben Bakterien. Ein wesentlicher Aspekt der Forschung betrifft die komplizierten Wechselwirkungen zwischen elektroaktiven Bakterien und bioelektrochemischen Systemen, die noch nicht vollständig verstanden sind und weiter untersucht werden müssen.

Gleichzeitig wird in der Studie der Einfluss verschiedener Parameter wie Spurenelemente, pH-Wert und Salze auf die Produktivität untersucht, um deren Auswirkungen auf die Optimierung des Rieselbettreaktors zu ermitteln. Durch die Untersuchung dieser Schlüsselaspekte trägt diese Forschung zur Förderung der nachhaltigen Biokraftstoffproduktion bei und steht im Einklang mit dem allgemeinen Ziel, erneuerbare Ressourcen für eine umweltbewusstere Energielandschaft nutzbar zu machen.

Table of Content

1 Introduction

1.1 General introduction

Sustainability is today always an issue when considering energy. It's crucial that resources provide us with enough energy to satisfy our needs—to heat our homes, power our cities, and drive our vehicles. However, it's also crucial to consider how long these resources can be used. Non-renewable resources are finite and will be depleted by their consumption. In contrast, there are resources that will essentially never run out. These are called renewable resources (National Geographic Society et al., 2022). Renewable and sustainable resources are part of a worldwide effort to reduce greenhouse gases and combat climate change.

Sustainable raw resources have a variety of advantages. They can offer cleaner energy solutions and are already more ecologically benign than non-renewable resources such as fossil fuels.

But also, from political perspective it is important to think about alternatives. An issue that is very topical these days is independence regarding external energy providers. Current political issues and the new geopolitical and energy market realities require to accelerate clean energy transition and increase Europe's energy independence (European Commission, 2024). Suitable renewable and sustainable resources are a long-term solution since they may be utilized continually. They help to reduce dependency on external energy sources.

There are different kinds of renewable resources. Each of these resources has advantages and disadvantages, and the availability of resources might affect how successful they are.

One of these renewable resources is plant biomass which can be converted to liquid biofuels such as ethanol or, alternatively, butanol. The capturing of CO_2 emissions and the utilization of CO_2 for biofuel production (for instance butanol) is a promising sustainable process with high environmental benefit.

Feedstocks, for example, biomass or metropolitan strong waste are gasified into syngas (CO, H_2 and CO_2) for this process, which is then converted into biofuels and chemicals utilizing microbial catalysts (Liu et al., 2013).

At the Institute of Environmental Biotechnology at IFA-Tulln (IFA; Institute of Agrobiotechnology), a BEST (Bioenergy and Sustainable Technologies) -funded research project is currently underway. The project deals with the production of bio-butanol from natural deposits through a process including syngas-fermentation and electrofermentation techniques. Figure 1 provides an illustration of the proposed overall procedure:

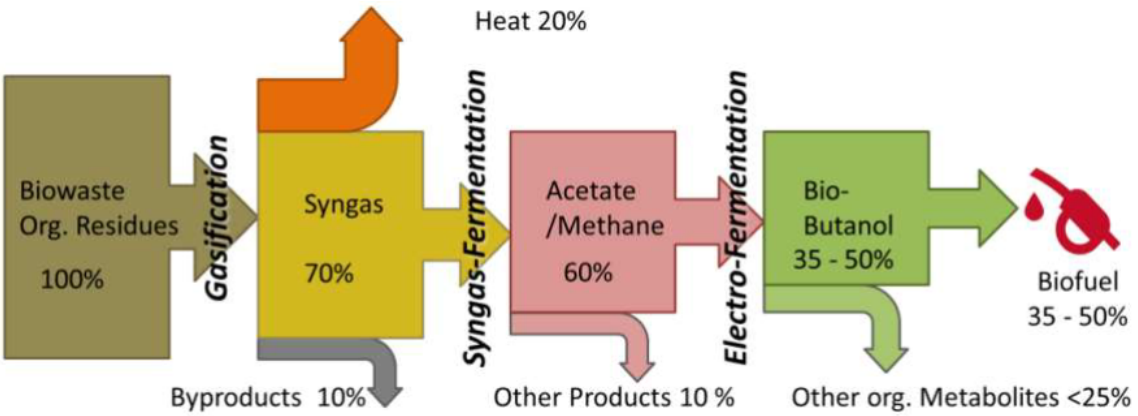

Figure 1: Bio-electric syngas technology for the production of biomass derived biofuels and platform chemicals - Proposed conversion of biomass through a cascade of conversion technologies: gasification, biological syngas- and electro-fermentation. (Source: https://www.best-research.eu/en/competence_areas/all_projects/view/677, accessed on 2024, March 13)

The process consists of 3 main steps which can be divided in: gasification, syngas fermentation and electro-fermentation.

Syngas or biogas production from biomass of varying or minor quality is the first step. Syngas with high concentrations of CO, H_2, and CO_2 can be produced by gasifying biomass and other carbonaceous materials. Wood waste, agricultural byproducts, municipal organic waste, and pulp and paper industry waste are examples of low-cost feedstock material (BesTECH. (n.D.). The next step, syngas fermentation, combines thermochemical and biochemical processes. It takes advantage of the simplicity of the gasification cycle and the precision of the fermentation system to produce bio-based products (BesTECH. (n.D.).

In the third step, syngas fermentation uses special microorganisms to turn the produced gases into alcohols and organic acids, mainly ethanol and acetic acid. In addition to selecting the most suitable microbial production strains, essential tasks include testing improved gas fermenters and optimizing electrode designs.

In my master thesis I was focusing on the third step which aimed to improve chain elongation and alcohol production using syngas- and electro-fermentation techniques.

1.2 Fermentation of biofuels

1.2.1 Historical background of biofuel fermentation

Anaerobic fermentation is a metabolic process where microorganisms, such as bacteria & yeasts convert sugars or other natural carbon sources into products like acids, alcohols, or gases under anaerobic conditions. Human utilization of fermentation spans thousands of years, deeply embedded in cultural and industrial practices like food and beverage production, biofuel, and pharmaceuticals.

In ancient times, fermentation primarily served as a tool for food preservation, especially when fruits, grains, or plant materials were exposed to air or moisture. Around 5,000 BCE, Sumerians and Egyptians began with the production of wine and beer. Despite lacking precise knowledge of the manufacturing process or the reasons behind fermentation, they often perceived it as a divine wonder.

Over time, humans gained insights into deliberately harnessing the potential of microorganisms. In the production of fermented foods and beverages, there emerged a practice of selecting and propagating specific strains of yeast or bacteria. An example of this is the domestication of bread-making yeast in ancient Egypt around 4,000 BCE.

In the nineteenth century, scientist Louis Pasteur proposed that microorganisms are the catalysts for fermentation, sparking significant advancements in fermentation techniques. Pasteur also discerned that different bacteria are responsible for various types of fermentations (Manaa et al., 2021).

Today, microorganisms are recognized as valuable resources in biotechnology, exemplified by the widespread use of fermentation. This process finds applications in various industries, including the production of alcoholic beverages, dairy products, bread, sauerkraut, and vinegar. Additionally, anaerobic fermentation plays an increasingly important role in the production of biofuels, chemicals, drugs, and various other biotechnological processes. Today, biofuels, such as bioethanol and biobutanol, are generated by microbial syngas fermentation. In this transformative biological process, microorganisms, particularly yeast and specific anaerobic

bacteria, convert sugars and other feedstocks obtained from biomass into biofuels. These biofuels not only decrease greenhouse gas emissions but also offer renewable substitutes to traditional fossil fuels (Manaa et al., 2021).

1.2.2 ABE-fermentation

Acetone-butanol-ethanol fermentation (ABE) is a microbial process that converts carbohydrates into solvents such as acetone, butanol, and ethanol.

This has historically been done using solventogenic clostridium species, particularly *Solventogenic clostridia*, which has been used industrially for solvent production since the early 20th century.

The main metabolites produced during ABE fermentation are butanol, acetone and ethanol, accompanied by the generation of CO_2 and H_2. The fermentation process is divided into the acidogenic- and the solventogenic phase. Figure 2 shows a simplified overview of ABE fermentation in *S. clostridia* (Li, 2023).

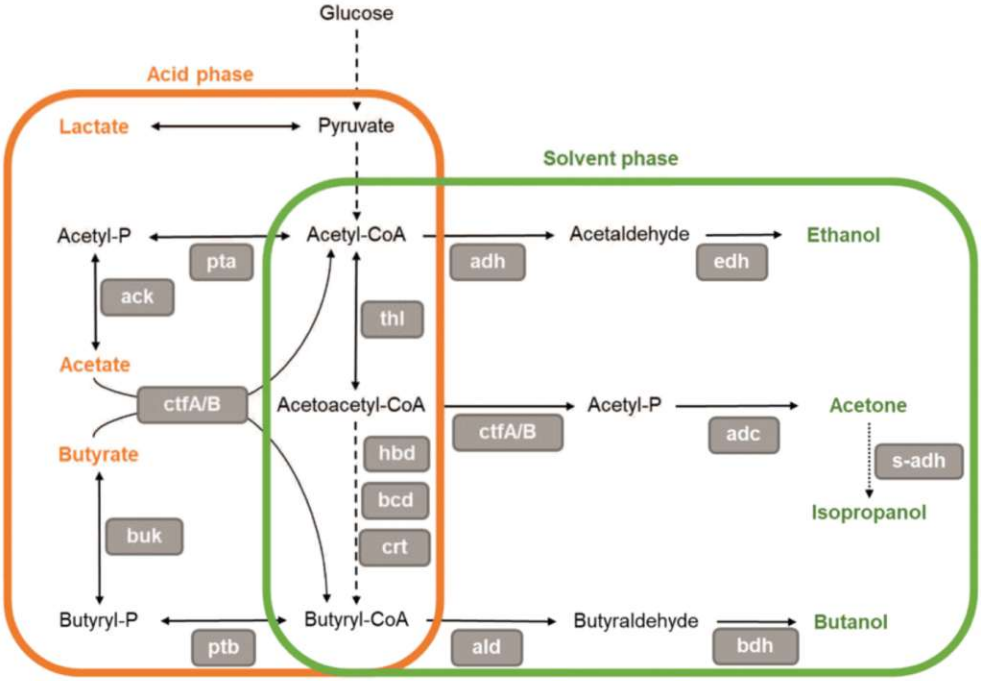

Figure 2: Simplified acetone-butanol-ethanol fermentation in solventogenic clostridia (Source: Diallo et al., 2001)

1.2.3 Gas fermentation

While ABE fermentation specifically produces solvents such as acetone, butanol, and ethanol from carbohydrate-based substrates, gas fermentation utilizes gaseous substrates like CO, CO_2, and H_2 to produce various biofuels and biochemicals.

Syngas fermentation is a specific type of gas fermentation, in which feedstocks such as biomass or municipal solid waste are gasified into syngas (CO, H_2 and CO_2) which is then used as carbon and energy source and transformed by specific microorganisms into biofuels and chemicals (Liu et al., 2013).

There are currently a variety of ways to capture CO_2 from flue gases, and the subsequent CO_2 fixation by microbial syngas fermentation is in addition also beneficial for the environment (Steger, 2022). Items like alcohols and acids like formic acid and acidic acid can be produced by some anaerobic bacteria through the conversation of H_2 and CO/ CO_2

Usually acetogenic bacteria are used in syngas-fermentation. They use pathways like the Wood-Ljungdahl pathway also termed the reductive Acetyl-CoA pathway, which allows them to use the H_2 and CO/ CO_2 in syngas as carbon and energy source and to produce acetic acid. This diverse group uses a variety of habitats showing different morphologies and physiological characteristics (Steger, 2022).

One of the advantages of syngas fermentation is clearly the use of low pressure and temperature compared to traditional methods such as Fischer-Tropsch synthesis or conventional chemical processes. Also, no specific ratio of CO/ CO_2 to H_2 is required which makes this process not complicated (Ellacuriaga et al., 2023).

From an ecological perspective, it is important to consider the positive impact of using waste gases, which are frequently produced by industrial processes and biomass gasification, and reducing the impact they have on the environment. Syngas-fermentation allows to convert CO_2 into valuable products and contributes to the mitigation of greenhouse gas emissions.

With all these advantages, there are also technological challenges. As syngas-fermentation is a new technology, there are yet some difficulties and challenges regarding process optimization and scale up. This includes the inhibition of organisms through product concentration, gas-liquid mass transfer limitation and low volumetric productivity compared to sugar fermentation (Manna et al., 2024).

As this is a new field, there is a lot of research ongoing to optimize this process, which was also a big part of this work and will be explained in the next chapters.

1.2.3.1 Bioreactor Concepts for Syngas Fermentation

Reactor types such as stirred tanks, bubble columns, gas lift and loop reactors are generally suitable for syngas fermentation. Fixed cell reactor concepts such as trickle bed or membrane reactors are also considered as possible alternatives. The different concepts are visualized in figure 3 (Katharina Stoll, 2019).

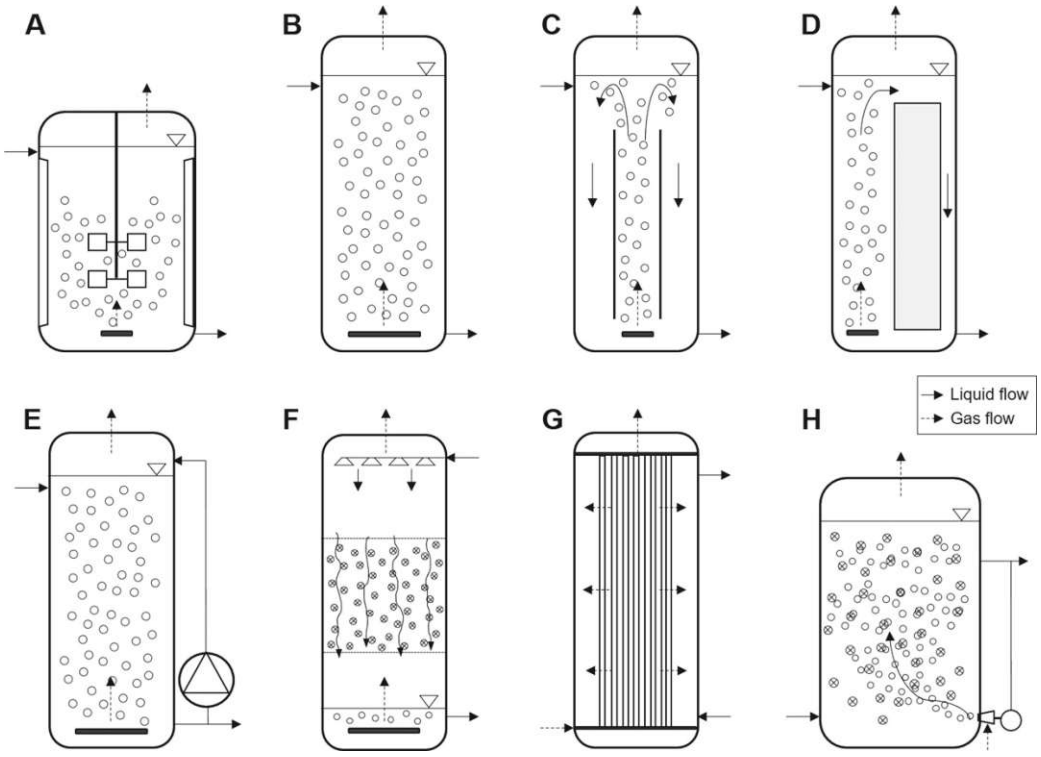

Figure 3: Schematic description of different reactor types. A: Continuous stirred tank reactor (CSTR), B: bubble column (BC), C: gas lift reactor (GLR, internal circulation), D: gas lift reactor (external circulation), E: loop reactor with external pump, F: trickle bed reactor (TBR), G: membrane reactor (hollow fiber membrane bioreactor, HFMBR), H: moving bed biofilm reactor (MBBR). (Stoll et al., 2019)

A CSTR (continuous stirred tank reactor) is a well-mixed reactor where reactants are continuously added, and products are continuously removed. Stirring ensures uniform distribution of reactants and maintains constant temperature and concentration throughout the reactor.

In a bubble column, gas is bubbled through a liquid medium, creating bubbles that rise through the column. The interaction between the gas bubbles and the liquid promotes mixing and mass transfer, making it suitable for gas-liquid reactions and biological processes.

A GLR (gas lift reactor) with internal circulation utilizes gas injection at the bottom of the reactor to create uplift and induce liquid circulation. This promotes mixing and enhances mass transfer, making it useful for gas-liquid reactions and biological treatments. A GLR with external circulation is similar to GLR with internal circulation, but in this case, gas injection occurs externally, leading to liquid circulation within the reactor. This configuration offers better control over gas-liquid contact and circulation patterns.

In a TBR (trickle bed reactor), liquid reactants flow downward over a packed bed of solid catalyst or support material, while gas is bubbled through the bed in a concurrent flow. This configuration maximizes contact between reactants and catalyst, making it ideal for heterogeneous catalytic reactions.

A membrane reactor incorporates semi-permeable membranes to separate reactants and products, allowing selective transport of specific components while retaining others. This design enhances reaction kinetics and product purity, particularly in gas-liquid or liquid-liquid systems.

In an MBBR (moving bed biofilm reactor), biofilm grows on movable support media within the reactor, providing a high surface area for microbial attachment and growth. This promotes biological treatment processes such as wastewater treatment by enhancing biofilm formation and substrate utilization (Stoll et al., 2019).

In my experimental investigations, trickle bed reactors were used. The experimental setup is detailed in 2.6.

1.2.3.2 Cell immobilization and biofilm formation

In gas fermentation, reactor configurations mentioned in figure 3 can be particularly valuable due to the slow growth rate of the microorganisms involved. These reactor types allow high cell densities and therefore high conversion rates.

Cell immobilization is a process, in which microorganisms are fixed on a surface or fixed in a carrier substance so they stay there and are immobile in the solution. The microorganisms obtain resilience against environmental challenges (pH, temperature, organic solvents, salts, inhibitory substrates and products, toxins, self-destruction) thanks to immobilization, which also shields the cells from shear pressures. Immobilized cells may be kept active, viable, and productive for an extended length of time, which makes it easier to carry out continuous culture

procedures and improves operational stability. Even at the high dilution rates of the continuous operating mode, cell wash-out is prevented (Zhu et al., 2007).

For biofilm formation, initially, microorganisms in the fluid adhere to a surface. Then, these microorganisms begin to produce an extracellular matrix, which is a mixture of proteins, polysaccharides, and other substances. This matrix acts as a glue, holding the microbial cells together and forming a protective barrier around them. As cellular aggregation increases and the extracellular matrix expands, it creates a structured layer known as a biofilm (Alhayek et al., 2023).

1.2.4 Electro-fermentation

Traditional microbial fermentation has been utilized to create a wide range of goods, including biofuels, chemicals, and food items. Conventional fermentation techniques do have certain drawbacks, though, such as limited product yields, sluggish reaction times, and susceptibility to environmental factors. By incorporating electrochemical principles into fermentation systems, electro-fermentation seeks to get beyond these constraints Zheng et al., 2020).

In gas fermentation reactor configurations as mentioned in figure 3 may be of particular value, due to the slow growth rate of the involved microorganisms. These reactor types allow high cell densities and thus high conversion rates.

Electro-fermentation is a new bioengineering technique that combines traditional microbial fermentation with electrochemical techniques to improve the reducing or oxidizing metabolism. Bioelectrochemical systems use electrodes and electrical stimulation or carry out the reduction reaction with a certain potential through the transfer of electrons between the electron acceptor and electron donor (Zheng et al., 2020). Electro-fermentation is a process that increases microbial activity, supports targeted metabolic pathways, and regulates fermentation parameters by applying an electrical potential or current to a fermentation system (Zheng et al., 2020).

1.2.4.1 Bioelectrochemical Systems (BES)

Before the concept of bioelectrochemical systems (BES) was discovered, it has been observed in nature that certain microorganisms have the ability to generate electricity through microbial metabolism through their membranes to or from their extracellular environment (Arends et. Al, 2012).

Bioelectrochemical systems are unique systems in which electrodes are combined with biological elements like bacteria or enzymes in order to facilitate electron transport and transform chemical energy into electrical energy or useful products. BESs have drawn a lot of interest recently because of their promise for producing valuable chemicals, treating wastewater, and generating sustainable energy.

The chemical energy of organic waste, such as low-strength wastewaters and lignocellulosic biomass, can be converted by bioelectrochemical systems (BESs) into microbial fuel cells (MFCs) or in microbial electrolysis cells (MECs), or other products created at the cathode by an electrochemical reduction process. (Pant et al., 2012)

Since Michael Potter first investigated in 1911 the generation of an electrical current by a number of microorganisms, which convert chemical energy into electrical energy by degrading a variety of substrates, especially organic compounds from waste water, bioelectrochemical systems have been widely used in the form of MFCs (Zheng et al., 2020).

Electron Transfer in the Bioelectrochemical System

For bioreduction, the immobilized microorganisms on the anode absorb electrons from the electrode. The extracellular electron transfer (EET) mechanism is a key factor in how well bacteria use electrons and consume energy. The EET might be classified into three mechanisms: direct electron transfer (DET), mediated electron transfer (MET) and indirect electron transfer (IET), as visualized in figure 5 (Zhao et al., 2018) (Sydow et al., 2014).

In general, three different modes of electron exchange are known:

1. Direct electron exchange (DET, through direct contact between the microbial cells and the solid-state electrode (cytochromes) or over large distance through pili (nanowires), which is relevant for this work.
2. Mediated electron exchange (MET) driven by soluble mediators like methyl viologen. To move electrons between an electrode and microorganisms, MET uses redoxactive

substances. Exogenous or endogenous electron shuttles are both possible, with hydrogen serving as an essential electron mediator.

3. Indirect electron transfer (IET) that is based on a wide range of microbial electron donors and acceptors such as hydrogen (Sydow et al., 2014). Regarding IET, additional electroactive substances can be secreted that mediate between the organisms and the electrode (Sydow et al., 2014).

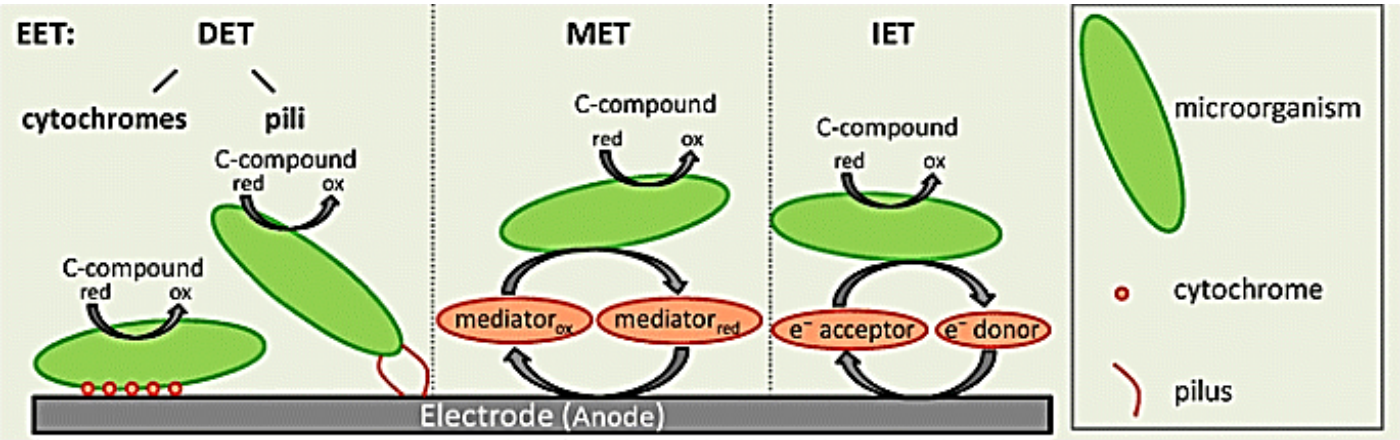

Figure 4: Electroactive bacteria - different modes of electrochemical exchange (Source: Sydow et al., 2014)

As direct electron exchange is most relevant for this project, this way of electron exchange is explained in more detail.

Direct electron exchange between microorganisms and electrodes can take place in (BES) through specific processes and structures like cytochromes or pili. The movement of electrons from the microbial cells to the electrode surface is facilitated by these elements. Cytochromes are proteins that are found in the periplasmic space or on the outer membrane of some bacteria. These proteins contain heme groups capable of both accepting and donating electrons. By acting as a bridge for the passage of electrons between the microbial cells and the electrode, cytochromes are essential for (EET).

Some microbes have outer membrane cytochromes. The electrode surface is directly contacted by these cytochromes when they protrude from the cell. A direct electron exchange channel is created when the electrons produced during microbial metabolism are transported to the cytochromes on the outer membrane and subsequently to the electrode. Other bacteria use periplasmic cytochromes for electron transport. The periplasmic space, or space between the cell's inner and outer membranes, is where these cytochromes are found. Direct contact or conductive materials are used to transmit the electrons from the cytochromes to the electrode.

Some microbes may directly exchange electrons without the usage of cytochromes by using pili or nanowires. Pili are tiny, hair-like protrusions that are attached to the outside of microbial cells. Since they may function as conductive filaments, electrons can go from the cell to the electrode. The bacteria and the electrode may make direct electrical contacts thanks to these pili-mediated electron transfer routes.

In BES, bacteria use oxidation processes to break down organic substances or other electron donors. As a result of the release of electrons from the donor molecule during the oxidation process, the donor becomes the oxidized form. The bacterial outer membrane cytochromes or pili need to receive the electrons that have been released during the oxidation process. The cytochromes or pili act as pathways for the movement of electrons. To get to the electrode surface, the liberated electrons can either go down the conductive pili or directly interact with the heme groups found in cytochromes.

An electrical current is produced as a result of the flow of electrons from the microorganisms at the anode to the electrode surface and the following reduction processes at the cathode (Mohan et al., 2019) (Zheng et al., 2020).

Regardless of whether cytochromes or pili are used to promote the direct electron exchange, it frequently takes place within biofilms created by microorganisms on the electrode surface. Because of the close proximity of the microorganisms, the electrode, and their electron transfer components due to the biofilm structure, electron transfer might occur (Edel et al., 2022), (Zheng et al., 2020).

1.2.4.2 Bioelectrochemical reactor concepts

In bioelectrochemical reactor concepts, there are two main categories: divided and non-divided reactor configurations.

Non-divided reactor concept

The anode and cathode compartments are not physically separated from one another in a non-separated reactor arrangement by a barrier or membrane. The membrane serves the purpose of spatially segregating the distinct electrochemical reactions transpiring at the anode and cathode interfaces. the objective entails the provision of electrons to bacteria residing at the cathode. These electrons must be sourced externally, as the applied voltage solely facilitates electron transport from the anode to the cathode without generating new electrons;

otherwise, the reactor would accumulate a negative charge. For instance, electrons can be derived from the oxygen present in water, thereby effecting its conversion into molecular O_2 (O_2 gas). However, O_2 is not conducive for anaerobic bacteria. Alternatively, beyond membranes, another substance may be deployed to donate electrons (e.g., Fe^{2+}).

Divided reactor concept

Anode and cathode compartments are physically divided in a separated reactor arrangement, often by a membrane or a barrier. This division makes it possible to independently regulate the cathodic and anodic environments, which may be advantageous in some applications. When certain microbial populations or operational conditions are sought at the anode and cathode, divided reactor arrangements are frequently utilized. They offer flexibility in the bioelectrochemical system's performance and efficiency by enabling the independent regulation of each compartment.

Figure 8 shows an example for divided reactor concepts - a two-chamber system. The anode and cathode compartments are physically divided from one another in a two-chamber arrangement by a membrane or barrier. In the experiments performed during this work, bacteria consume electrons from the working electrode (cathode). This can occur directly on the surface of the electrode or catalysed by a mediator.

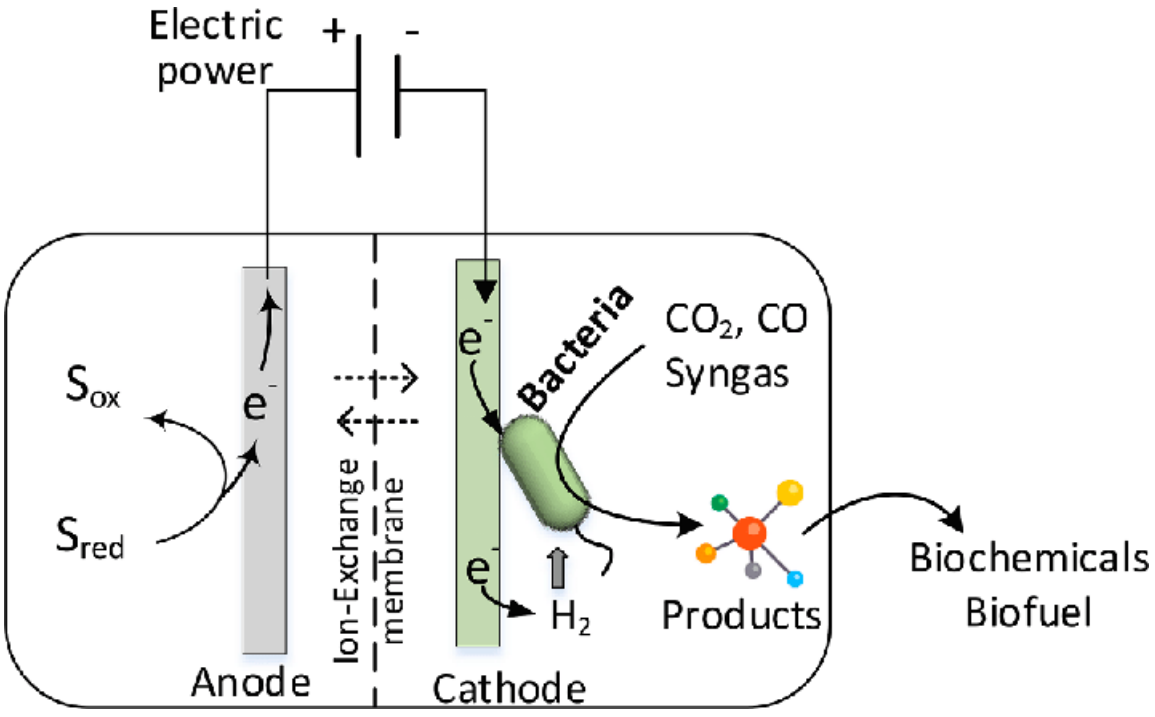

Figure 5: Concept of gas electro-fermentation: microbial electrosynthesis platform supporting gas fermentation. [S red and S ox : Substrate reduced, and Substrate oxidized]. (Source: Suman Bajracharya et al., 2022)

In general, a two-chamber system is used in bioelectrochemical reactors to offer a regulated and optimal individual environment for both the anodic and cathodic process.

In the context of bioelectrochemical reactors, such as Microbial Fuel Cell Systems (MFCS), a two-chamber system is often employed to create distinct environments for the anodic and cathodic processes. This setup allows for precise control and optimization of each stage of the electrochemical reactions. Generally, electric current can only move electrons from one electrode to the other.

Corresponding reactions for electron uptake or release must occur at both electrodes. A possible process at the anode involves the oxidation of OH^- to O_2:

$$2OH^- \rightarrow O_2 + 2e^-$$

At the cathode, H^+ is reduced to H_2:

$$2H^+ + 2e^- \rightarrow H_2$$

H_2 is subsequently consumed by the microorganisms. Alternatively, two H^+ and two electrons can be absorbed separately. The molecular O_2 generated at the anode can be toxic for anaerobes; therefore, it is crucial to maintain a membrane barrier to prevent its contact.

Both the anodic and cathodic compartments can be selectively regulated in separated reactor configurations, allowing for independent manipulation of their respective environments. This capability is particularly advantageous in applications where specific microbial populations or operational conditions are desired at either the anode or cathode.

1.3 Microbial and Chemical Background

1.3.1 Microbial Pathway

For energy production and survival in the absence of oxygen, anaerobic bacteria use a variety of metabolic pathways. In the following those pathways which can be exploited for the production of renewable biofuels are described.

1.3.1.1 Wood Ljungdahl Pathway

Spanning various phylogenetic classes, the Wood–Ljungdahl pathway, also known as the acetyl-CoA pathway, comprises a series of biochemical reactions that uses CO_2 as a carbon source and generates acetyl-CoA. Specific bacteria employ this pathway in both oxidative and reductive directions (Ragsdale et al., 2016).

Acetogens are obligate anaerobic bacteria that synthesize acetyl-CoA and cell carbon from CO_2 through the Wood-Ljungdahl pathway. When an acetogen only produces acetate as a fermentation product, it is referred to as a homoacetogen or a CO_2-reducing acetogen (Ragsdale et al., 2016). The discovery of the Wood-Ljungdahl pathway coincides with the revelation of *Clostridium aceticum*, the first isolated organism that was shown to grow by converting hydrogen gas and carbon dioxide to acidic acid (Ragsdale et al., 2008). *C. aceticum*, later reclassified as *Moorella thermoacetica*, belongs to the Thermoanaerobacteriaceae family, was first isolated, it attracted a lot of attention due to its unusual capacity to convert glucose almost stoichiometrically into three moles of acetic acid (Ragsdale et al., 2016).

ABE fermentation with *M. thermoacetica* involves the integration of two main pathways: glycolysis and the Wood-Ljungdahl pathway, to produce acetate:

Glycolysis: In the first part of the process, glucose is broken down via glycolysis into pyruvate. This occurs in the cytoplasm of the bacterial cell and yields a small amount of ATP and NADH.

Glucose ($C_6H_{12}O_6$) ($C_6H_{12}O_6$) + 2 ATP + 2 NAD^+ -> 2 Pyruvate ($C_3H_4O_3$) ($C_3H_4O_3$) + 2 ATP + 2 NADH

1. **Acetyl-CoA Formation via Wood-Ljungdahl Pathway**:

- **CO_2 Fixation**: In the Wood-Ljungdahl pathway, carbon dioxide is fixed and reduced to formate ($HCOO^-$)

- **Acetyl-CoA Synthesis**: Formate is further reduced to CO, which combines with a methyl group derived from methyl-tetrahydrofolate (methyl-THF) to form acetyl-CoA. (Holden, 2009)

The overall reaction can be summarized as:

$$CO_2 + 4H_2 + 2\text{Methyl-THF} + CoA \rightarrow 2\ \text{Acetyl-CoA} + 2H_2O + 2THF$$

2. **Acetate Production**:

Acetyl-CoA can be hydrolyzed to release acetate and coenzyme A (CoA).

$$\text{Acetyl-CoA} + H_2O \rightarrow \text{Acetate} + CoA$$

Wood Ljundahl pathway is the largest carbon fixation pathway in anaerobic conditions (Souza et al., 2019). Autotrophic carbon assimilation and energy conservation are achieved through the reductive use of the pathway (Ragsdale et al., 2016). Organisms use H_2 as an electron donor, and CO_2 as an electron acceptor and through this pathway acetate can be produced technically from acetyl-CoA. Figure 6 shows an overview of the acetogenesis and the Wood-Ljungdhal Pathway of CO_2 fixation.

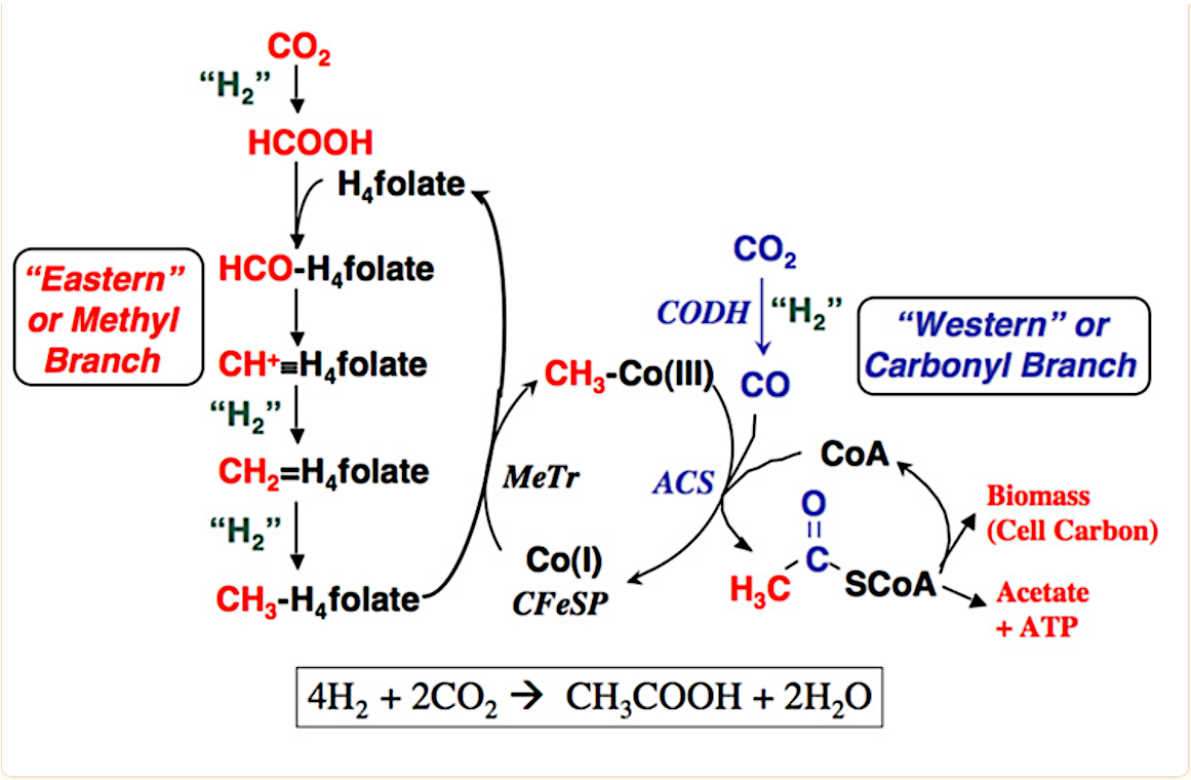

Figure 6: Acetogenesis and the Wood-Ljungdahl Pathway of CO2 Fixation (Source: Ragsdaleet al., 2016)

1.3.1.2 Reverse ß-oxidation

This metabolic pathway is responsible for chain elongation of carbon chains. Reverse β-oxidation is a metabolic pathway used by acetogenic bacteria to synthesize Acetyl-CoA from Acetate (Kallscheuer et al., 2017), see figure 7. This pathway is "reverse" because it is in the opposite direction of classical β-oxidation, which typically breaks down fatty acids to produce acetyl-CoA.

In general, β-oxidation is a common metabolic strategy for fatty acid degradation. In this four-step process, two carbon atoms are removed from the fatty acid chain in one cycle as acetyl-CoA. However general ß-oxidation strategies are not limited to the breakdown of monocarboxylic acids (fatty acids) but may also include the use of aromatic compounds, amino acids, and dicarboxylic acids.

Each enzymatic step of the β-oxidation cycle is reversible, offering the possibility of using the reversed metabolic pathway for applied purposes (Kallscheuer et al., 2017).

In such cases, 3-oxoacyl-CoA thiolase, which catalyzes the final step of chain reduction in the catabolic direction, mediates the condensation of the initial acyl-CoA molecule with acetyl-CoA in the anabolic direction (Kallscheuer et al., 2017).

The carbonyl group at C3 is progressively reduced and dehydrated to yield an extended chain product (Kallscheuer et al., 2017).

In recent years, several β-oxidation pathways have been studied in detail, and the reversal of these pathways were observed in the last years (Tarasava et al., 2022).

Microorganisms utilize reverse ß-oxidation pathway for several reasons. Acetate is a common metabolite found in anaerobic environments. By using reverse β-oxidation, microorganisms can efficiently convert acetate into acetyl-CoA, which serves as a central metabolic intermediate for various biosynthetic pathways. The conversion of acetate to acetyl-CoA through reverse β-oxidation also generates reducing equivalents such as NADH or ferredoxin, which can be used for energy production via oxidative phosphorylation or other metabolic pathways (Kallscheuer et al., 2017) (Tarasava et al., 2022).

With just four core enzymes and no need for ATP, the iterative non-decarboxylative elongation of carbon molecules with varying chain lengths and functional groups are made possible by the reverse ß-oxidation (rBOX) pathways (Tarasava et al., 2022). By dodging the regulatory system of the fatty acid degradation pathway and creating a thermodynamic pull toward chain elongation, the local β-oxidation can be functionally reversed (Tarasava et al., 2022) .

The fact that the rBOX cycle reactions do not require ATP makes it more energy efficient. As acetyl-CoA is a common precursor, there are no limitations to flux, and various carbon sources can be used. The biochemistry of the pathway enzymes allows for a wide range of exit points and flexible precursor input, allowing for great combinatorial potential and the production of numerous products (Tarasava et al., 2022).

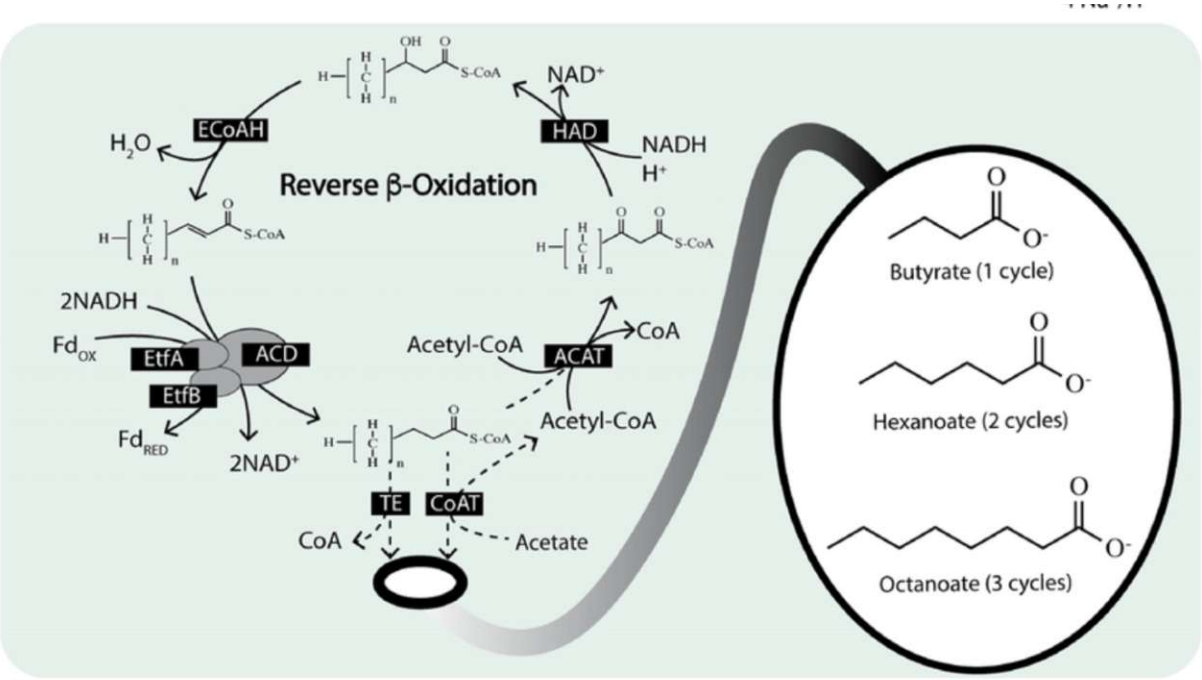

Figure 7: Metabolic pathways involved in chain elongation. (Source: Scarborough et al., 2020)

1.3.1.3 Solventogenesis

Solventogenesis is a metabolic process, by which specific anaerobic microorganisms like Clostridium species, produce bulk chemicals like solvents. Clostridia used in microbial fermentations use a variety of carbon sources and produce intermediates like pyruvate that can be further processed for more energy, depending on the species and the environment.

Under certain conditions, the bacteria switch their metabolic pathways after the acidogenesis stage and begin converting the accumulated organic acids into solvents. Acetate, butyrate and caproate are converted to their respective alcohols: ethanol, butanol and hexanol are produced as a result of this metabolic shift (Diallo et al., 2021).

The bacteria excrete the solvents into the surrounding environment as byproducts. Figure 8 displays a simplified acetone-butanol-ethanol metabolic pathway in *solventogenic clostridia*

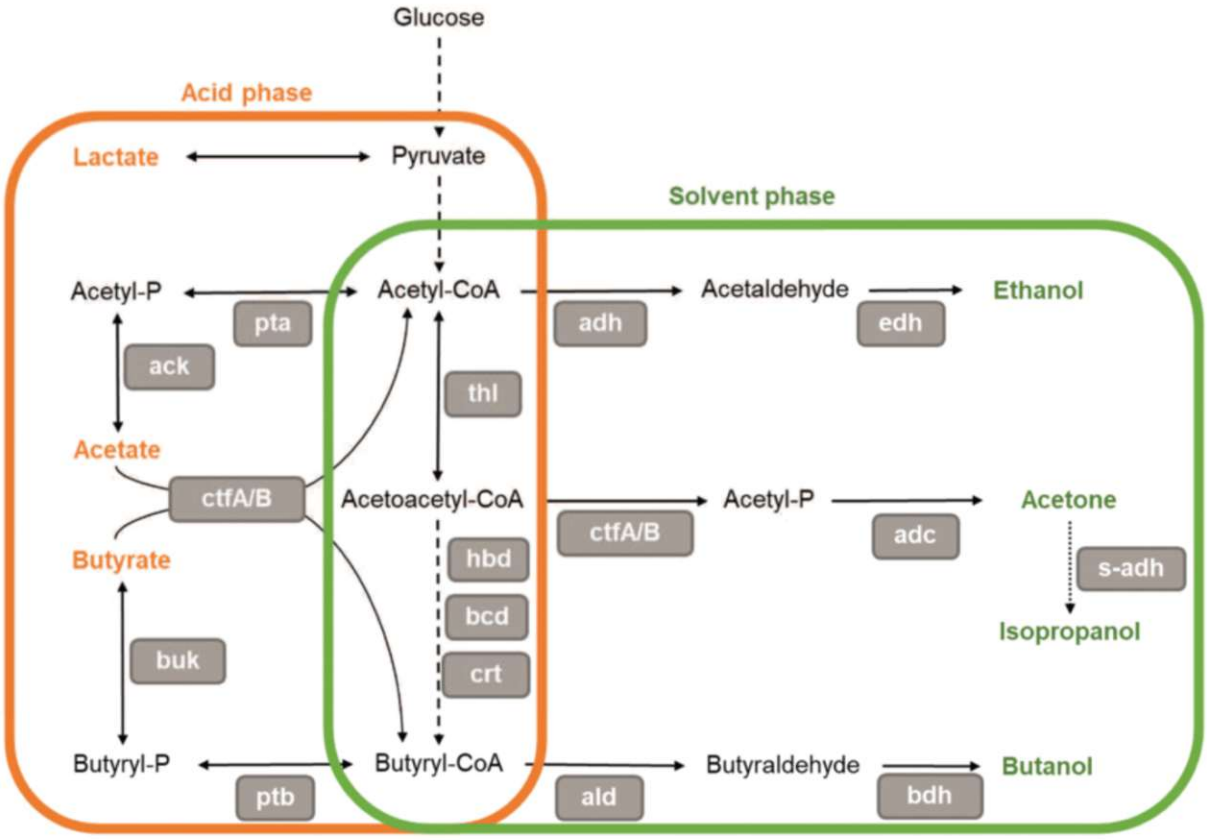

Figure 8: Simplified acetone-butanol-ethanol metabolic pathway in solventogenic clostridia (Source: Diallo et al., 2021)

Ten Clostridium species are known to be solventogenic; *C. acetobutylicum*, *C. beijerinckii*, *C. pasteurianum*, *C. saccharobutylicum*, and *C. saccharoperbutylacetonicum* being the most studied. During the twentieth century, these species were utilized in industry for the production of acetone through the ABE fermentation process (Diallo et al., 2021).

Solventogenic microorganisms, particularly *C. acetobutylicum*, are from high interest, because of their capacity to produce significant solvents like butanol. Due to the fact that these solvents can be utilized as alternative sources of energy or as precursors for the synthesis of various chemicals, this procedure has attracted interest in industrial biotechnology for the production of biofuel and biochemicals.

In syngas fermentation, where acetogens use gases like CO, CO_2 and H_2, it is assumed that solventogenesis also happens alongside acetate production using the same pathway as in ABE fermentation.

2 Aim of the study

The project focused on exploring the process of syngas fermentation, which involves the conversion of syngas into alcohols through biological pathways. It was integrated into the BESTECH project, which aimed to produce alcohols via pyrolysis and syngas- or electro-fermentation routes.

Initial investigations included experiments with pure gases to assess feasibility. The utilization of electro-fermentation, an area with limited prior experience at the institute, was a key aspect of the study.

Furthermore, the project involved evaluating various parameters to optimize electro-fermentation, including pH, media composition, and the influence of trace elements and salt concentration on the process.

3 Materials and methods

3.1 Used devices and instruments

Table 1 below lists the equipment and materials that were used to collect and analyze the various samples.

Table 1: Materials and equipments used

Equipment
Carbon cloth (model 1071) (45x40 cm) - Fuelcellstore
Carrier "Bioflow 9"/PE schwarz 800m2/m3 – RVT Process Equipment
Cassette for squeeze pump - Heidolph
Cathode for Elena reactor: PP4200 - deltaplastic
Centrifuge Eppendorf centrifuge 5430
Column/medium bottle - own construction IFA Tulln
Cuvette VWR
Electric heating jacket - own construction IFA Tulln
Gas distributor – own construction IFA Tulln
Hose (flexible) for squeeze pump - PharMed-PT
Hose for gas PUN-H-6X1 – FESTO
Hose for medium PUN-H-6X1 – FESTO
HPLC: Agilent 1260 infinity II Column: coregel ion 300 Detector RI
Incubator: Universal heating cabinet Memmert UL50
Magnetic stirrer plates Cimarec i Poly
Magnetic stirring plate “TB1” - VELP SCIENTIFICA
Magnetic stirring plate “TB2” - VELP SCIENTIFICA
Magnetic stirring plate “TB3” – IKAMAG REO
Manometer Digitron 2086P
Mass flow controller - Bürkert
Milligas counter - Ritter

Typ: MGC-1 V3.4 PMMA
Needle Ø 0.60 x 25 mm B.Braun
Needle Ø 0.80 x 120 mm B.Braun
Needle Ø 1.20 x 40 mm B.Braun
OD-measuring instrument - HachLange Dr-2800
pH meter for analytics: Mettler Toledo FiveEasy Plus
pH meter for media prep.: WTW Multi 340i
Photometer: Hach Lange GmbH
Potentiostat (Multi)PalmSense 4
Rotilabo hose connector - Carl Roth GmbH+Co.KG
Safeflow valve for sampling – B.Braun
Soap film flowmeter 1-10-100 mL - hP
Squeeze pump Pumpdrive 5201 - Heidolph
Syringe 10 mL NORM-JECT
Syringe 1mL NORM-JECT
Syringe 2 mL NORM-JECT
Syringe 20 mL NORM-JECT
Syringe 5 mL NORM-JECT
Syringe 50 mL NORM-JECT
Temperature probe medium bottle - own construction IFA Tulln
Three-way valve - Fresenius
Vortex shaker: Phoenix Instrument RS-VF10

3.2 Solutions

Chemicals used
BES
$C_6H_9NO_6$ - Acros
$CaCl_2$ * 2 H_20 -VWR CHEMICALS
$CaCl_2$ * $2H_2O$ – VWR CHEMICALS
Carrez reagent 1 (10.65%) $K_4[Fe(CN)_6]*3H_2O$ - Roth
Carrez reagent 2 (28.8%) $ZnSO_4*7H_2O$ – VWR CHEMICALS
CH_3COONa - Roth
$CoSO_4$ * 7 H_2O -VWR CHEMICALS
$CuSO_4$ * 5 H_2O - Sigma Aldrich
$FeSO_4$ * 7 H_2O - Roth
Glucose stock (300 g/L)
H_2SO_4 (0.025 mol/L) - Roth
H_3BO_3 – Sigma Aldrich
K_2HPO_4 - Roth
$K_2HPO_4*3H_2O$ - Sigma
$KAl(SO_4)_2$ * 12 H_2O Roth
KH_2PO_4 – Roth
L-Cysteine – HCl * H_20
Meat Peptone
$MgSO_4$ * $7H_20$ - Roth
$MnCl_2$ * 4 H_20 - Roth
MQ-H_2O
Na – Acetate - Roth
Na_2CO_3 (50 g/L) - Roth
Na_2MnO_4 * 2 H_2O - Roth
Na_2SeO_3 * 5 H_2O - Sigma Aldrich
Na_2WO_4 * 2 H_2O - Sigma Aldrich
NaCl - Pan
$NaHCO_3$ buffer solution 10x - Roth

NH_4Cl - VWR CHEMICALS
$(NH_4)_3C_6H_5O_7 \cdot H_2O$– VWR CHEMICALS
NiCl, SeO_3 , WO_4 stocks - Merck
$NiCl_2$ * 6 H_20 - Merck
Reduction Stock 150x
Resazurin Stock 1
RO-H_2O for blank and dilutions
Salt solution
Trace element stock 100x
Trace metal solution - Roth
Tryptone
Tween 80
Vitamin solution - Roth
Wolin´s trace metal solution
Vitamin Stock 100x - Roth
Wolfe´s vitamin solution
Yeast extract - Oxid
$ZnSO_4$ * 7 H_20 - Roth

3.3 Microorganisms

For this project anaerobic bacteria were used. Different bacteria constellation was used for the different experiments. In Table 2, there is an overview of the anaerobic organisms.

Table 2: Microorganisms used in this study

Microorganism	Origin	Metabolism	Products	Cultivation Temperature
Clostridium carboxidivorans	DSMZ 15243	Autotrophic Anaerobic	Acetate Ethanol Butyrate Butanol Caproate Hexanol	37 °C
Megasphaera sueciensis	DMSZ 17042	Heterotrophic Anaerobic	Butyrate (C4) Caproate (C6) Caprylate (C8)	30 °C
Mixed culture	Anerobic sludge from biogas tower	Heterotrophic Anaerobic/facultative	Actetate Ethanol	30 °C

3.3.1 Precultures & trial inoculation

For precultures, cyrostocks were taken out from freezer (-80 °C), which were stored in 35% glycerol. They were transferred to serum flasks under anaerobic conditions, working in the laminar flow cabinet.

The cyro stock was transferred to a sterile serum bottle under constant N_2 flow to prevent oxygen contamination.

While it is important to ensure anaerobic conditions for precultures, trials were conducted under non-sterile conditions.

With the help of sterile syringe, 1.5 mL of preculture were transferred in 120 ml flasks with 50 ml relevant preculture medium and flasks were flushed with proper gas combination for 1-3 minutes and the flasks were incubated at relevant temperature as described in Table 2.

3.4 Used media

In this section, specific media and their compositions that were used to conduct the experiment, are mentioned.

3.4.1 Medium for acetogens (used in trickle bed reactor trial)

Table 3 lists the composition of the medium for *C. carboxidivorans*

Table 3: Medium for acetogens

Compound	Composition for 1 L
K_2HPO_4*3H_2O	0.6 g
KH_2PO_4	0.33 g
NH_4Cl	1.0 g
$MgSO_4$*7H_2O	0.1 g
Hefeextrakt	2.0 g
BES	8.0 g
Autoclave 121°C, 20 min After autoclaving the following was added	
Vitamin stock 100x	10.0 mL
Reduction stock 150x	6.67 mL
Trace element stock 100x	10.0 mL
$NaHCO_3$ buffer solution 10x	100.0 mL
Adjust pH to 6.3 with HCl /NaOH	

3.4.2 Media used for trickle bed reactors with electricity

Table 4 lists the composition of the medium for trickle bed reactor Elena & Zorro.

Table 4: Media for Elena & Zorro reactors

Compound	Composition for 1 L
KH_2PO_4	1.0 g
NaCl	1.0 g
NH_4Cl	0.25 g
$MgSO_4*7H_2O$	0.21 g
KCl	0.1 g
$CaCl_2*H_20$	0.04 g
Resazurin stock 1 [1% w/v]	1.0 mL
Autoclave 121°C, 20 min After autoclavation the following was added	
Wolin´s trace metal solution	10.0 mL
Wolfe´s vitamin solution	10.0 mL
Adjust pH to 6.3 with HCl /NaOH	

3.4.3 Media for *C. carboxidivorans*

Table 5 lists the composition of the media for *C. carboxidivorans.*

Table 5: Media for C. carboxidivorans

Compound	Composition for 1 L
NH_4Cl	1.0 g
KH_2PO_4	11.73 g
K_2HPO_4	2.406 g
$MgSO_4 * 7H_20$	0.1 g
Yeast extract	2.0 g
$FeSO_4 * 7 H_2O$	0.026 g
Wolfe´s mineral solution	20.0 mL
NiCl, SeO_3, WO_4 stocks	1.0 mL

Autoclave 121°C, 20 min After autoclaving the following was added	
Wolfe´s vitamin solution	10.0 mL
L-Cysteine [100g/L]	0.5 g
Na_2CO_3 [50 g/L]	1.0 g
Adjust pH to 6.3 with HCl /NaOH	

3.4.4 Preculture media for *C. carboxidivorans* / 104c

Table 6 &7 lists the composition of the media for *C. carboxidivorans* preculture.

Table 6: Preculture media for C. carboxidivirans

Compound	Composition for 1 L
Tryptone	5.0 g
Meat peptone	5.0 g
Yeast extract	10.0 g
Resazurin stock 1 [1% w/v]	1.0 mL
Salt solution	40.0 mL

pH was adjusted to pH 6.0 & the media was transferred into serum flasks (50 mL) and sparged with N_2 / CO_2 (80/20) for at least 30 minutes. The flasks were autoclaved at 121° C for a duration of 15 min. After autoclaving, following ingredients were added under laminar flow in a working bank:

Table 7: Components added after autoclaving for C. carboxidivorans preculture

Compound	Composition for 1 L
L-Cysteine – HCl * H_20 (100 g/L)	0.5 g
Na_2CO_3 (50 g/L)	1.0 g
Glucose stock (300 g/L)	5.0 g

3.4.1 Salt solution for *C. carboxidivorans* preculture medium

Table 8: Salt solution for C. carboxidivorans preculture medium

Compound	Composition for 1 L
$CaCl_2$+2$H_2$0	0.25 g
$MgSO_4$ * 7H_2O	0.5 g
K_2HPO_4	1
KH_2PO_4	1
$NaHCO_3$	10
NaCl	2

3.4.2 Preculture media for *M. suciensis*

Table 9 lists the composition of the media for *M. suciensis* preculture.

Table 9: Preculture media for M. suciensis

Compound	Composition for 1 L
Tryptone	10.0 g
Meat extract	10.0 g
Yeast extract	5.0 g
Tween 80	1.0 g
K_2HPO_4	2.0 g
$C_2H_3NaO_2$	5.0 g
(NH_4)2 * $H_2$0 * citrate	1.86 g
$MgSO_4$*7$H_2$0	0.2 g
$MnCl_2$ * 4 $H_2$0	0.06 g

3.4.3 Standard media for trials with *M. suciensis*

Table 10 lists the composition of the standard media for trials with *M. suciensis*.

Table 10: Standard media for trials with M. suciensis

Compound	Composition for 1 L
KH_2PO_4	1.0 g
NaCl	1.0 g
NH_4Cl	0.25 g
$MgSO_4$ * 7 H_2O	0.211 g
KCl	0.1 g
$CaCl_2$ * $2H_2O$	0.04 g
CH_3COONa	2.46 g
Resazurin stock 1 [1% w/v]	1.0 mL
Wolin´s trace metal solution	10.0mL
Wolfe´s vitamin solution	10.0 mL

Medium was adjusted to pH 6,3 and filled up in flasks.

3.4.4 Media for mixed cultures

Table 11 lists the composition of the media used for mixed cultures.

Table 11: Media for mixed cultures

Compound	Composition for 1 L
KH_2PO_4	1.0 g
NaCl	1.0 g
NH_4Cl	0.25 g
$MgSO_4$ * 7 H_2O	0.211 g
KCl	0.1 g
$CaCl_2$ * $2H_2O$	0.04 g
Resazurin stock 1 [1% w/v]	0.001 g

Wolin´s trace metal solution	10.0 mL
Wolfe´s vitamin solution	10.0 mL
Cystein * HCl	0.5 mL

The pH of the medium for mixed cultures was adjusted to 6.3

3.4.5 Media for trace element trials

For trace element trials, *C. carboxidivorans* autotrophic media was used.

Table 12: Media for trace element trials

Compound	Composition for 1 L
NH_4Cl	1.0 g
KH_2PO_4	0.33 g
K_2HPO_4	0.45 g
$MgSO_4$*7 H_2O	0.1 g
$FeSO_4$*7 H_2O	0.026 g
Wolfe´s mineral solution	20.0 mL
NiCl stock	1.0 mL
WO_4	25.0 µL
SeO_3	50.0 µL
Resazurin stock 1 [1% w/v]	1.0 mL
After autoclaving add:	
Wolfe´s vitamin solution	10.0 mL
L-Cysteine 100 g/L	0.5 g
Na_2CO_3 (50 g/L)	1.0 g

After adding remaining ingredients after autoclaving , pH was adjusted to 6,2.

For the trace elements trials, five times the concentration of normally used trace elements were added to the medium.

3.4.6 Wolin´s mineral solution

The Wolin´s mineral solution was added to the relevant medium after autoclaving.

Table 13: Wolin´s Mineral Solution

Compound	Composition for 1 L
Nitrilotriacetic acid	1.5 g
$MgSO_4 * 7H_2O$	3.0 g
$MnSO_4 * H_2O$	0.5 g
NaCl	1.0 g
$FeSO_4 * 7 H_2O$	0.1 g
$CoSO_4 * 7 H_2O$	0.18 g
$CaCl_2 * 2 H_20$	0.1 g
$ZnSO_4 * 7 H_20$	0.18 g
$CuSO_4 * 5 H_2O$	0.01 g
$KAl(SO_4)_2 * 12 H_2O$	0.02 g
H_3BO_3	0.01 g
$Na_2MnO_4 * 2 H_2O$	0.01 g
$NiCl_2 * 6 H_20$	0.03 g
$Na_2SeO_3 * 5 H_2O$	0.3 mg
$Na_2WO_4 * 2 H_2O$	0.4 mg
Distilled water	1 L

3.4.7 Stock solutions used for *C. carboxidivorans* autotrophic media

Table 14: Stock solution used for C. carboxidivorans autotrophic media

Compound	Composition for 1 L
Ni-Stock [5mL]	
Nitrilotriacetic acid	0.03 g
$NiCl_2*6H_2O$	0.003 g
Se-Stock [5mL]	

Nitrilotriacetic acid	0.03 g
Na_2SeO_3	0.0198 g
W-Stock [5 mL]	
Nitrilotriacetic acid	0.03 g
$Na_2WO_4*2H_2O$	0.04 g

3.4.8 Production of media

To prepare the desired medium, the components listed in the tables before were dissolved in RO-H_2O in a Schott flask. Subsequently, the various stock solutions, mentioned above of the respective formulation, were added. After completion of the media, their pH was checked and, if necessary, pH is adjusted to the given pH as listed above using NaOH or HCl.

Since mixed culture was used in most of the experiments, the media did not have to be sterile, and autoclaving was therefore not necessary. The culture media were prepared before the experiments in a bigger scale. The anaerobic conditions were achieved during the test preparations of the reactor experiments without gassing the culture media with N_2 beforehand.

3.5 Serum flask trials

3.5.1 Trace element trials

For the development and metabolic activity of bacteria, trace elements are important nutrients that must be available in small quantities. Iron, selen, cobalt, nickel, molybdenum, zinc, and manganese are examples of such trace elements. They perform crucial functions in cellular metabolism and act as cofactors for enzymatic processes.

Although there isn't much evidence on how trace elements affect the elongation of chains and the synthesis of alcohol during anaerobic gas fermentation, some research. (Pranhita et al., 2018) showed that they presumably have an impact through altering the activity of certain enzymes and metabolic pathways.

In this thesis, I was focusing on the trace elements selenium and molybdenum because they delivered the best results.

3.5.1.1 Reactor design and setup

Flasks for trace elements

120 mL serum flasks (as triplicate) were used for trace element trials. 30 mL of medium for trace elements was added together with the relevant amount of trace elements (which was 5 times higher than the "normal" amount in the medium described in table 10) into serum flasks together with 1 mL of relevant culture (see table 14) and pH adapted to pH 5. Afterwards, the flasks were gassed with a H_2/CO_2 gas mixture, consisting of H_2/CO_2 in the ratio of 80/20 % [%v/v], to 1.5 bar overpressure. During this process, a needle (gas supply needle) with the gas inlet was pushed through the rubber stopper of the flask into the medium. After opening the gas valve, another needle for the gas outlet is inserted through the rubber stopper and the serum flasks are rinsed with the gas for a few minutes. Afterwards, the needle for the gas outlet was then pulled out of the head area and continued to be gassed until an overpressure of 1,5 bar was reached and the needle for the gas inlet was pulled out of the flask. The flasks were then cultivated in a shaking incubator at 30 °C and 130 rpm. No electrodes were used for this experiment. For control trials, the same procedure was done, except adding (higher amount of) trace elements to the medium. On weekly basis, the residual pressure was checked using a manometer. To investigate the pH of the medium together with the amount of acetate, butyrate, caproate, ethanol, butanol and hexanol in the medium, 1mL of the sample was taken from the liquid phase and the bottles were gasified to 1,5 bar overpressure.

3.5.1.2 Reactor design and setup

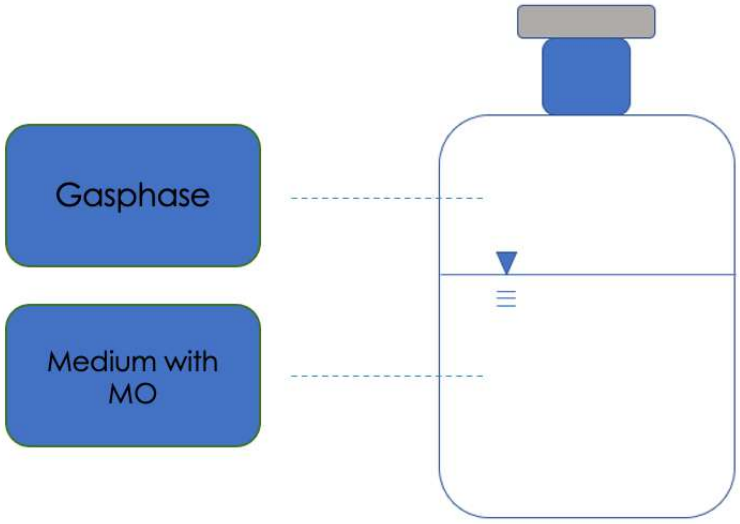

Figure 9: Flask setup for trace element & lower pH trials

4 x 120 mL serum flasks (as single replicate) were used for this experiment. 30 mL of medium of *Zorro* reactor described in 2.6.2 was added into serum flasks and pH adapted to pH 4,5 (for 3 flasks). To achieve the desired pH conditions, 30 mL of culture in each flask was treated with 4.2 mL of 0.5 M HCl. As one flask served as control, the pH was adjusted to pH 5,3. Afterwards, the flasks were gassed with a H_2/CO_2 gas mixture, consisting of 80% H_2 & 20% CO_2, to 1.5 bar overpressure. The gasification was done as described before. The flasks were then cultivated in a shaking incubator at 30 °C and 130 rpm. No electrodes were used for this experiment. On weekly basis, the residual pressure was checked using a manometer. To investigate the pH of the medium together with the amount of acetate, butyrate, caproate, ethanol, butanol and hexanol in the medium, 1 mL of the sample was taken from the liquid phase and the bottles were gasified to 1,5 bar overpressure.

Figure 10: Flask for salt trial

3.5.2 Salt trials

During experimentation with trickle bed bioreactor (see 2.6), an intriguing phenomenon was observed: whenever the pH was adjusted using a 1 M NaOH solution, there was a noticeable increase in electricity consumption. This observation suggested a potential link between pH adjustment with NaOH, increased electricity consumption, and enhanced biofilm formation. Biofilms are complex microbial communities attached to surfaces, and they can significantly impact bioreactor performance by serving as barriers, improving gas exchange, and enhancing overall system stability. To explore this connection further, a trial was started outside of the above-mentioned trickle bed bioreactor using NaCl, KCl and a mixture of both as salts.

3.5.2.1 Reactor design and setup

Electroflasks for salt trails

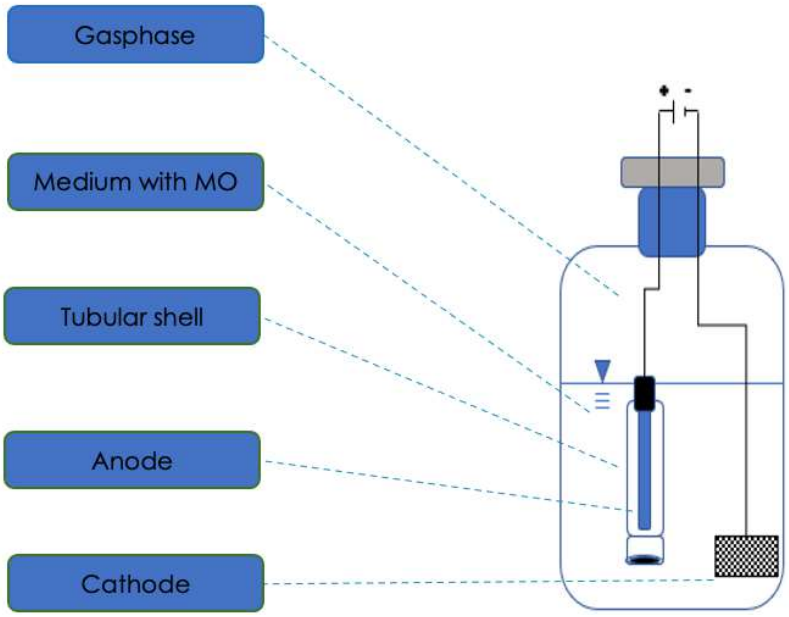

Figure 11: Flask set up for salt trials

For this experiment an electrochemical "reactor" was designed using 120 mL serum flasks. The setup was modified: one with a membrane separating the anode and cathode chambers, another with electrodes but no membrane. For this experiment the one with membrane was used.

The cathode material selected for this setup is plain carbon cloth. Carbon cloth provides a high surface area for microbial attachment and efficient electron transfer to support microbial growth in electrochemical systems. The anode material is stainless steel electrode E316L (Nirosta V2A), as stainless steel electrodes are corrosion-resistant and have good electrical conductivity, making them suitable for anodic reactions in electrochemical bioreactors. The electrodes were introduced through a drilled hole in the rubber cap of an electro-flask.

Each experimental approach involves three serum flasks (120 mL) (as biological triplicate) with mixed culture concentration of 110 mM in a 30 mL medium with a total chloride concentration of 220 mM. Afterwards, the anode chamber was filled with medium to avoid air bubbles on the membrane.

The cathode and anode were placed in the serum flask and filled chamber, respectively. Finally, an aluminum cap was used to crimp the butyl rubber stopper into the flask. It is important to make sure that the electrodes inside the serum flasks do not contact each other. Afterwards a gas mixture (80% H_2 / 20% CO_2) into each flask to create the desired anaerobic environment (as described in the experiment for trace elements before) and the bottles were gasified to 1,5 bar overpressure.

The electroflasks were then attached to a voltage supply source after being placed inside an incubator on a stirrer plate. Voltage is supplied by a stainless steel wire threaded through a rubber and vinyl cap to the bulb. The ends of the wires are attached to the carbon fabric and immersed in the medium.

Figure 12: Electroflasks for salt trial

3.6 Trickle-bed reactor

Trickle-bed reactors are known for efficient gas-to-liquid mass transfer with low energy consumption. They work by allowing microorganisms to form biofilms on carrier materials while the medium trickles downward and gas flows in various directions.

While trickle-bed reactors have been studied for bio-methanation processes, their use in acetic acid production is less common.

One challenge in scaling up gas fermentation is the initial start-up phase of Trickle-Bed Reactors. The experimental configuration initially consisted of three trickle-bed reactors.

Two further Trickle-bed reactors were built, each operated under electrical current.

The primary objective of this experiment was to systematically investigate the potential impact of electricity on chain elongation and alcohol production within the fermentation system.

3.6.1 Reactor set up

The trickle-bed reactors were set up parallel as visualized in figure 13 and consisted of a glass column, with an empty column volume of 387 mL each, 45 cm high and a diameter of 3 cm. The packing height of the carriers (Biofow nine PE black, RTV Process Equipment GmbH, Germany) filled up about 33.5 cm of the column (Steger et al., 2022). The gas inside each column took up about 316 mL of space.

At the top and bottom of these glass columns, there were special caps with connectors for gas and liquid. These connectors made sure the gas and liquid went in and out evenly. After the liquid went through the columns, it was collected in big bottles. Then, the liquid was pumped back into the columns at a rate of 9.8 mL per minute using a peristaltic pump (PD 5201, Heidolph, Germany).

Each big bottle had three tubes connected to it: one for taking out liquid, one for circulating the liquid, and one to keep the pressure right. Before the liquid went into the columns, it split into two smaller tubes to spread the liquid evenly over the materials inside.

To keep everything at the right temperature (around 30°C), heating jackets were wrapped around the glass columns and big bottles. The liquid's acidity level (pH) was corrected by adding 1 M NaOH solution once a day (if needed).

The gas mixture of H_2 and CO_2 came from a pressurized gas cylinder. To control how much gas went into the columns, a mass flow controller was used. Traps were put in the gas tubes to catch any extra liquid that might get in and cause problems.

The gas went into the bottom of the columns, moved through them, and came out at the top. Used gas was measured with milligascounters (MGC-1 V3.4 PMMA, Ritter, Germany). The gas flow rate in each column was around 3.8 mL per minute (Steger et al., 2022).

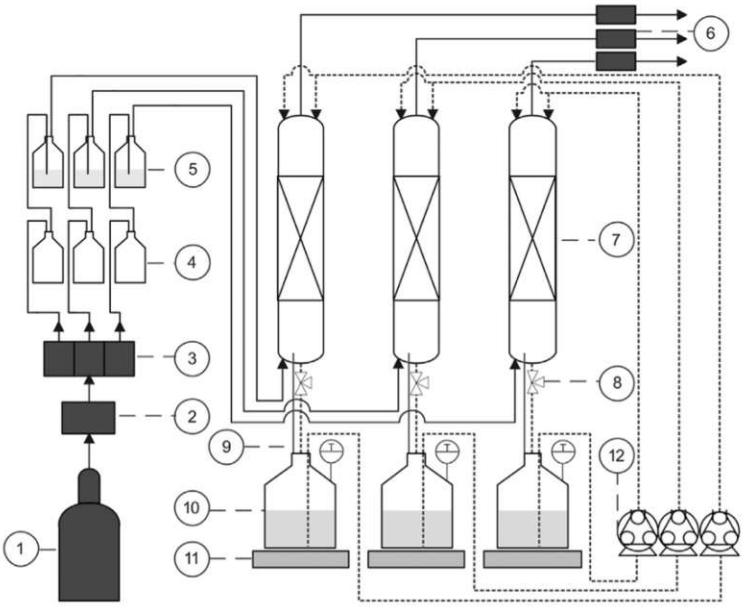

Schematic drawing of three parallel TBs with gas cylinder (1), MFC (2), gas distributer (3), liquid traps (4), humidification flasks (5), MGCs (6), three columns with heating jackets (7), sampling ports (8), pressure balancing tubes (9), three medium collection flasks (10) which were located on magnetic stirrers (11) and contained magnetic stir bars, and peristaltic pumps (12).

Figure 13: Trickle bed reactor set up of FR1, FR2 & FR3 (Source: Steger et al., 2022)

The reactors were named as FR1, FR2, FR3 (FR1 – FR3 as described in figure 14).
The two reactors operated under electrical current were named Elena & Zorro, which will be described below. The experiment of Elena served as a control to Zorro.

Figure 14: Trickle bed reactors - from left to the right: FR1, FR2 & FR3

3.6.2 Trickle-bed reactor with electricity- reactor set up

The setup of these two reactors has some similarities to the reactors described before in figure 11. This section will only be focusing on the differences. The introduction of electricity to this context, the reactor Elena was equipped with an electrode configuration that enabled the controlled application of electrical current. For the cathode of "Elena" we used polypropylene and added 40% carbon black, that was heated and shaped, as polypropylene doesn't break down easily.

A total of 125 cathode pieces, each with a resistance of 200 ohms, were meticulously arranged along a 1.3-meter wire. This arrangement was designed to facilitate efficient electron transfer and enhance the reactor's electrochemical capabilities. The anode of the reactor consisted of

a stainless-steel rod and the reactor volume was 400 mL, offering space for the electrochemical reactions and processes taking place within. The application of electrical potential, measured in volts, was carefully controlled to ensure optimal conditions for the desired electrochemical process. Elena maintained a maximum potential of 0.74 volts at a flow rate of 5 mL per minute. The reactor operated at a controlled temperature of 30 °C.

The construction of Zorro paralleled that of the previous setup, with the exception of the cathode component. For Zorro's configuration, commercially available polylactide (PLA) and polypropylene (PP) pellets were employed. At IFA, 30% carbon black (Russ) was incorporated into the polylactide to enhance its conductivity. After adding the carbon black, the polylactide was heated and shaped using hot extrusion. In this instance, a 3x3 plain carbon cloth (Model 1071) was utilized. No visible biofilm was observed on Zorro's setup, suggesting its absence.

There was the assumption that the reason behind this could be polylactide degradation. However, no noticeable indicators were detected for this degradation, including the absence of biofilm. Nonetheless, there remained a doubt if degradation has occured.

This was the reason for the construction of the second reactor Elena using the cathode mentioned above to prevent degradation. This adjustment was intended to see if we could reproduce the results obtained with Zorro.

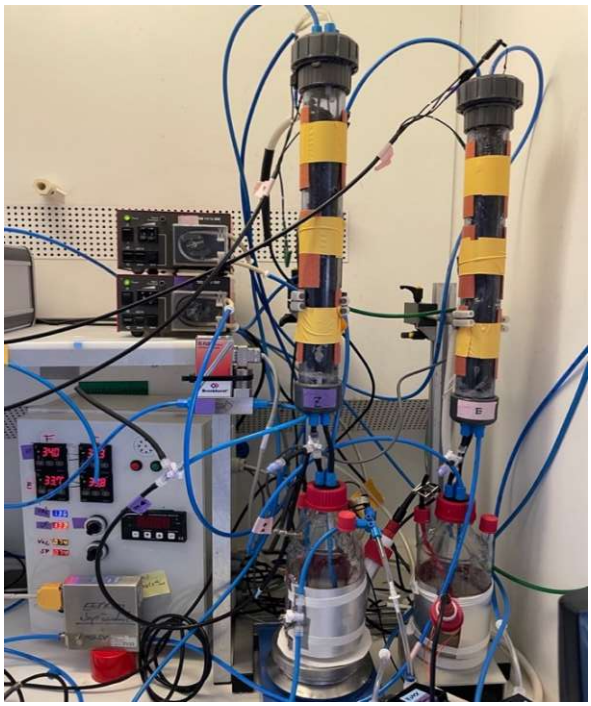

Figure 15: Trickle bed reactors - from left to right: Zorro & Elena

Medium and inoculation - Zorro reactor

The experiment employed a total volume of 400 mL within the Zorro reactor. The selected medium used for the experiment was tailored for the growth and cultivation of *M. sueciensis* (Table 4).

The first inoculation was performed with acetogenic microorganisms with 1x50 mL of liquid each from the F1 reactor & the F2 reactor, described above. In this process, the microorganisms were subjected to centrifugation of 10 minutes at 12700 rpm, and the resulting pellet was resuspended in a small quantity of RO water. Subsequently, this microbial suspension was transferred to the Zorro reactor. A secondary inoculation was performed some weeks later, introducing bacteria of the genus Megasphaera into the Zorro reactor. These microorganisms were sourced from 2x 50 mL pre-culture that had been propagated in a glucose-rich medium and then transferred in an acetate medium. Similar to the initial inoculation, the microorganisms were centrifuged, the pellet was collected, and it was suspended in few ml of RO water.

Medium and inoculation – Elena reactor

The experiment was conducted within a reactor with a total volume of 400 mL. The selected medium used for the experiment was tailored for the growth and cultivation of *M. suciensis* (Table 4).

To prepare for the inoculation, 3.2 grams of 2-(N-morpholino)ethanesulfonic acid (MES) were introduced to a 50 mL volume in the column. This step involved the addition of BES to suppress the methanogenic activity of archaea.

For the initial inoculation, microorganisms were obtained from two sources, 50 mL from F1 and 50 mL from F2. The collected microorganisms from F1 and F2 were centrifugated for 20 minutes at a speed of 3,800 rpm. The resulting microbial pellet was then carefully resuspended in approximately 10 mL of a 0.9% NaCl solution and transferred to the reactor.

3.6.3 Sampling and sample evaluation

For the serum flask trials, sampling was carried out every week to analyze pH, OD and the production of long chain hydrocarbons / alcohols. For the trickle bed reactor trials, this was done on a daily basis.

Regarding the sampling of serum flask trials, 1mL of the sample was taken (as biological triplicate) from the liquid phase and the bottles were gasified to 1,5 bar overpressure. The sampling of trickle bed reactors, sampling was carried out through a 3-way valve.
The measurement of the optical density was measured at a wavelength of 600 nm using a the HachLange Dr-2800.

The pH of the sample was measured with a pH meter. It was necessary to monitor the pH levels in the trickle-bed reactors (TB) to ensure that the pH did not fall below 5.5. In the event of a decrease in pH, adjustments were made by 1M NaOH.
This process was facilitated through the introduction of NaOH via a tubing system into the TB medium bottle.
The detection of alcohols and long-chain hydrocarbons was accomplished through the utilization of High-Performance Liquid Chromatography (HPLC).

3.6.4 High pressure liquid chromatography – HPLC

To identify the products formed, high press liquid chromatography (HPLC) was used. With a refractive index detector and a Coregel ION 300 column, the Agilent 1260 Infinity II was the instrument used. A 0.01 M H_2SO_4 solution served as the eluent.
Prior to analysis, the samples were subjected to Carrez clarification to remove solid fractions that could potentially interfere with the HPLC analysis.
The first step of the sample preparation is sample purification through Carrez clarification. pH of the samples should be between 4 to 6 for subsequent measurements, therefore 200 µL of the supernatant was mixed with either 760 µL of 0.025 M H_2SO_4 in cases where the pH exceeded 6. 760 µL of MQ-H_2O was mixed instead for samples with pH values below 6 and 20 µL of Carrez solutions 1 and 2 were sequentially added to the samples. The introduction of Carrez solutions resulted in the precipitation of proteins, effectively purifying the samples and eliminating turbidity.
Then the samples were centrifugated at 12,400 rpm for 10 minutes. The supernatant was drawn up via syringe and passed through a membrane filter with a pore size of 0.45 µm before being transferred into HPLC vials. The measurements were conducted as single technical replicates

4 Results

In this chapter, the data and results of experiments mentioned above are presented & discussed.

4.1 Trace element trial

Trace elements play an important role in gas fermentation experiments as they serve as essential cofactors for many enzymatic reactions required for the metabolism of microorganisms in biological processes. These microorganisms require trace elements to activate enzymes involved in the conversion of gaseous substrates such as CO, CO_2 and H_2 into useful products such as biofuels and biofuels. Therefore, providing the right amount and composition of trace elements in the culture conditions is crucial to ensure optimal performance and productivity in gas fermentation processes.

Some studies showed that a higher concentration of trace elements may have a positive impact on product formation (Nimbalkar et al., 2018).

In this thesis the focus will be on the trace elements selenium (Se) and molybdenum (Mo) as they served the best results. The study involved various experimental trials, each focused-on combinations of microorganisms and trace elements. These trials were as follows:

1. A trial featuring *C. carboxidivorans* with selenium supplementation with concentration 5 times higher than in control flask (as described in table 12 & 15).
2. A trial involving *C. carboxidivorans* with molybdenum supplementation with concentration 5 times higher than in control flask (as described in table 12 & 15).
3. A trial combining *C. carboxidivorans* with *M. sueciensis*, with selenium supplementation with concentration 5 times higher than in control flask (as described in table 12 & 15).
4. A trial combining *C. carboxidivorans* with *M. sueciensis*, with molybdenum supplementation with concentration 5 times higher than in control flask (as described in table 12 & 15).

5. Two control trials, one with *C. carboxidivorans* and the other with a combination of combining *C. carboxidivorans* with *M. sueciensis* with “normal” amout of tracelements as used in medium described in table 12.

These distinct experimental trials allowed for the systematic exploration of the influence of selenium and molybdenum on various microbial combinations, providing valuable insights into their respective impacts within the experimental context.

Table 15: Overview of constellation of flasks used for trace element trials

Flask name	Microorganism(s) used in flask	Added trace element (5x higher than control)
C	*C. carboxidivorans* (C)	Selenium
C	*C. carboxidivorans* (C)	Molybdenum
C+M	*C. carboxidivorans* + *M. sueciensis* (C+M)	Selenium
C+M	*C. carboxidivorans* + *M. sueciensis* (C+M)	Molybdenum
Control	*C. carboxidivorans* (C)	--
Control	*C. carboxidivorans* + *M. sueciensis* (C+M)	--

In the initial phase of the experiment, all flasks exhibited identical values to the control group, as visually represented in figure 16. This control trial served as a reference point, characterized by the absence of caproate, hexane, and butanol, with only the presence of acetate, ethanol, and butyrate, which was the case for all flasks mentioned above.

Subsequently, in the following graph (figure 17 – 20), the concentrations of acetate, butyrate, caproate, ethanol, butanol, and hexane within the control flasks is presented. This graphical representation highlights the changes observed in these compounds over the experiment and provides insight into the dynamics of these components within the control trials.

The analysis of the trace element test is illustrated by the following diagrams.

Figure 16 depicts the trial's outset, where all flasks maintained identical conditions. In the subsequent graph (figure 17), the composition at the end of the experiment of the control flask

featuring *C. carboxidivorans* is delineated. Meanwhile, figure 18 illustrates the terminal state of the control flask containing a mixture of *C. carboxidivorans* and *M. sueciensis.*

Both control flasks exhibited a reduction in acetate production, alongside a concurrent decrease in butyrate production, indicative of butanol and ethanol production. Interestingly, there is minimal difference observed between the control flask containing only *C. carboxidivorans* and the control flask containing both *C. carboxidivorans* and *M. sueciensis*.

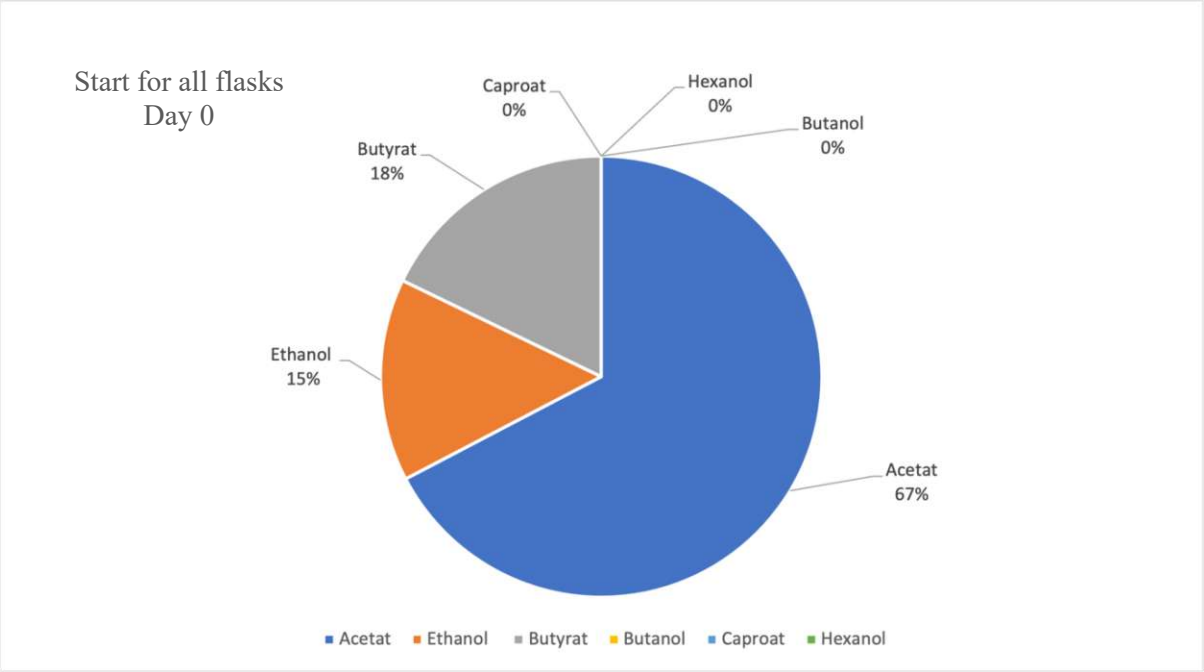

Figure 16: Ratio of main products including butanol, hexanol, acetate, butyrate, caproate & ethanol investigated during cultivation at the start of the experiment

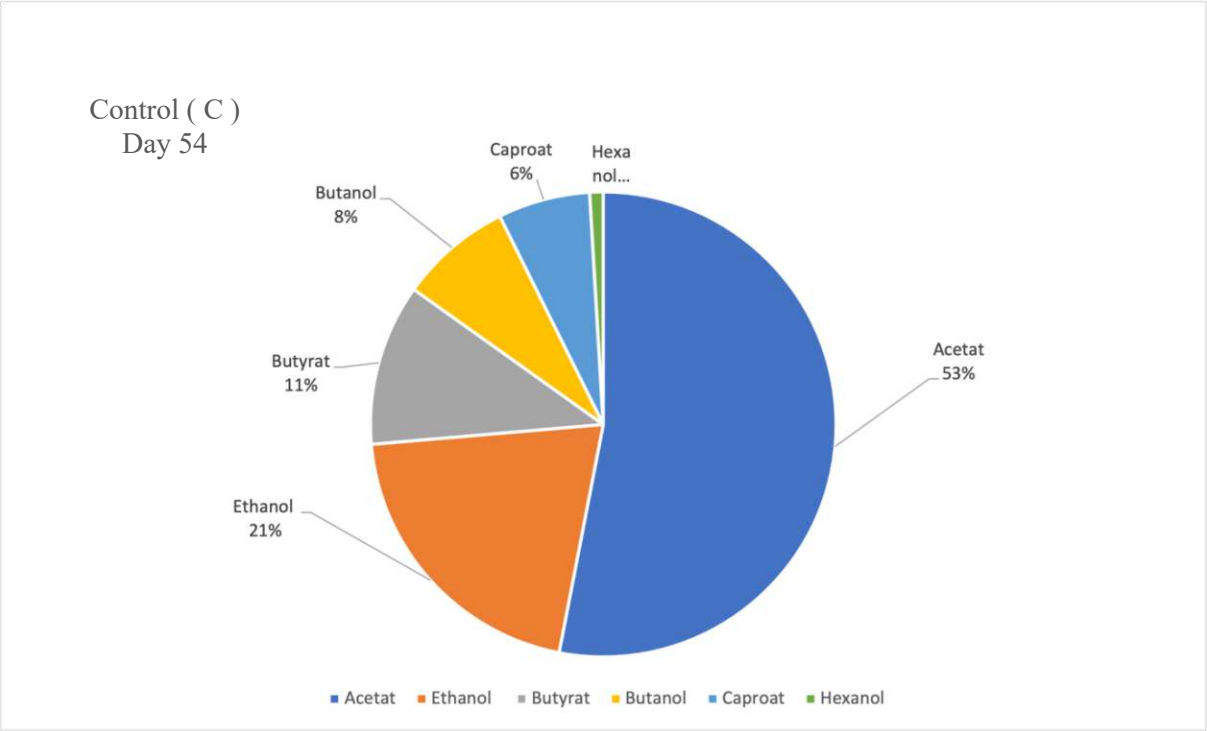

Figure 17: Ratio of main products including of acetate, ethanol, butyrate, butanol, caproate & hexanol in control flask with C. carboxydivorans at end of experiment after 54 days

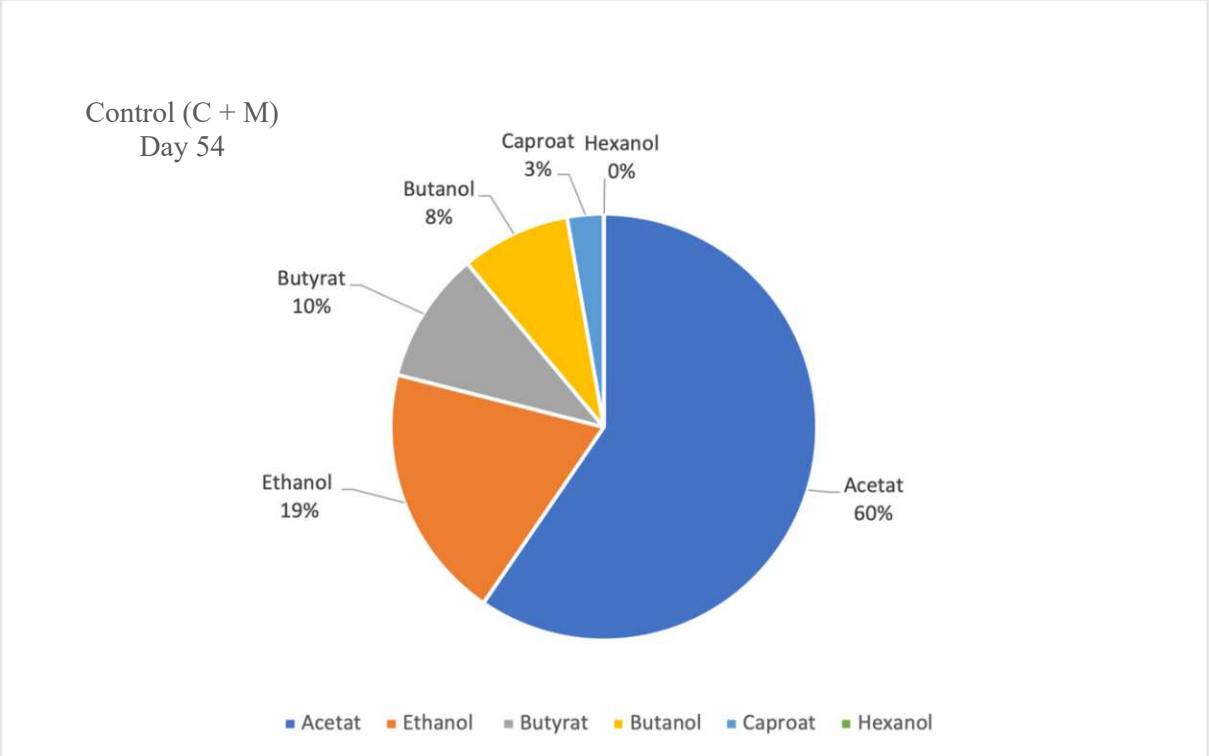

Figure 18: Ratio of main products including acetate, ethanol, butyrate, butanol, caproate & hexanol in control flasks with C. carboxidivorans and M. sueciensis at end of experiment after 54 days

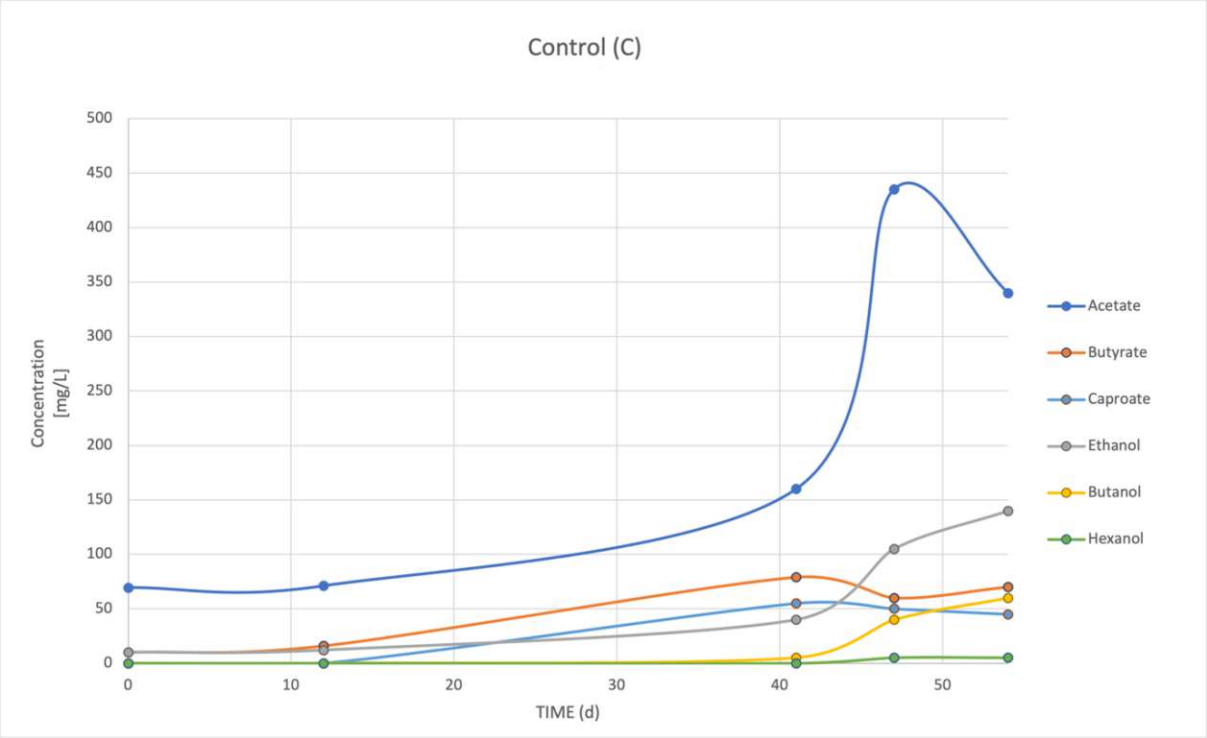

Figure 19: Concentration of acetate, ethanol, butyrate, caproate, butanol and hexanol in control flasks with C. carboxidivorans over time

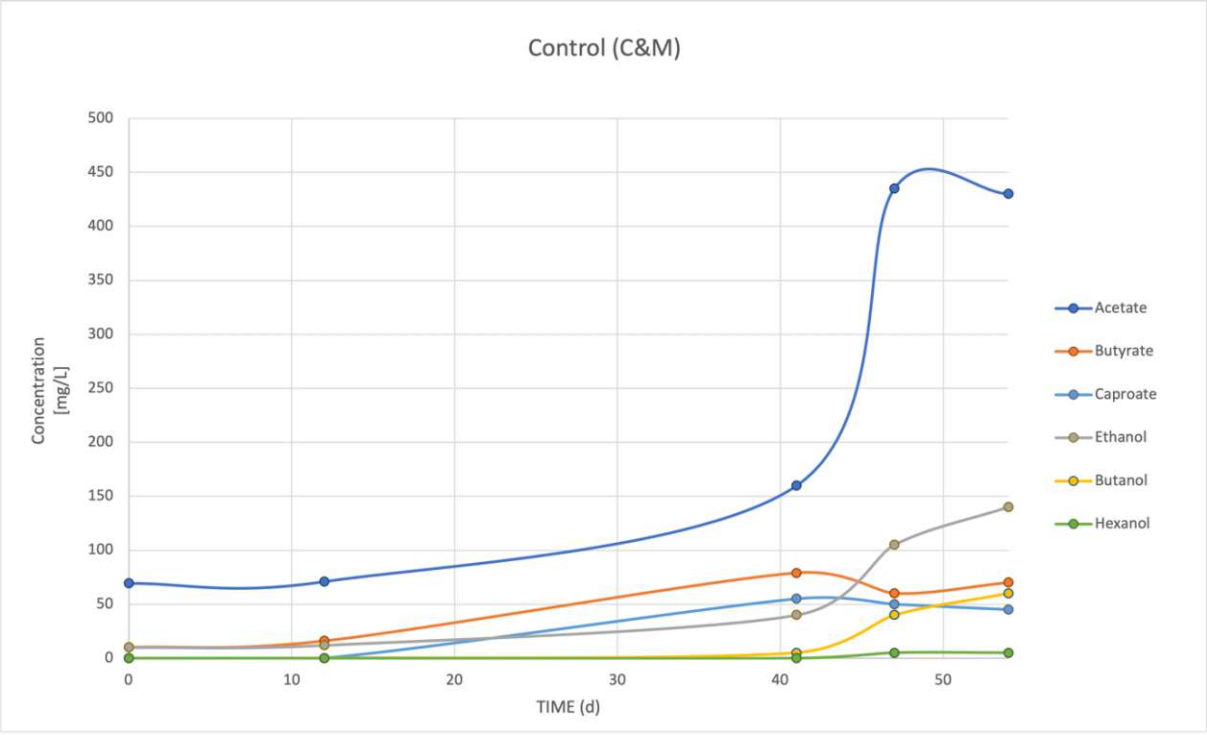

Figure 20: Concentration of acetate, ethanol, butyrate, caproate, butanol and hexanol in control flasks with C. carboxidivorans & M. suciensis over time

A notable effect becomes apparent with the introduction of an elevated quantity of trace elements, irrespective of the specific combinations employed.

The most prominent contrast is observed in the production of ethanol, notably in the flask where molybdenum serves as the trace element, coupled with *C. carboxidivorans* (figure 21-24). In this context, ethanol makes up 49% of the components acetate, caproate, butyrate & hexanol and in the combination flasks the ethanol production reached 55% when employing selenium as the trace element. This is in stark contrast to the control flask, where ethanol production was limited to 21%, indicating a substantially elevated production, approximately 2.62 times higher when compared to the control flask. Furthermore, there was a notable increase in butanol production compared to the control flask. In the control trial, the production of butanol amounted to 8%. However, in trials involving selenium and molybdenum as trace elements, the butanol production exceeded 20%, indicating a substantial elevation in butanol production, exceeding 2.5 times that of the control flask.

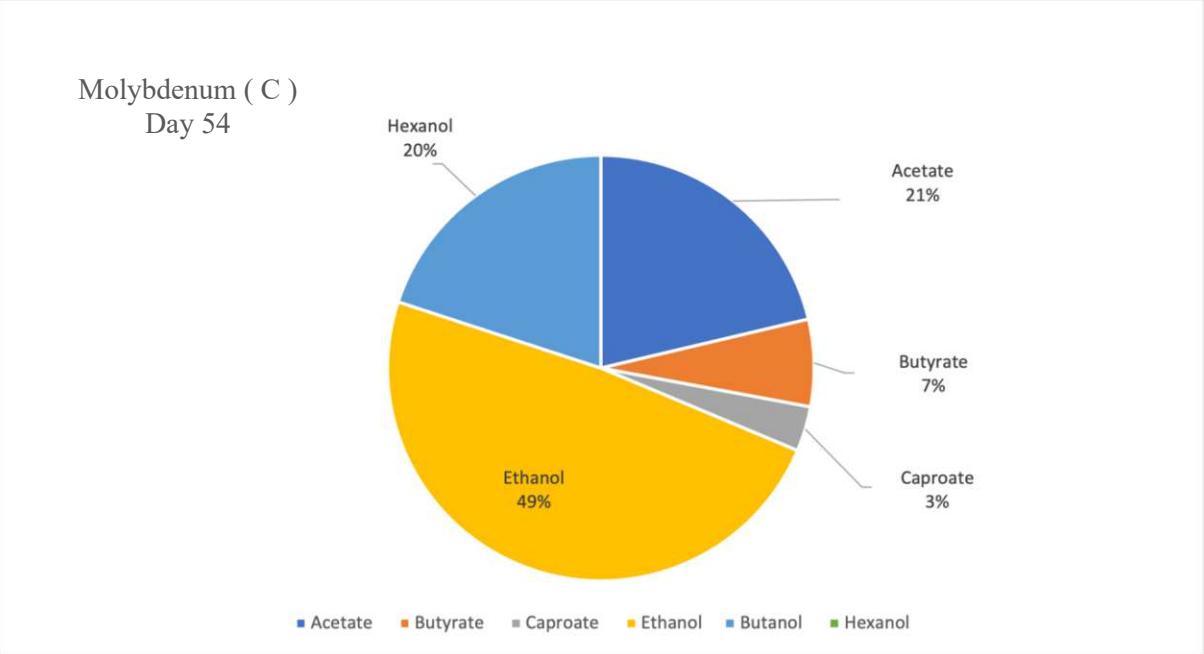

Figure 21: Ratio of main products including acetate, butyrate, caproate, ethanol, butanol & hexanol in flasks with molybdenum & C. carboxidivorans at end of experiment after 54 days

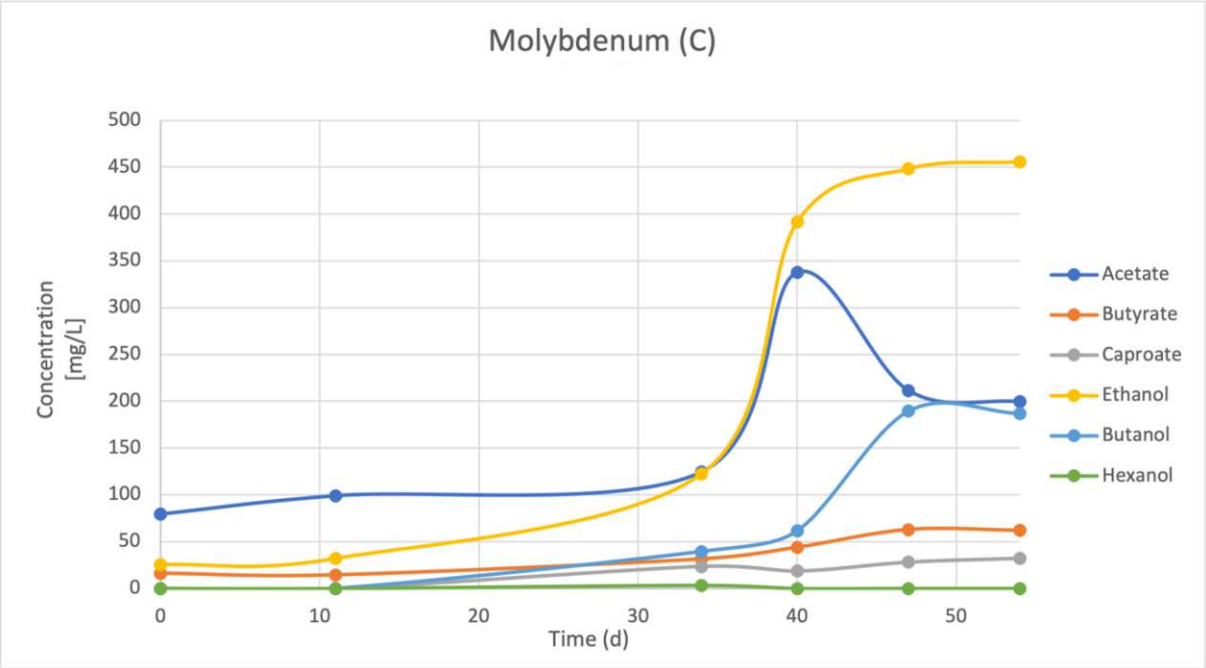

Figure 22: Concentration of acetate, butyrate, caproate, ethanol, butanol & hexanol in flasks with molybdenum & C. carboxidivorans over time

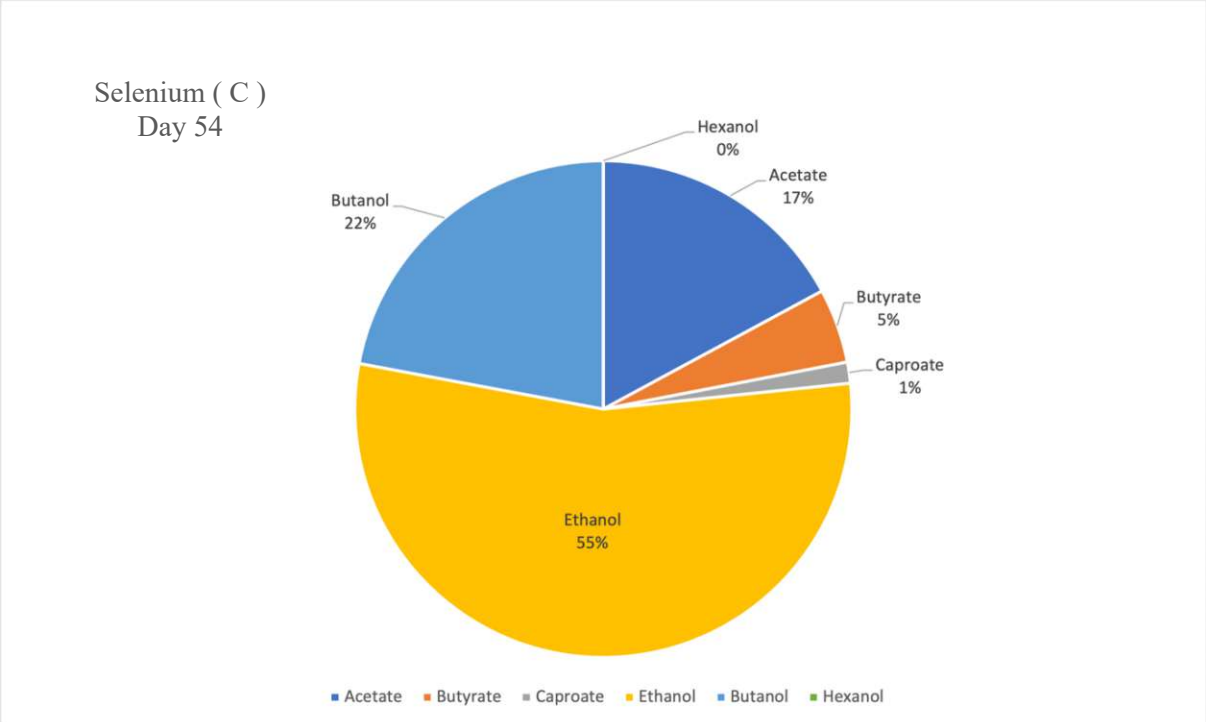

Figure 23: Ratio of main products including acetate, butyrate, caproate, ethanol, butanol & hexanol in flasks with selenium & C. carboxidivorans at end of experiment after 54 days

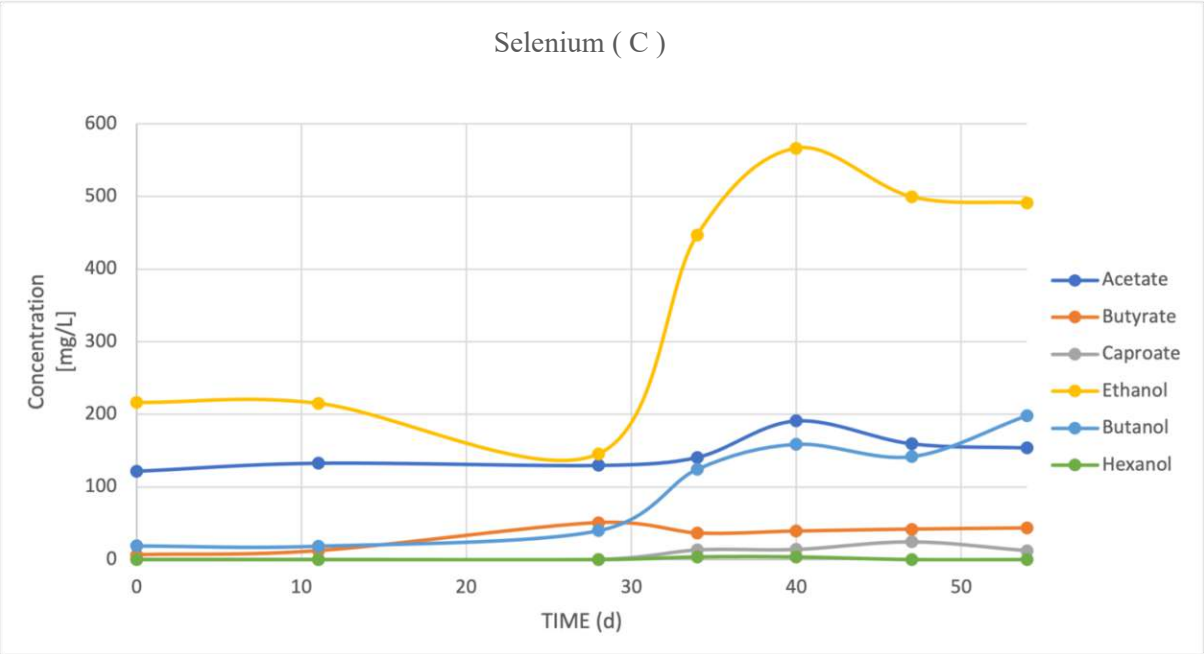

Figure 24: Concentration of acetate, butyrate, caproate, ethanol, butanol & hexanol in flasks with selenium & C. carboxidivorans over time

In the case of trials involving the combination of *C. carboxidivorans* and *M. sueciensis*, the alcohol production did not exhibit a substantial increase, as visualized in figure 25-28. However, it is noteworthy that chain elongation was notably more effective than in the control flasks, characterized by a higher concentration of butyrate and caproate, for which the *M. sueciensis* played a contributory role.

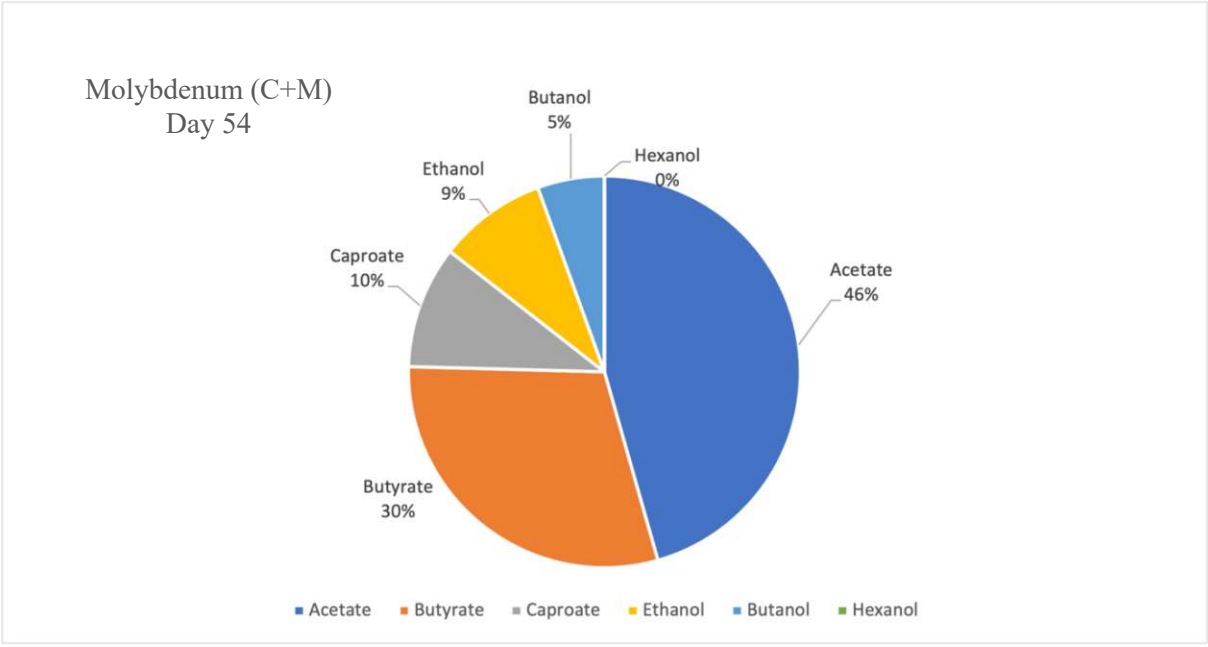

Figure 25: Ratio of main products including acetate, butyrate, caproate, ethanol, butanol & hexanol in flasks with molybdenum in combination with C. carboxidivorans & M. sueciensis at end of experiment after 54 days

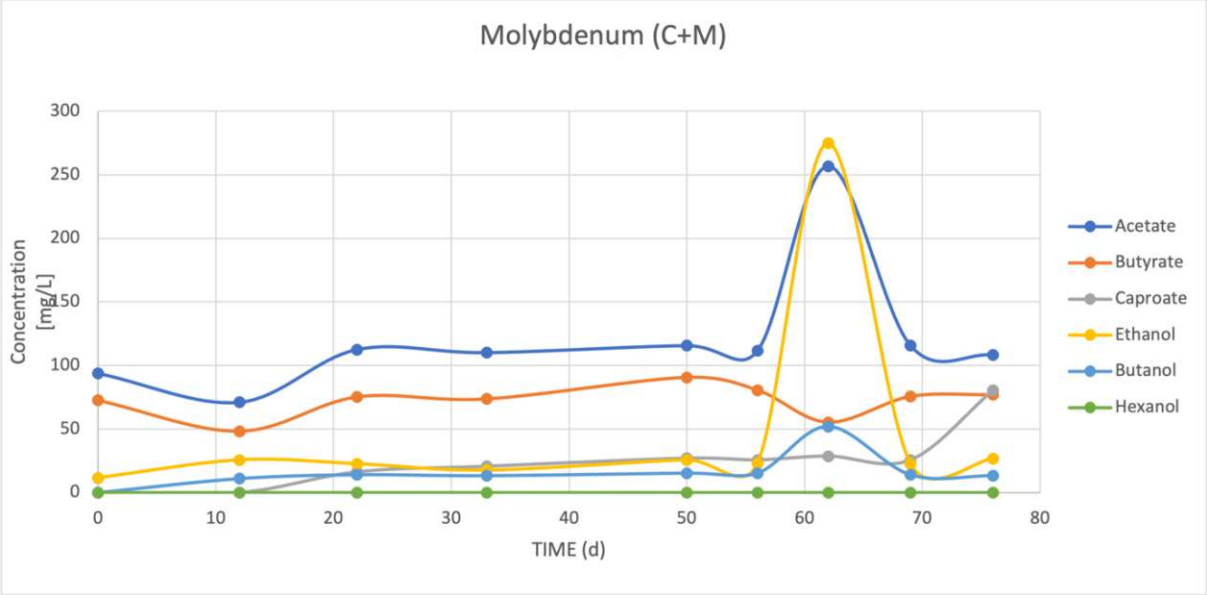

Figure 26: Concentration of acetate, butyrate, caproate, ethanol, butanol & hexanol in flasks with selenium in combination with C. carboxidivorans & M. sueciensis over time

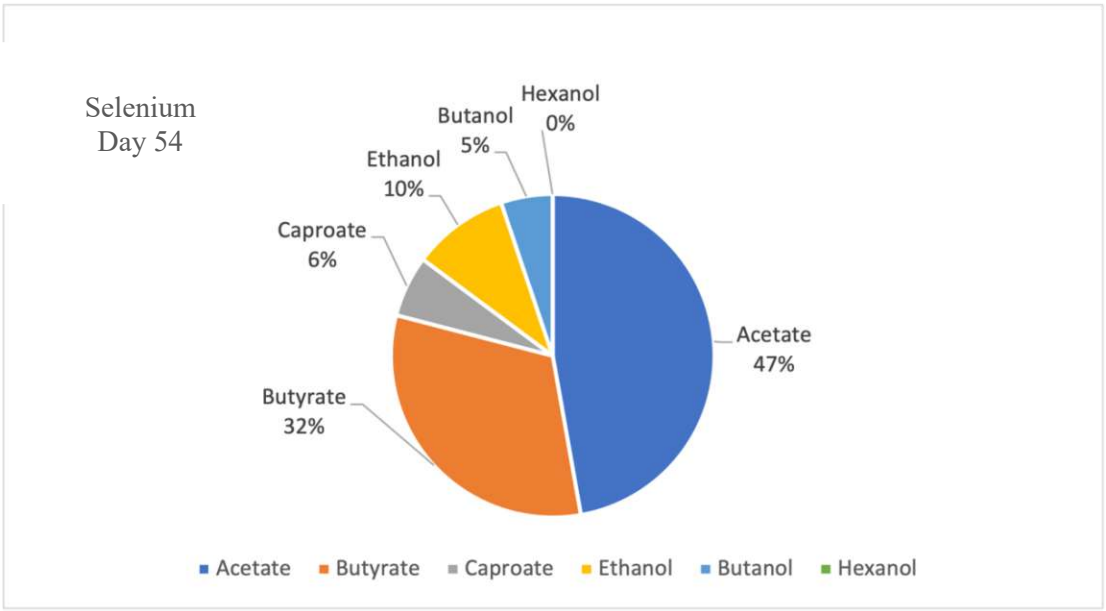

Figure 27 Ratio of main products including acetate, butyrate, caproate, ethanol, butanol & hexanol in flasks with selenium in combination with C. carboxidivorans & M. sueciensis at end of experiment after 54 days

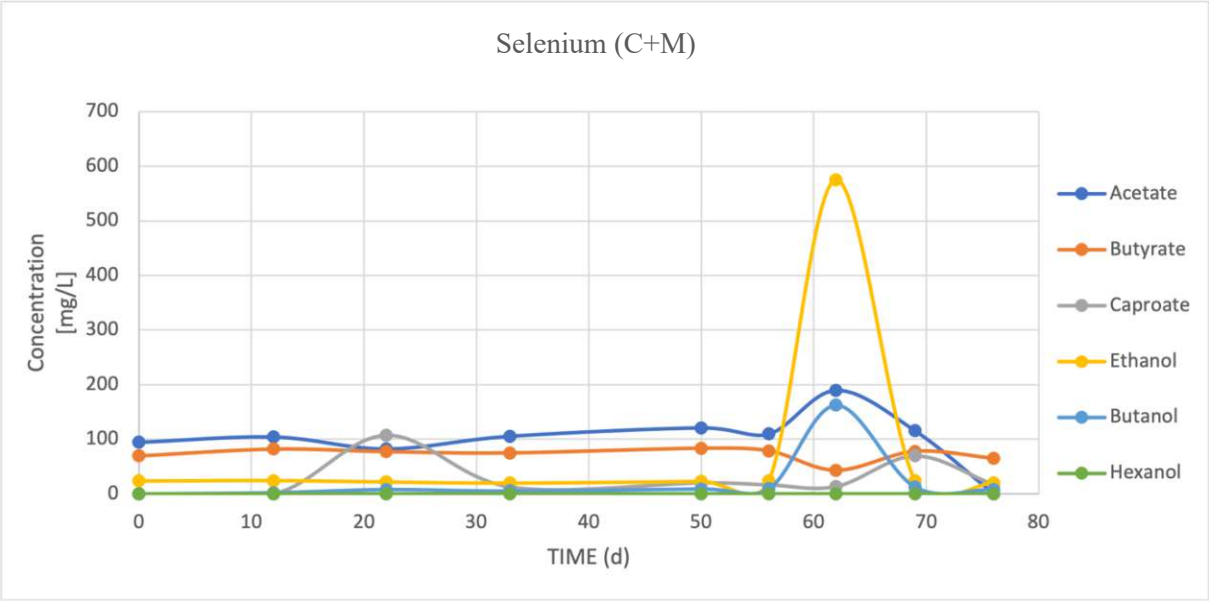

Figure 28: Ratio of main products including acetate, butyrate, caproate, ethanol, butanol & hexanol in flasks with selenium in combination with C. carboxidivorans & M. sueciensis over time

4.2 Lower pH trial

A further element that may have an impact on microbial activity and metabolic activities is the pH of the environment. In this experiment, the impact of a lower pH (pH 4.5) on *M. sueciensis* was investigated This is based on the assumption that the lower the pH, the higher the conductivity, as more hydronium ions are present in the solution.

A lower pH promotes the predominance of undissociated acetate species, thereby increasing its toxicity. This phenomenon is particularly relevant in the context of acetone-butanol-ethanol (ABE) fermentation, where a low pH facilitates the transition to the solventogenic phase. Similar observations have been reported in gas fermentation, suggesting the potential for enhanced alcohol production.

To establish a baseline for comparison, the control flask's pH was kept at 5.3.

The experimental setup for this experiment was described in 3.5.2.

The three flasks were arranged as follows:

Flask 1 & 2: pH 4.5

Flask 3: pH 5.3

The comparison between the initial and final stages of the experiment revealed minimal variation.

Figure 29 illustrates the initial ratios of the most important products of acetate, butyrate, caproate, ethanol, butanol and hexane of acetate, butyrate, caproate, ethanol, butanol, and hexane. In contrast, figure 30 depicts the final ratio of these substances, which have comparatively undergone minimal changes during this month.

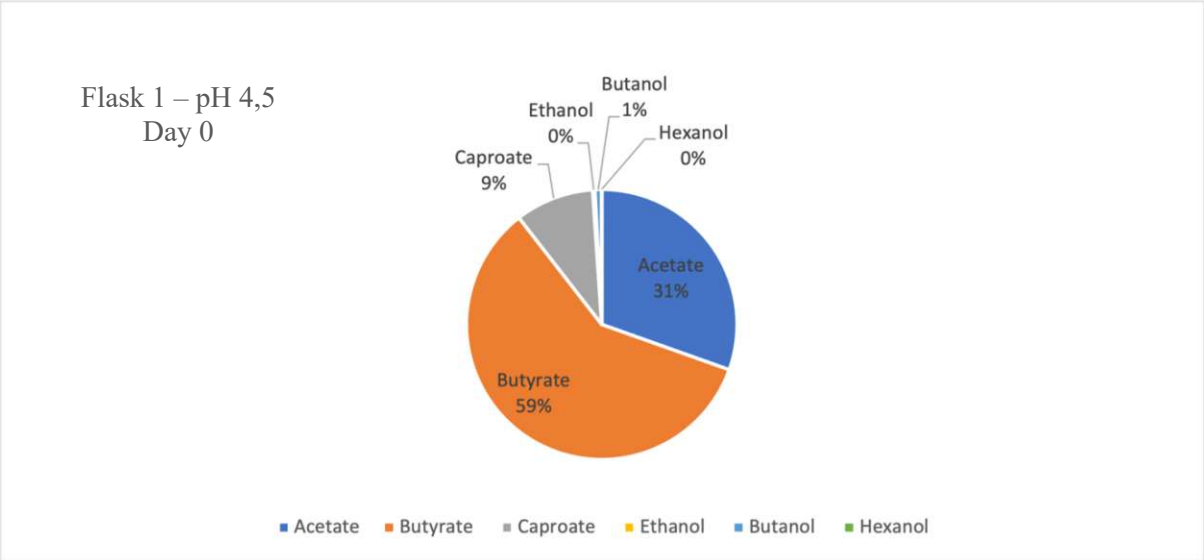

Figure 29: Ratio of main products including acetate, butyrate, caproate, ethanol, butanol & hexanol in flask 1 at beginning of experiment

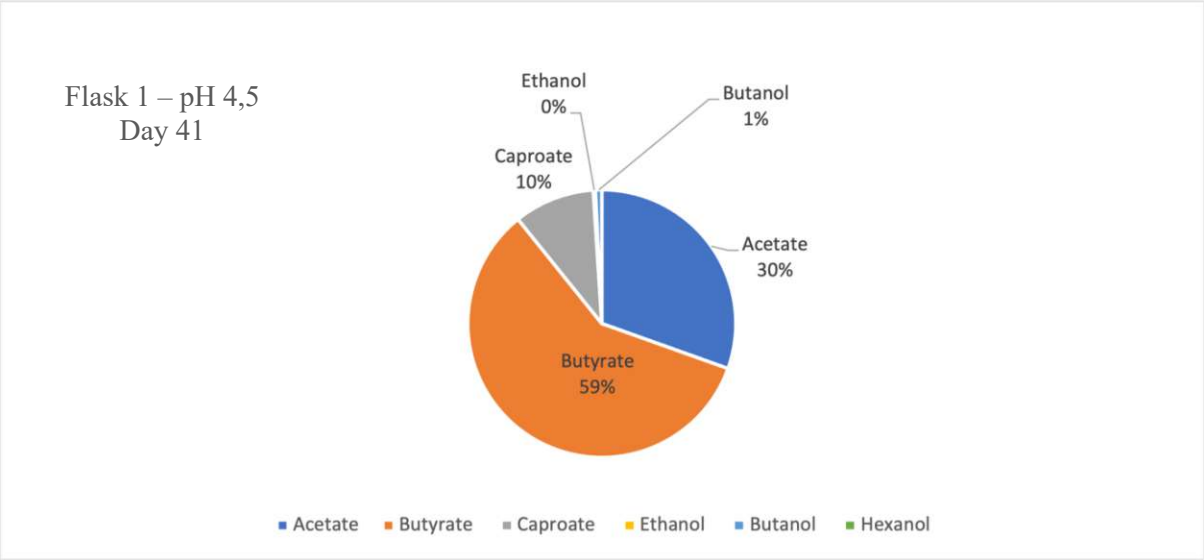

Figure 30: Ratio of main products including acetate, butyrate, caproate, ethanol, butanol & hexanol in flask 1 at end of experiment after 41 days

Figure 31 illustrates the concentration of acetate, butyrate, caproate, ethanol, butanol & hexanol in flask 1 over time.

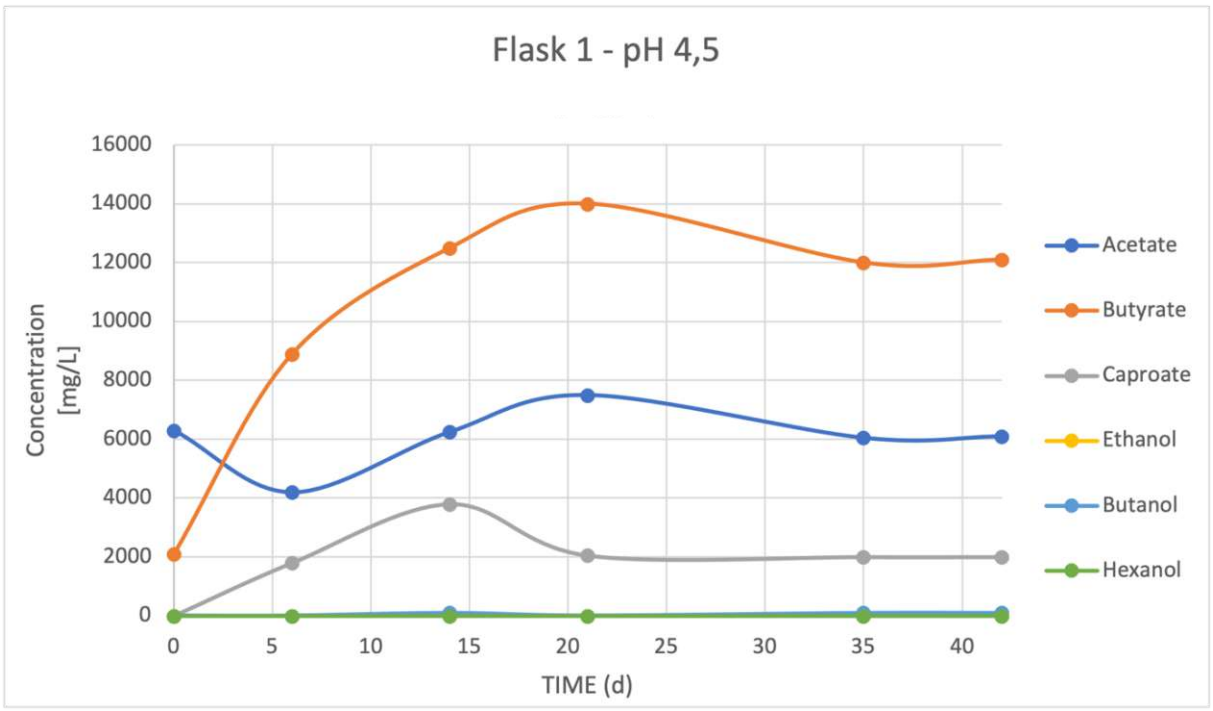

Figure 31: Concentration of acetate, butyrate, caproate, ethanol, butanol & hexanol in flask 1 over time

Flask 2 exhibits a similar trend when comparing both graphs in figure 32 and 33:

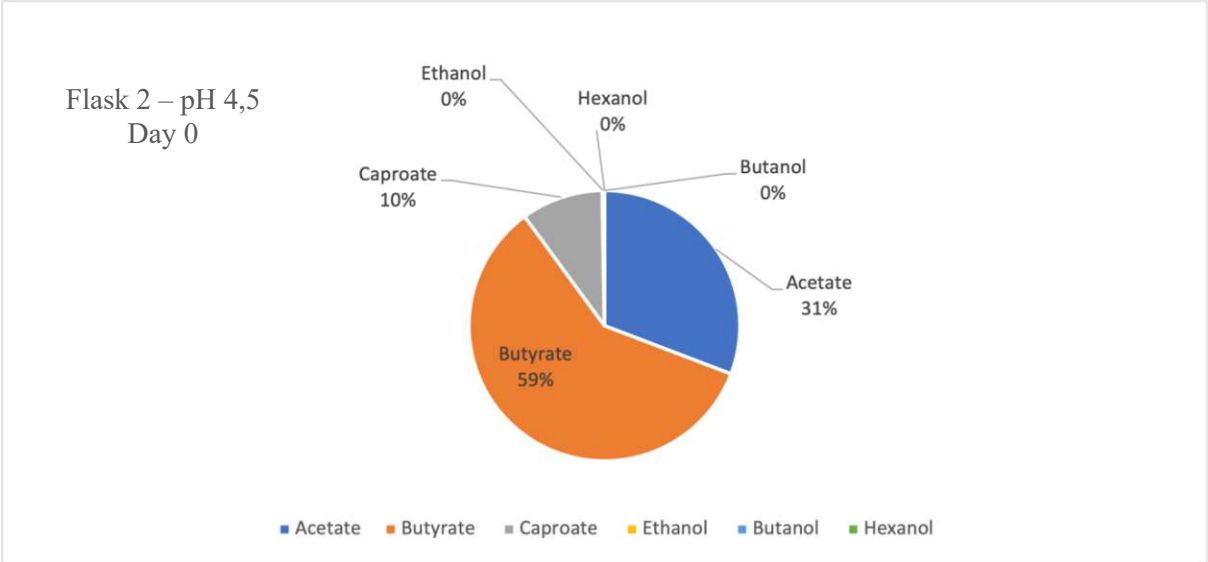

Figure 32: Ratio of main products including acetate, butyrate, caproate, ethanol, butanol & hexanol in flask 2 at beginning of experiment

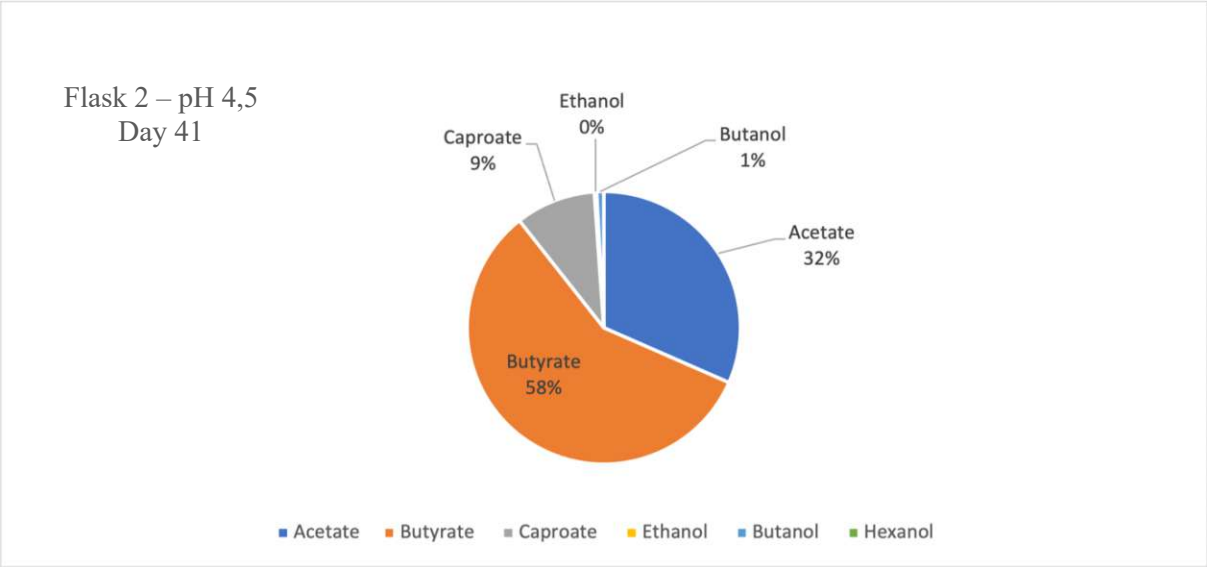

Figure 33: Ratio of main products including acetate, butyrate, caproate, ethanol, butanol & hexanol in flask 2 at end of experiment after 41 days

Figure 34 illustrates the concentration of acetate, butyrate, caproate, ethanol, butanol & hexanol in flask 2 over time.

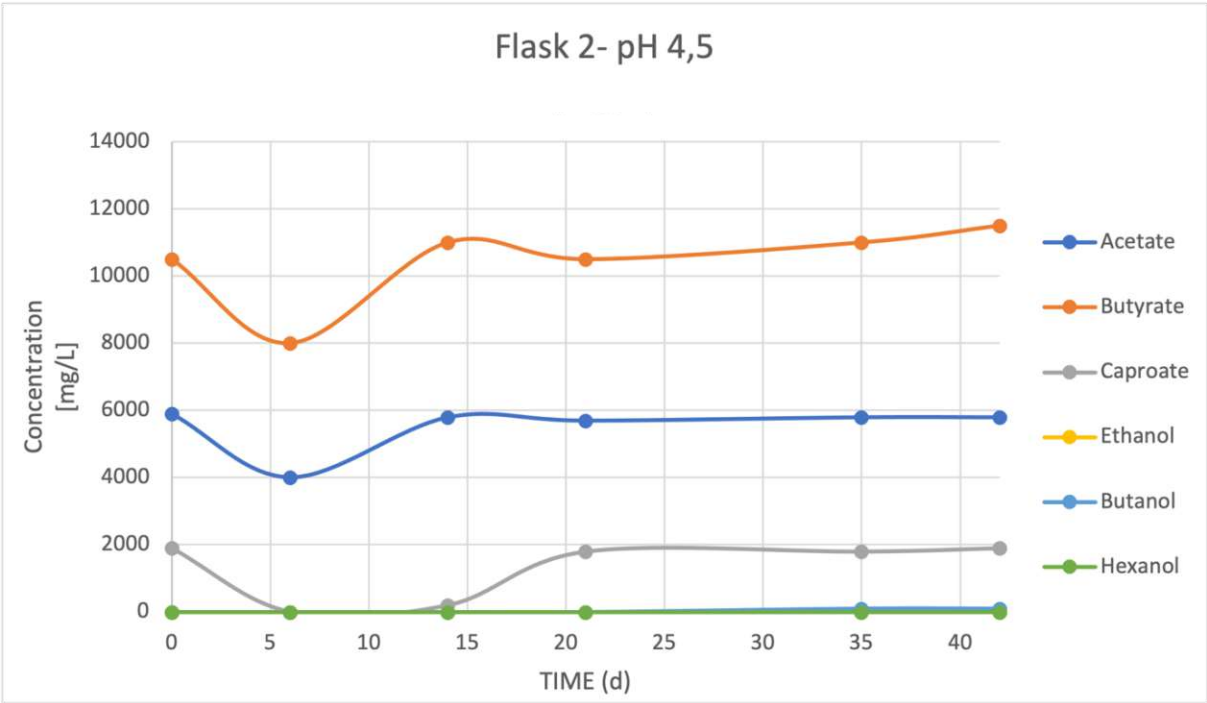

Figure 34: Concentration of acetate, butyrate, caproate, ethanol, butanol & hexanol in flask 2 over time

The intriguing aspect lies in comparing the values of flasks 1 and 2 with flask 3 (figure 35-37), which served as the control experiment. Comparatively, the values exhibit minimal variation, suggesting that the reduction of the pH to 4.5 had little impact.

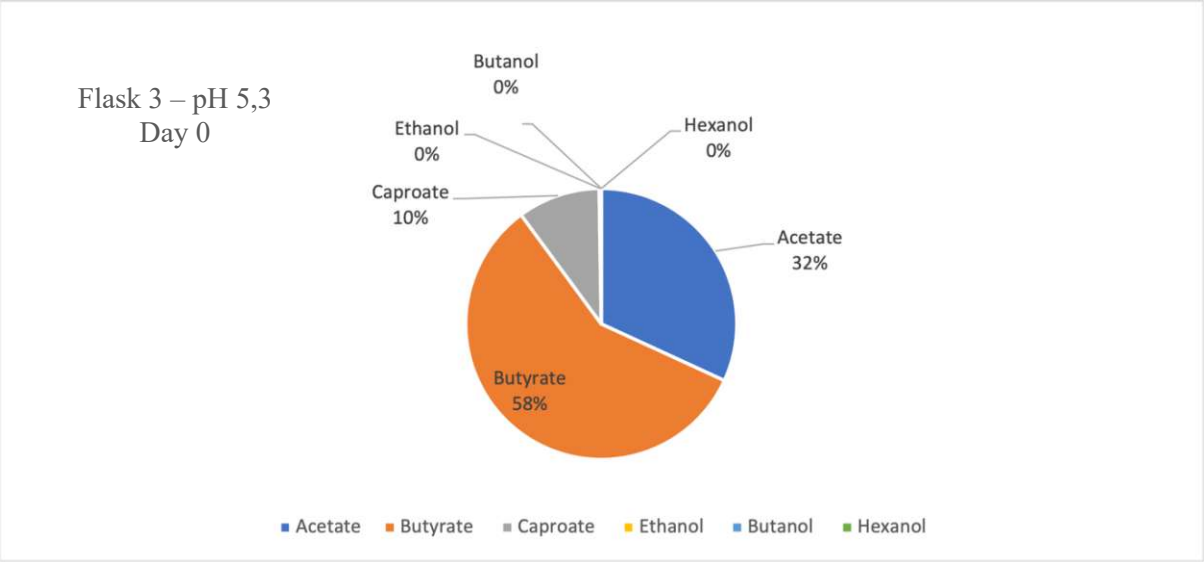

Figure 35: Ratio of main products including acetate, butyrate, caproate, ethanol, butanol & hexanol in flask 3 at beginning of experiment

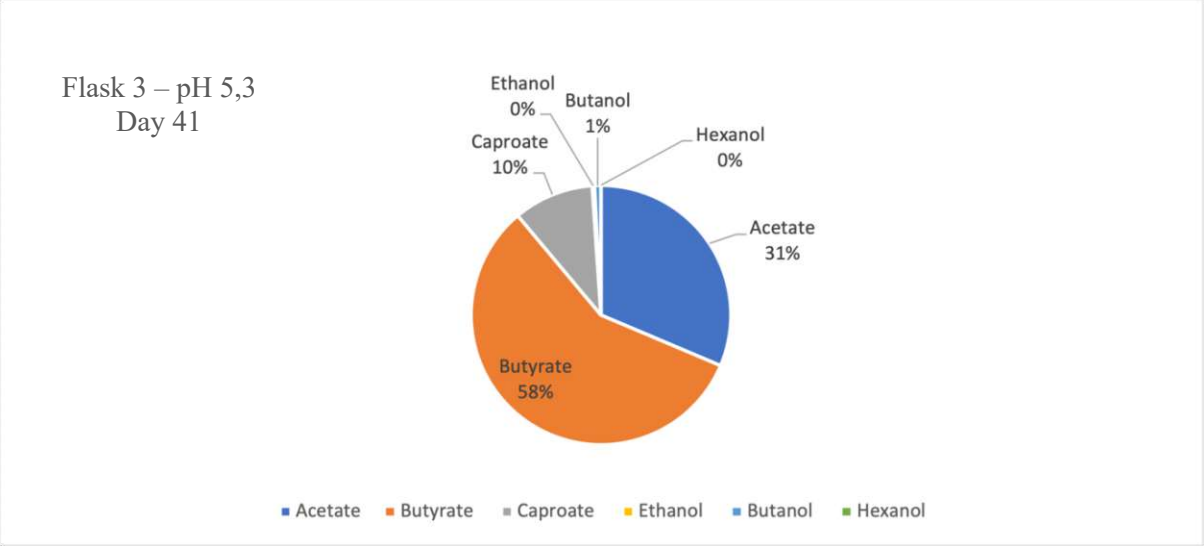

Figure 36: Ratio of main products including of acetate, butyrate, caproate, ethanol, butanol & hexanol in flask 3 at end of experiment after 41 days

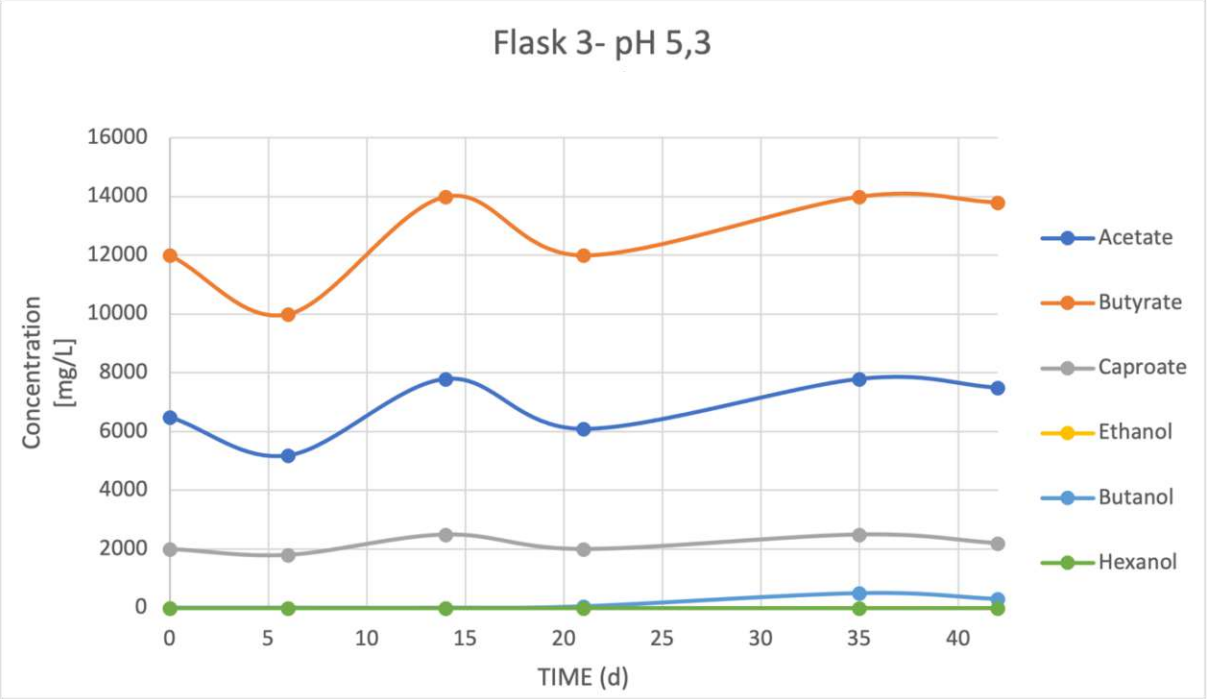

Figure 37: Concentration of acetate, butyrate, caproate, ethanol, butanol & hexanol in flask 3 over time

To further investigate, subsequent tests should explore pH levels lower than 4.5, as no perceptible distinctions were observed. This is particularly relevant as the thermodynamics of alcohol transformation are anticipated to be constrained below a pH of 4.5.

4.3 Salt trials

It was noticed that every time the pH in the trickle-bed reactor was adjusted using sodium hydroxide (NaOH), the electricity increased, which means an increase of the electrical conductivity due to the increase in salt concentration. This hinted to an increase in biofilm formation and better gas exchange.The assumption was that an increased salt concentration would result in higher currents and thus improved electron transfer. So, it was decided to investigate this more closely on a smaller scale.

The experimental design comprised three approaches, each involving three 30 mL flasks. The first set included three control flasks without an increased salt concentration. The second set involved three flasks with an end concentration of 220 mM NaCl added to the mixed culture. The third set comprised three flasks with 220 mM KCl and the last one involved three flasks with 220 mM NaCl/KCl mixture, aiming for a final concentration of 220 mM (equivalent chloride

ions from NaCl and KCl, summing up to 220 mM/L). This controlled experimentation aimed to assess the impact of salt concentrations on biofilm formation and associated electrical changes in a more confined setting.

Table 16: Overview of flasks set up

	Salt	Description
1	Control	(3x flasks) 110 mM mixed culture + medium (as described in table 12)
2	NaCl	(3x flasks) 110 mM mixed culture + 220mM NaCl in 30 mL
3	KCl	(3x flasks) 110 mM mixed culture + 220mM KCl in 30 mL
4	NaCl/KCl	(3x flasks) 110 mM mixed culture + 220mM NaCl/KCl in 30 mL

Figure 38 shows the Ratio of main products including acetate, butyrate, caproate, ethanol, butanol & hexanol control flask at beginning of experiment. In the control trial, conspicuous evidence of chain elongation is observed, indicated by a substantial increase in butyrate concentration, see figure 39 & 40. However, the alcohol production did not exhibit a significant elevation, reaching only 1%, see figure 39:

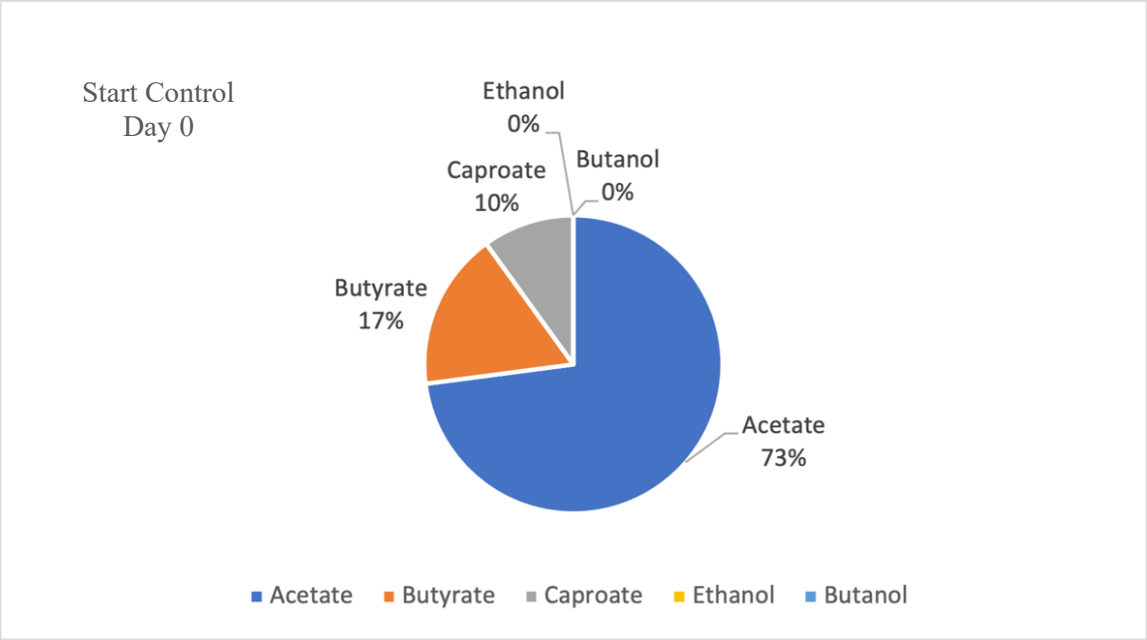

Figure 38: Ratio of main products including acetate, butyrate, caproate, ethanol, butanol & hexanol control flask at beginning of experiment

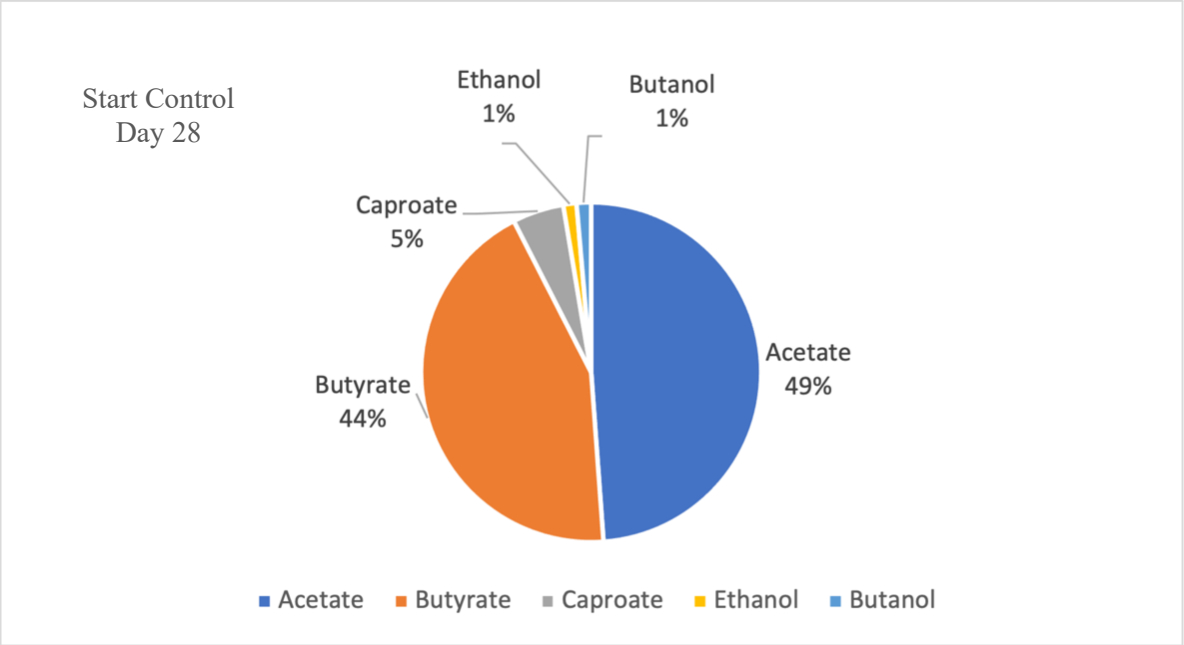

Figure 39: Ratio of main products including acetate, butyrate, caproate, ethanol, butanol & hexanol in control flask at end of experiment after 28 days

Figure 40 illustrates the concentration of actetate, caproate, ethanol, butanol & hexanol in control flask over time.

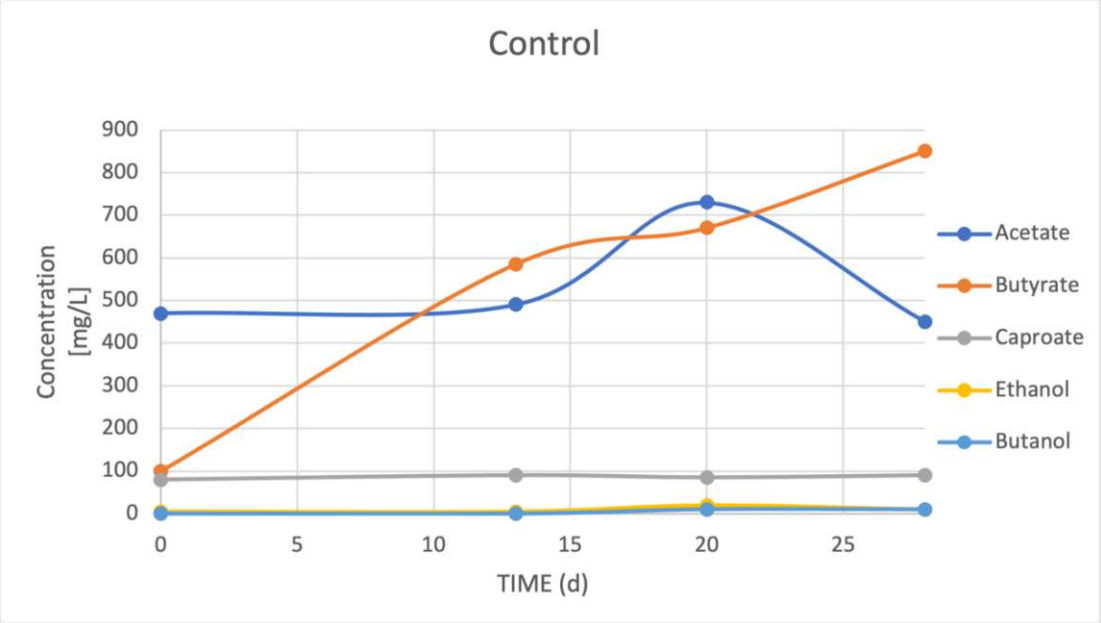

Figure 40: Concentration of acetate, butyrate, caproate, ethanol, butanol & hexanol in control flask over time

KCl trials

While chain elongation, was notably high in the control trial, the KCl trials demonstrated a substantial change in alcohol production, particularly with a 6% increase in ethanol production, as it is clearly visible in figure 41 & 42.

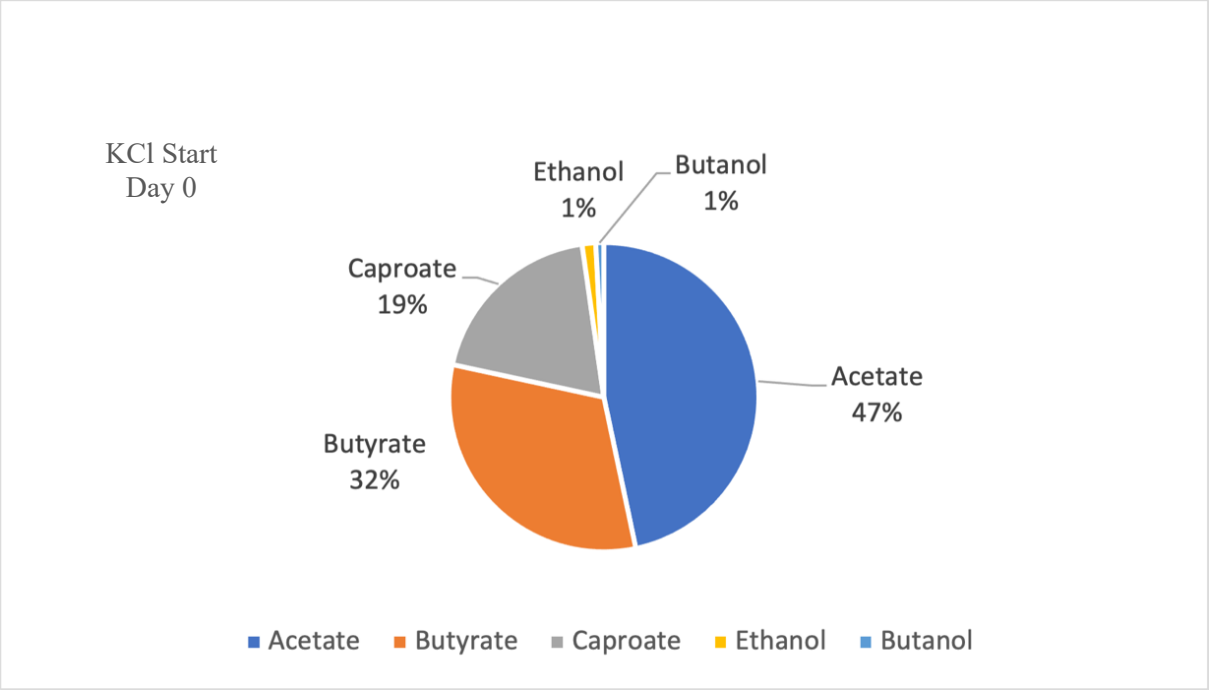

Figure 41: Ratio of main products including acetate, butyrate, caproate, ethanol, butanol & hexanol in KCl flasks at beginning of experiment

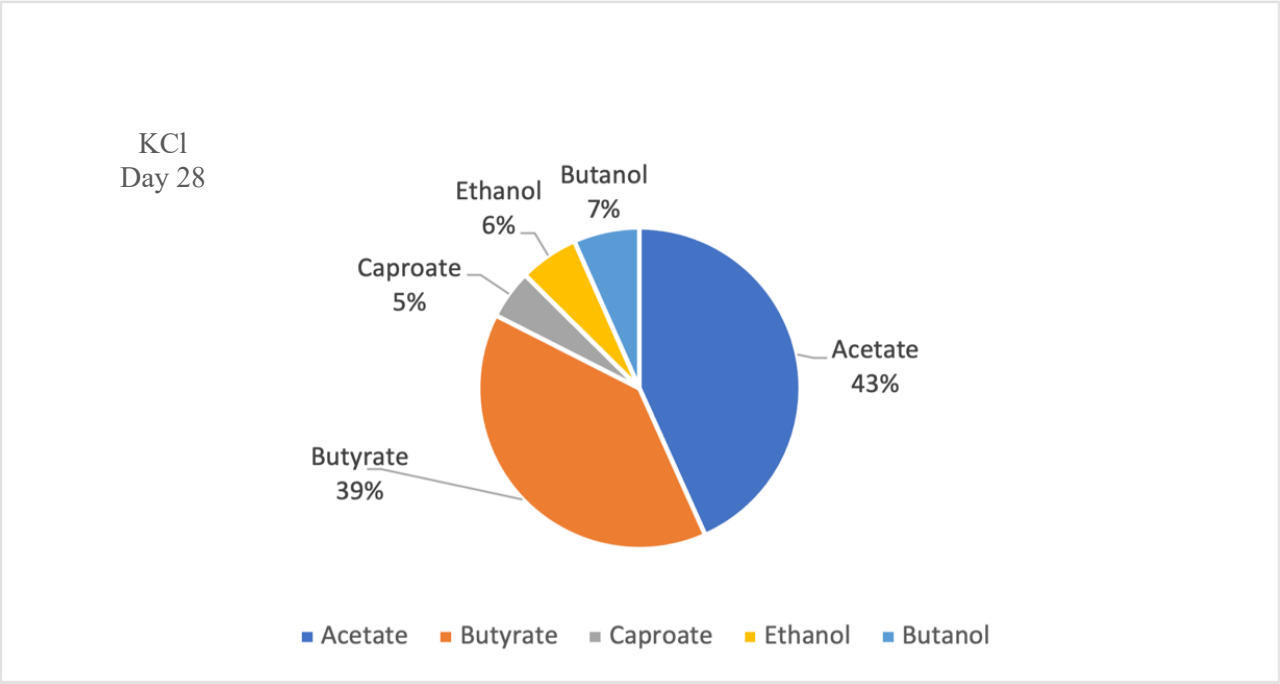

Figure 42: Ratio of main products including acetate, butyrate, caproate, ethanol, butanol & hexanol in KCl flask at end of experiment after 28 days

Figure 43 illustrates the concentration of acetate, butyrate, caproate, ethanol, butanol & hexanol in KCl flask over time.

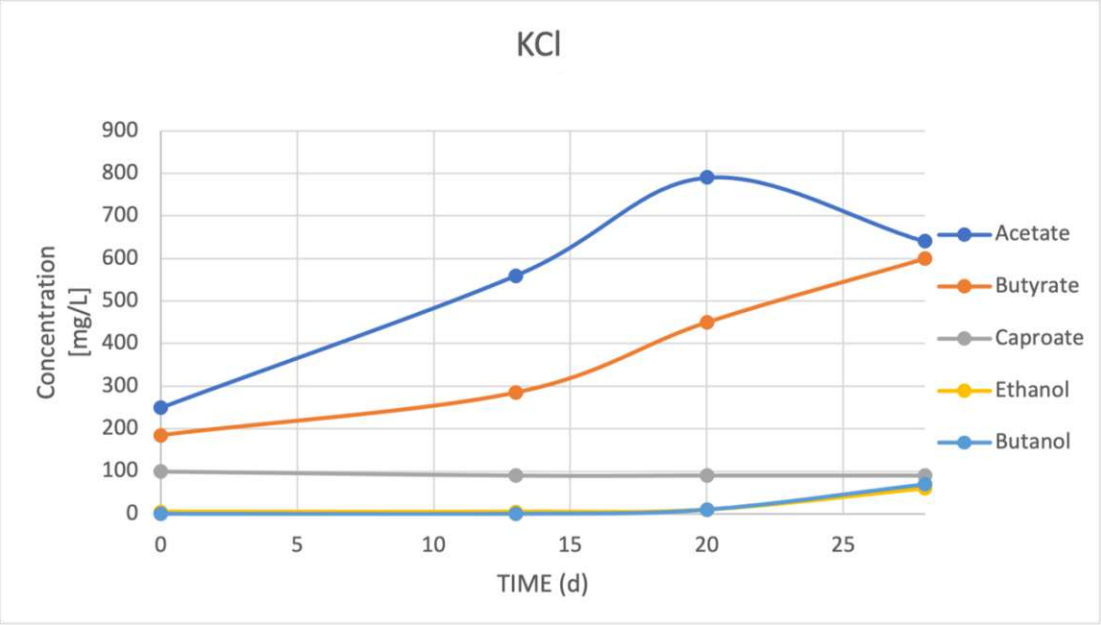

Figure 43: Concentration of acetate, butyrate, caproate, ethanol, butanol & hexanol in KCl flask over time

NaCl trials

The NaCl trials exhibited similarities to the control conditions, demonstrating enhanced chain elongation with comparable performance. However, alcohol production in the NaCl trials did not reach optimal levels, see figures 44-46.

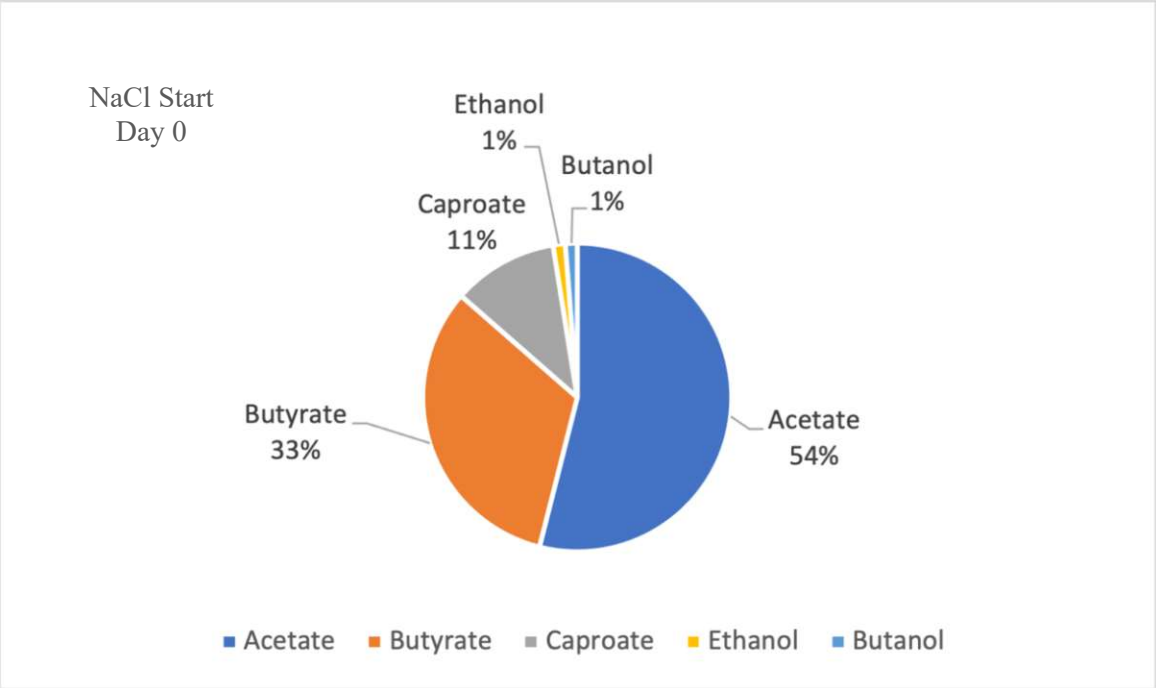

Figure 44: Ratio of main products including acetate, butyrate, caproate, ethanol, butanol & hexanol in NaCl flasks at beginning of experiment

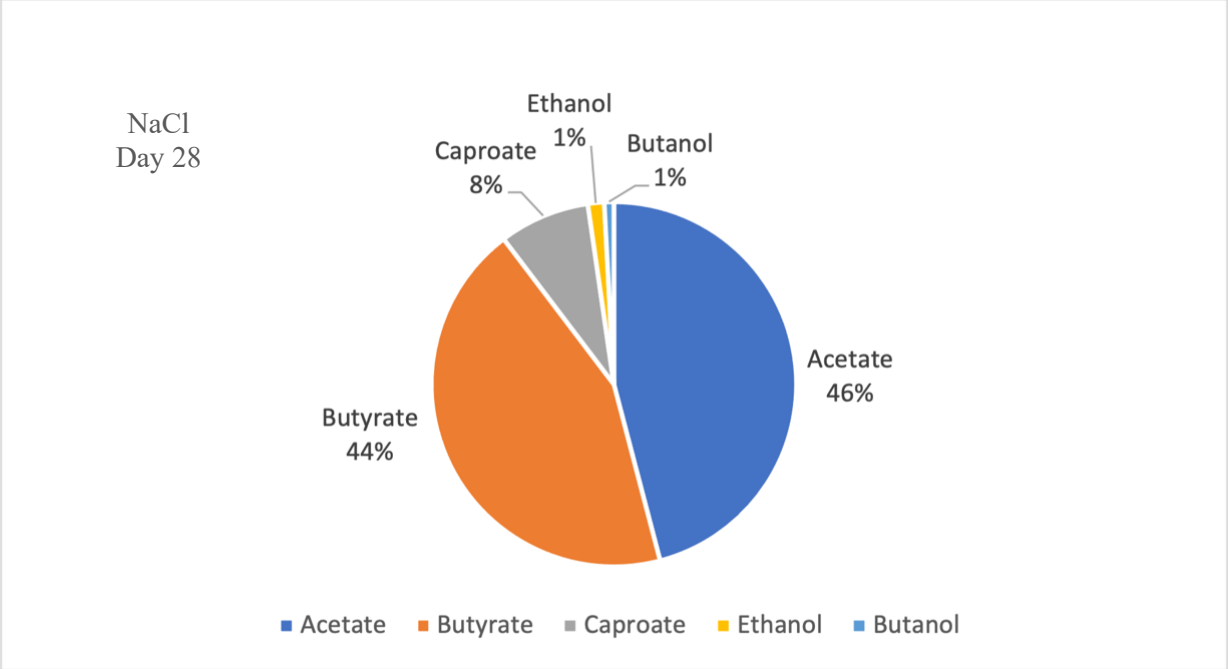

Figure 45: Ratio of main products including acetate, butyrate, caproate, ethanol, butanol & hexanol in NaCl flask at end of experiment after 28 days

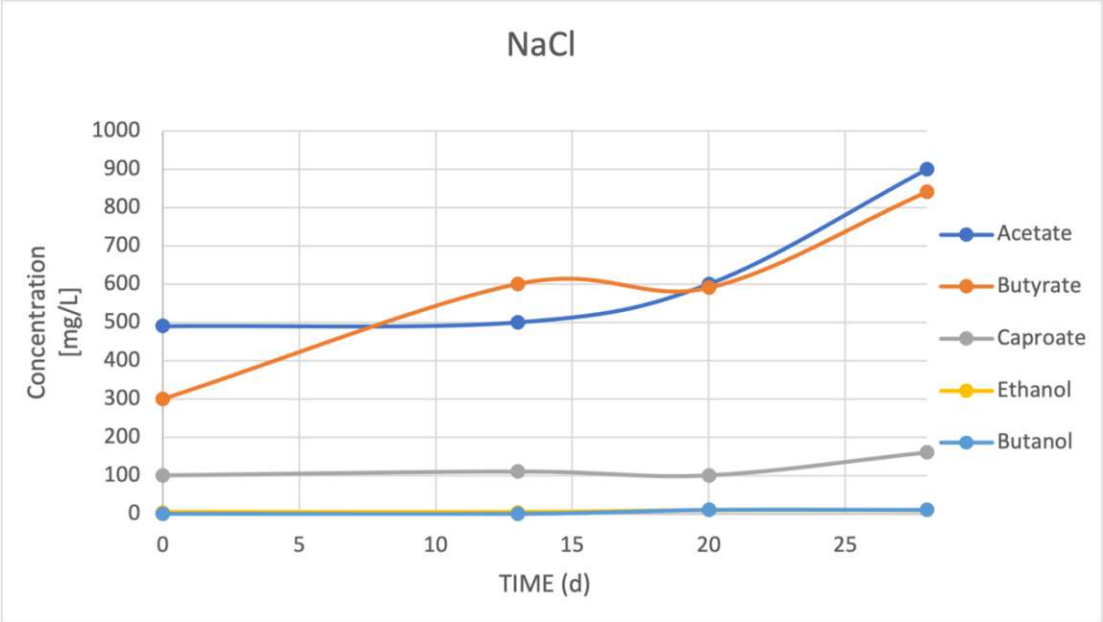

Figure 46: Concentration of acetate, butyrate, caproate, ethanol, butanol & hexanol in NaCl flask over time

NaCl/ KCl trials

In the trial involving a mixture of NaCl and KCl, chain elongation did not match the efficacy observed in the control trial. Additionally, there was noticeable alcohol production, reaching 4% ethanol production, exceeding the control, yet not reaching the levels achieved with KCl in isolation, see figures 47-49.

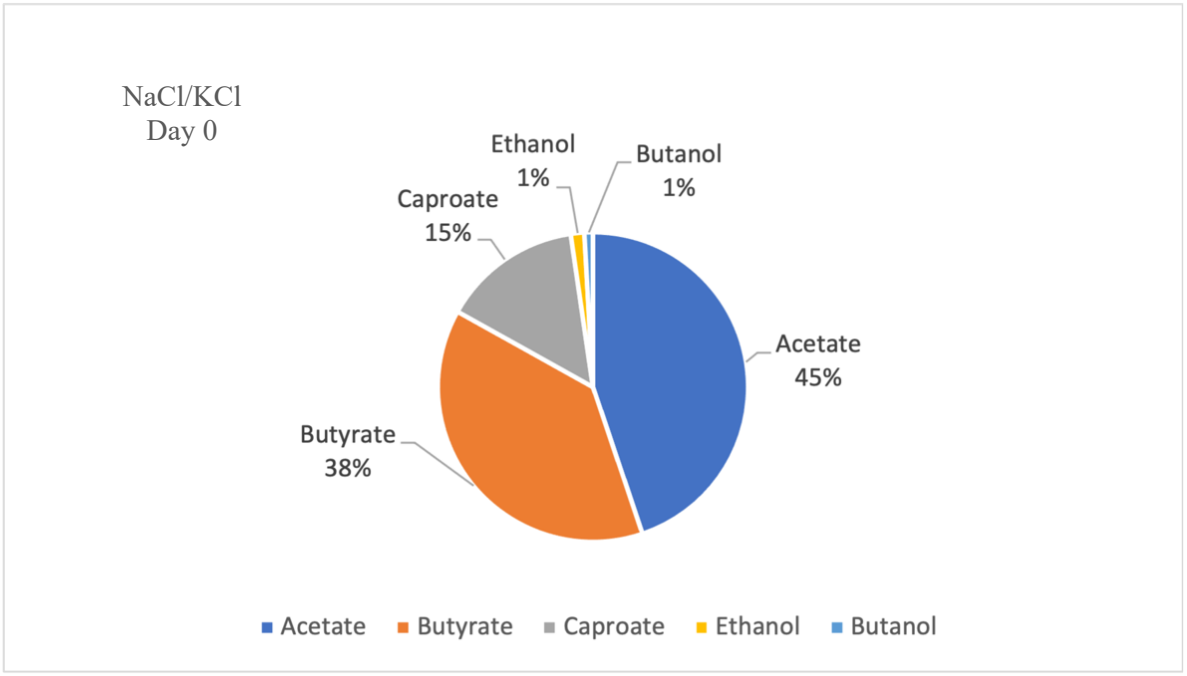

Figure 47: Ratio of main products including acetate, butyrate, caproate, ethanol, butanol & hexanol in NaCl/KCl flasks at beginning of experiment

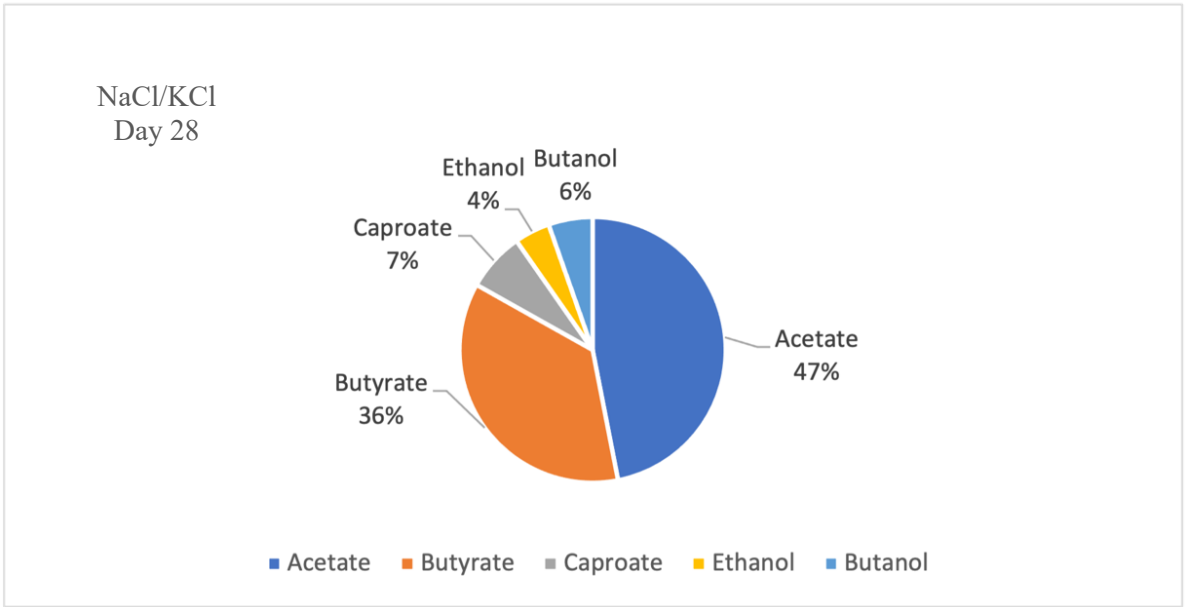

Figure 48: Ratio of main products including acetate, butyrate, caproate, ethanol, butanol & hexanol in NaCl/KCl flask at end of experiment after 28 days

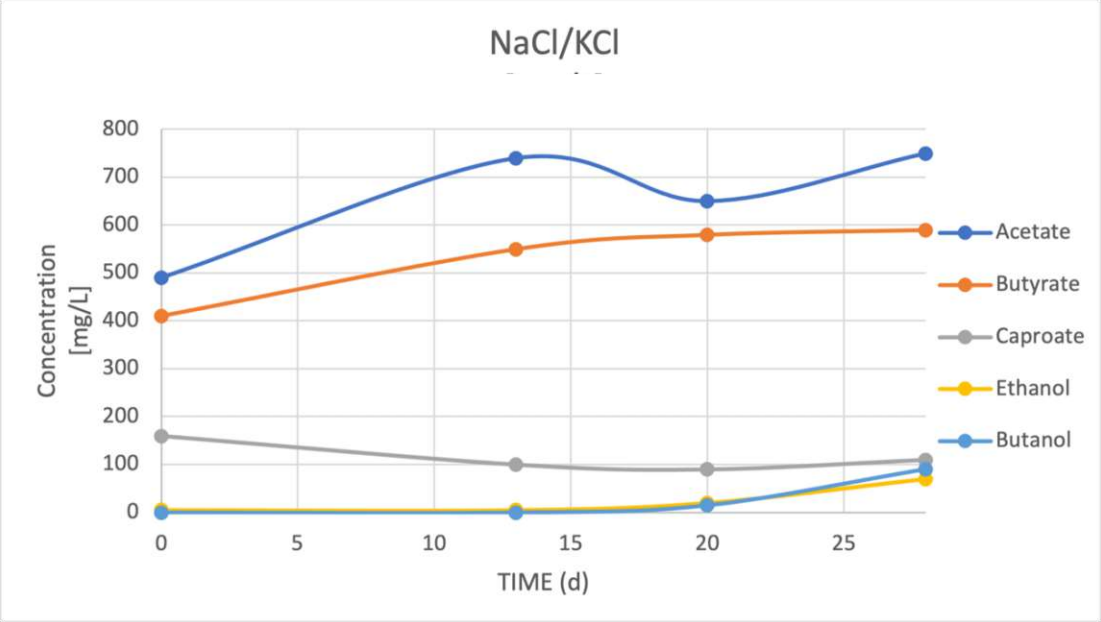

Figure 49: Concentration of acetate, butyrate, caproate, ethanol, butanol & hexanol in NaCl/KCl flask over time

Potential reasons for this discrepancy may include variations in microbial activity, substrate utilization preferences, or interactions between the chloride ions in the mixed salt solution. Further investigation is warranted to elucidate the underlying factors influencing these outcomes.

4.4 Trickle-bed reactor

This experiment aimed to optimize chain elongation and alcohol production in trickle-bed reactors. It was aimed to establish a continuous process. Batch experiments involving trace elements, pH reduction, and salt trials, as previously mentioned were conducted as preliminary trials to establish individual influences and optimal conditions.

Reactors FRI, FRII, and FRIII were initiated concurrently and representatives for syngas fermentation. In parallel, reactors Elena and Zorro were initiated to explore electro-fermentation, involving the application of an electric current.

In the context of the given experiment, reactors Elena and Zorro were specifically designed for electro-fermentation, where the application of electricity aimed to influence and potentially improve the outcomes of chain elongation and alcohol production when compared to traditional gas fermentation in reactors FRI, FRII, and FRIII In the Zorro setup, electrical current was applied for the first time. Before that, only conventional trickle bed reactors were in operation. Significant influence of electricity was observed, prompting validation through a subsequent trial employing a different growth/electrode material. In the Zorro configuration, polylactic acid with black carbon was used, while in the Elena setup, polyethylene with black carbon was used.

Here an overview of the setup of the reactors:

Table 17: Overview of trickle bed reactor set up

Reactor Name	Used Microorganisms	Electricity
FR I	• *M. sueciensis* & mixed culture • After 304 days: Addition of *C. ljungdahlii* to the reactor.	--
FR II	*M. sueciensis* & mixed culture	--
FR III	*M. sueciensis* & mixed culture + trace elements	--
Elena	MO from column FR I & 2	✓

Zorro	MO from column FR I & 2 + *M. sueciensis*	✓

Figures 50-52 illustrate the concentration of acetate, butyrate, caproate, ethanol, butanol & hexanol in trickle bed reactor FR1, FR2 & FR3 over time. In the reactors FR1 & FR3, the production of acetate, butyrate, and caproate exhibited a notable increase, indicating the successful occurrence of chain elongation. However, alcohol production remained low throughout most of the experiment.

In FR2, chain elongation was lower compared to FR1 and FR3. However, there is clear evidence that chain elongation is happening in this specific situation.

After 162 days, a medium swap was conducted to ensure the reproducibility of previously generated data. The old medium was suctioned and frozen, and 400 mL of new medium (Megasphaera medium, table 9) without acetate and cysteine was added. BES was dosed at 3.4 g for 400 mL, resulting in a concentration of 40 mM. Following this intervention, there was a noticeable improvement in chain elongation, although the data did not reach the initial levels, and the exact reason for this variance remains unclear.

As depicted in figures 50, 51, and 52, a discernible elevation in the concentrations of butyric acid and caproic acid is evident across all three columns (FR1, FR2, and FR3), encompassing diverse reactors with varying quantities. The production of ethanol and butanol remained nearly at 0 mg/L, except for in reactor FR2. Prior to the medium swap, a relatively high concentration of butanol was present in the medium, which subsequently returned to nearly 0 mg/L following the medium swap. The underlying cause for this phenomenon remains unclear.

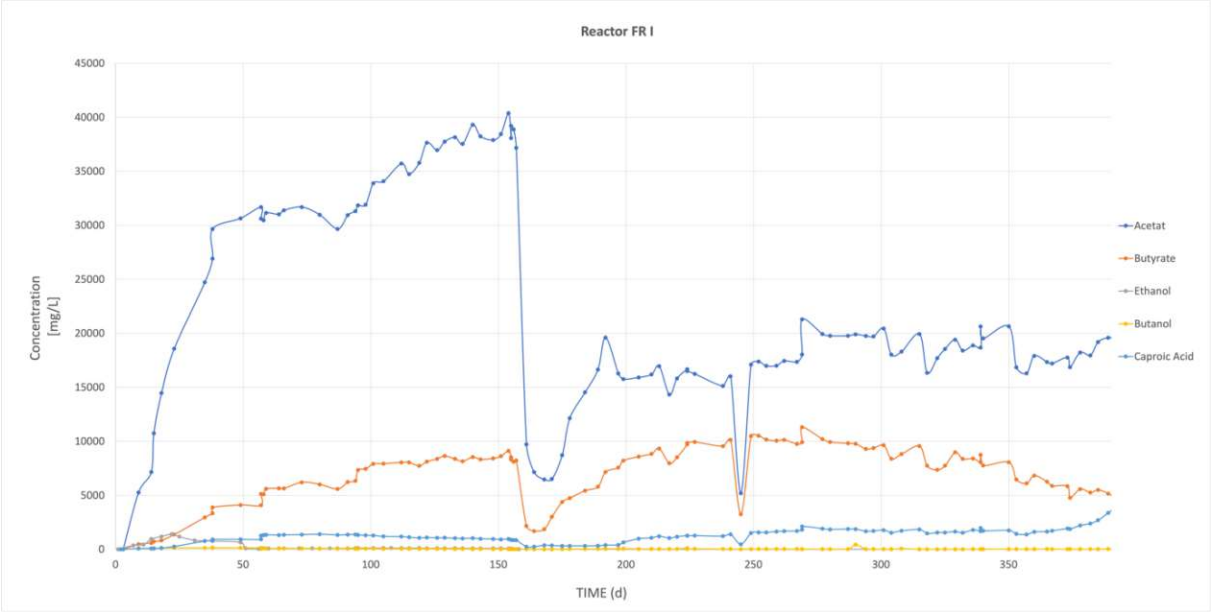

Figure 50: Concentration of acetate, butyrate, caproate, ethanol, butanol & hexanol in trickle bed reactor FR1 over time

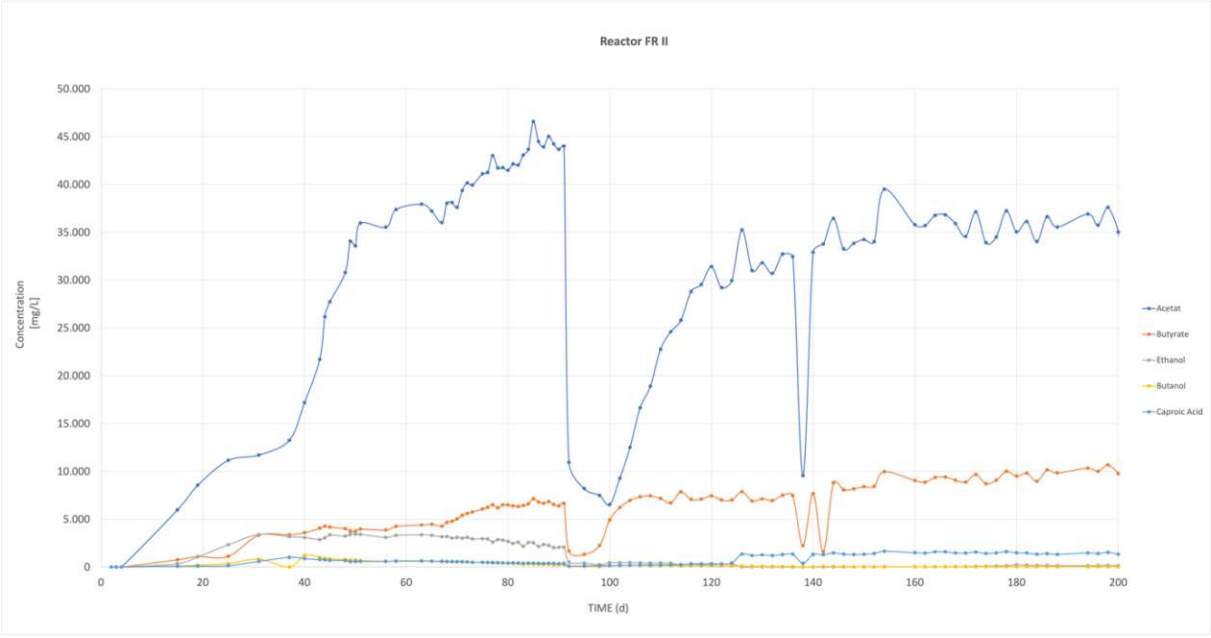

Figure 51: Concentration of acetate, butyrate, caproate, ethanol, butanol & hexanol in trickle bed reactor FR2 over time

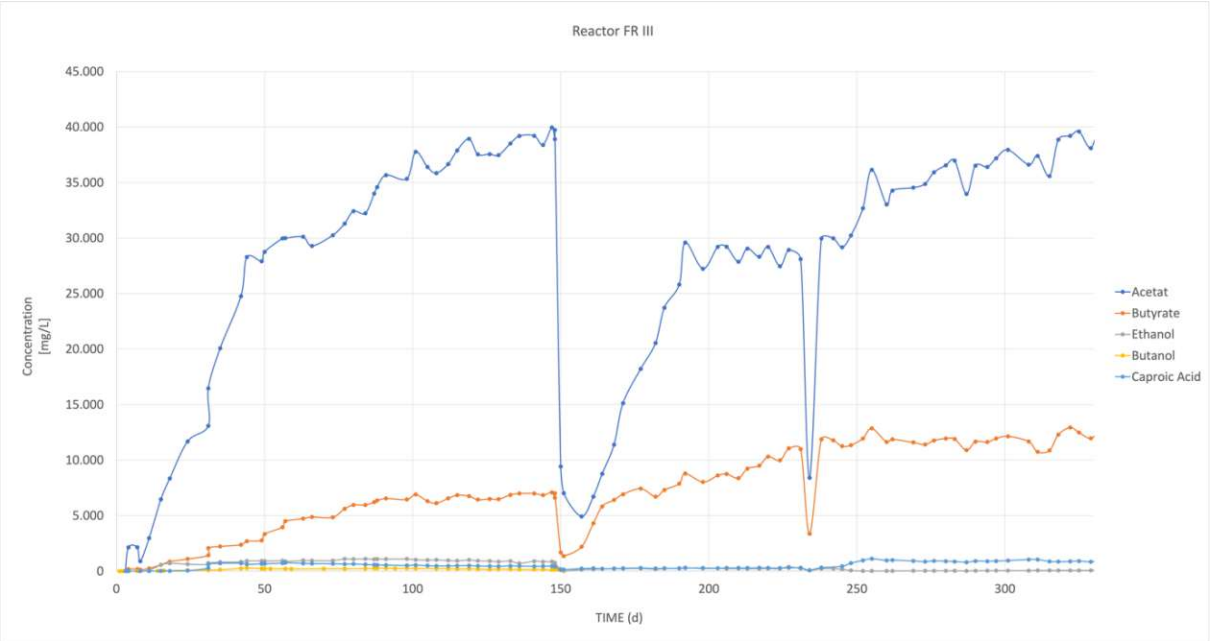

Figure 52: Concentration of acetate, butyrate, caproate, ethanol, butanol & hexanol in trickle bed reactor FR3 over time

Zorro & Elena reactors

Regarding the Zorro reactor, the chain elongation, leading to high concentrations of caproate and butyrate, is notably evident, especially up to day 80 (see figure 53). It is noticeable that electricity had a positive influence on chain elongation. The highest concentrations observed until day 80 of caproate is 2 g/L and of butyrate was 15 g/L. Alcohol production was also noticeable, reaching a peak concentration of 403 mg/mL of butanol by this date (see figure 53).

After 80 days, Zorro also underwent a medium swap, indicated by the downturn in the graphs of individual products. Subsequently, the acetate content increased sharply, and chain elongation could be identified by the rising concentrations of caproate and butyrate. However, the concentrations were not as high as before the medium swap. It was observed that no biofilm formed, and the reason for this remains unclear.

The electrical conductivity is depicted in figure 54. In general, the graph shows that after 80 days, the electrical conductivity decreased, and the initial value was no longer reproducible. This is most likely associated with the inability to form a biofilm, leading to a decrease in conductivity.

Figure 53: Concentration of acetate, butyrate, caproate, ethanol, butanol & hexanol in trickle bed reactor Zorro over time

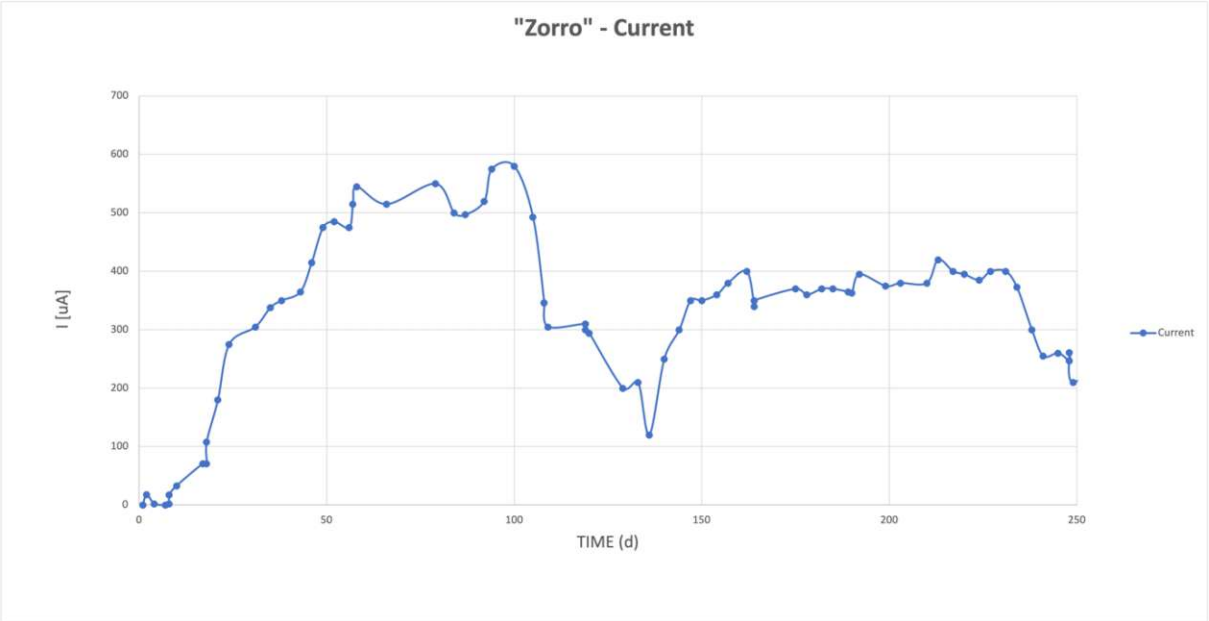

Figure 54: Electrical conductivity of Zorro reactor over time

Figure 55 illustrates the pH change of Zorro over time:

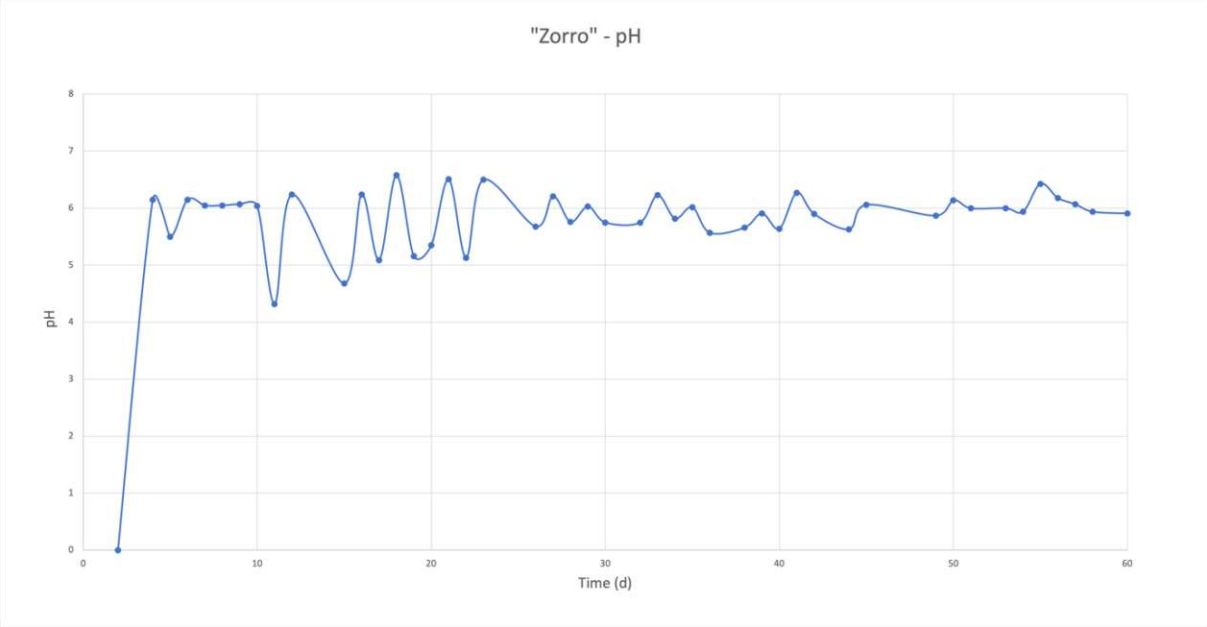

Figure 55: pH of Zorro over time

Elena served as a control experiment compared to Zorro. The modification of the cathode aimed to promote biofilm formation. After 66 days, a medium swap was conducted, incorporating trace elements Ni, Se, and W (Wolin's Mineral Solution) to assess potential improvements (see figure 56). However, the addition of trace elements did not induce significant changes.

Similar to Zorro, the acetate concentration increased after the medium swap, while butyrate exhibited a post-swap elevation as observed previously. The caproate concentration reached its highest value of 2 g/L before the medium swap, and although it increased post-swap, it did not return to the initial value, suggesting that more time might be needed. Nevertheless, successful chain elongation is noticeable, and alcohol production, with a peak butanol concentration of 2 g/L, was achieved.

After 95 days, the gassing composition was changed from H_2/CO_2 to $H_2/CO_2/CO$. The rationale behind this alteration was the potential positive impact of CO on alcohol production and chain elongation. From this date, a slight increase in caproate and butanol concentrations is discernible (see figure 56). However, a more extended observation of the CO's effects would be necessary for more accurate and comprehensive results.

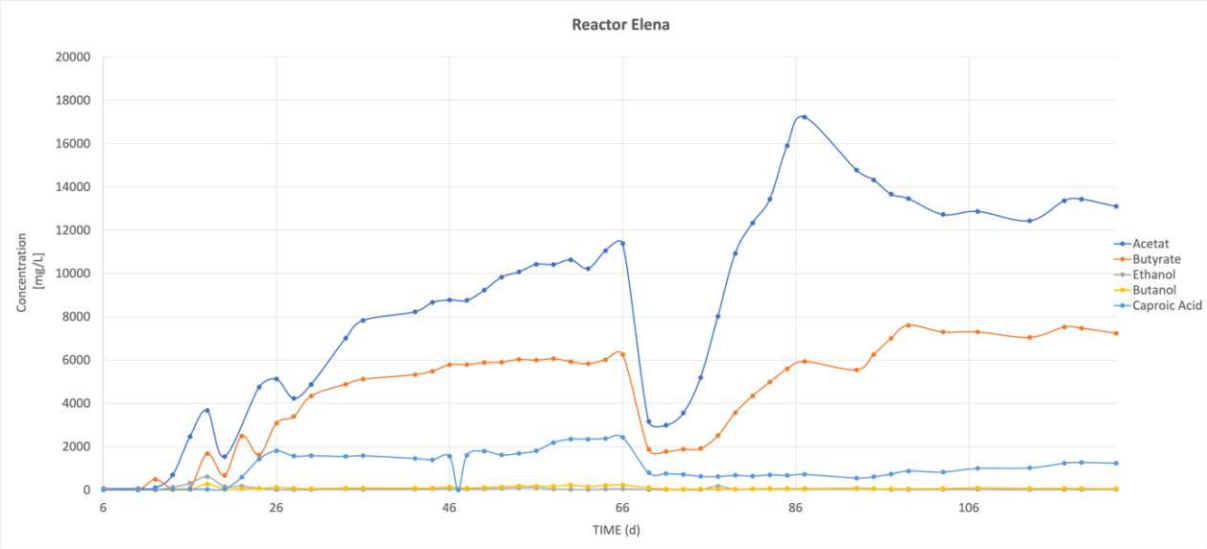

Figure 56: Concentration of acetate, butyrate, caproate, ethanol, butanol & hexanol in trickle bed reactor "Elena" over time

In comparison to Zorro, biofilm formation in Elena was more obvious (figure 57). This observation is also evident in graph 58, where the electrical conductivity increased with the development of the biofilm. The abrupt decline in electrical conductivity (figure 58) is attributed to the change in gassing mentioned above.

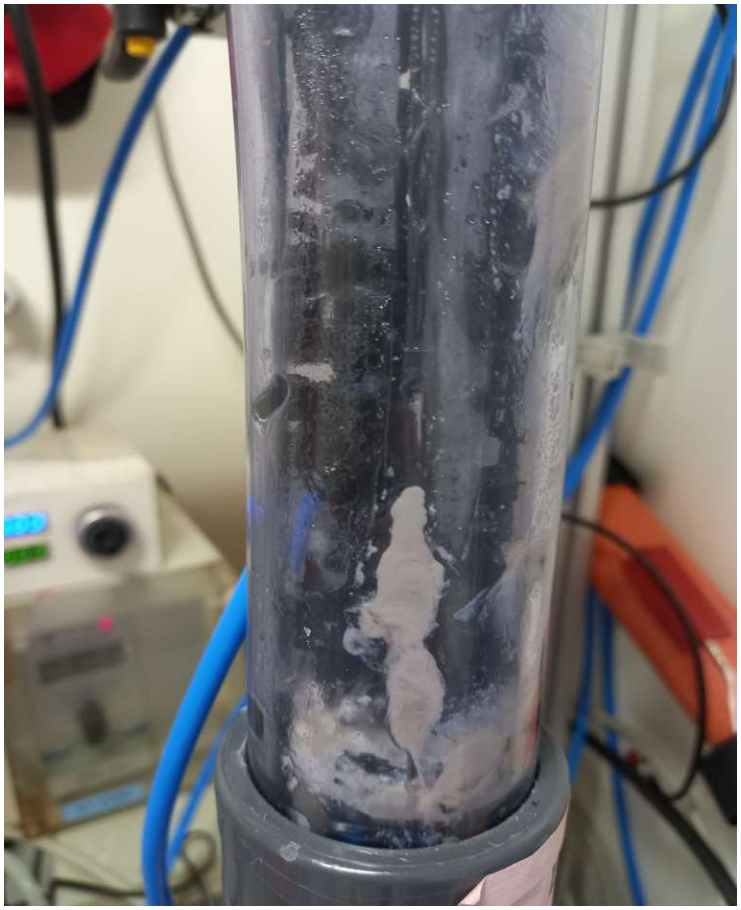

Figure 57: Biofilm formation in Elena reactor

Figure 58 illustrates the electrical conductivity of Elena over time.

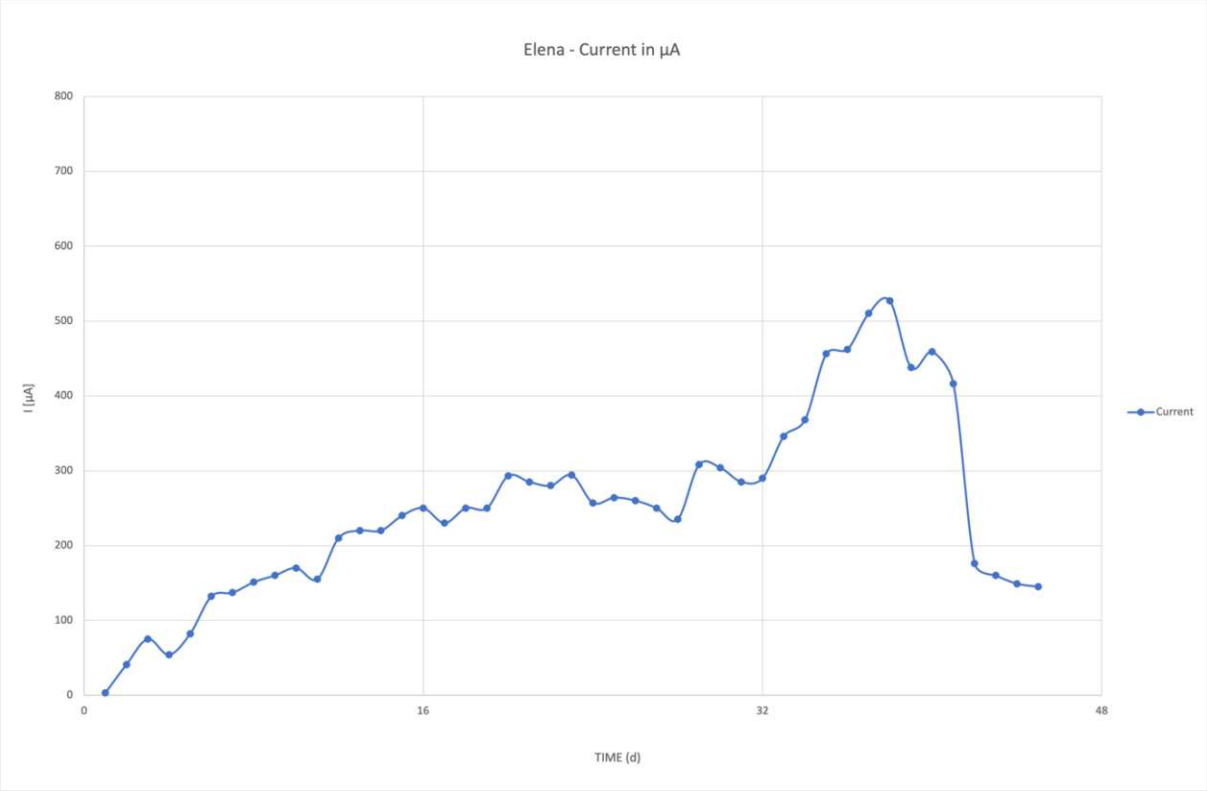

Figure 58: Electrical conductivity of Elena reactor over time

Figure 59 illustrates the pH change of Elena over time:

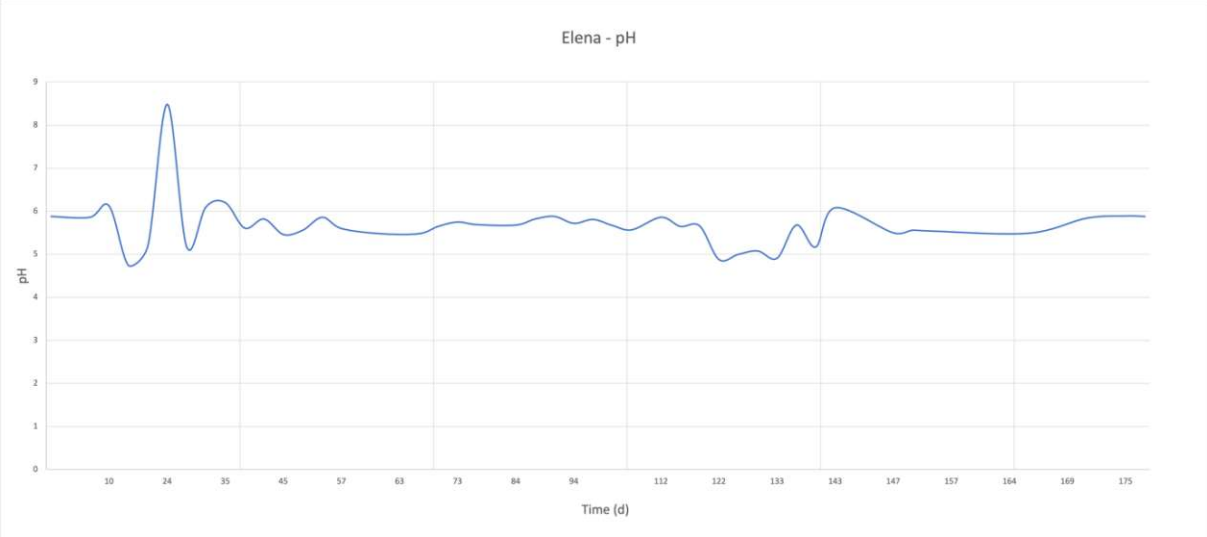

Figure 59: pH of "Elena" over time

5 Discussion

5.1 Flask trials

Trace element – trials

The impact of trace elements on the production of alcohol and chain elongation is a crucial aspect of anaerobic gas fermentation, as highlighted by various studies (Nimbalkar et al., 2018) (Marcel et al., 2022). Trace elements, such as iron, selenium, cobalt, nickel, molybdenum, zinc, and manganese, play essential roles in bacterial metabolism and enzymatic processes. While their specific influence on chain elongation and alcohol synthesis in anaerobic fermentation remains relatively understudied, various research suggests that they likely affect these processes by modulating enzyme activity and metabolic pathways.

In the article Role of Trace Elements as Cofactor: An Efficient Strategy toward Enhanced Biobutanol Production , Nimbalkar et al., (2018) highlight the significant positive impact of trace elements on butanol production and chain elongation. Addition of nickel chloride (100 mg/L) and sodium selenite (1 mg/L) resulted in an increase in total solvent and butanol concentrations, with nickel chloride and sodium selenite achieving the highest total solvent production of 16.13 g/L and butanol concentration of 10.81 g/L, compared to 7.88 g/L total solvent production and 5.34 of butanol production without additional trace elemnts. This means that adding nickel chloride and sodium selenite doubled the amount of butanol produced compared to when these elements were not added. This indicates that the addition of specific trace elements can improve the efficiency of the fermentation process by boosting both the concentration of desired alcohols and the overall yield.

In our experiment, the focus was on investigating the effects of selenium (Se) and molybdenum (Mo) as trace elements. The results showed significant differences in ethanol production, particularly notable when comparing molybdenum and selenium. Ethanol production increased by approximately 2.6 times (maximum achieved concentration was about 0,6 g/L) when selenium was used as the trace element, compared to the control flask. Similarly, there was a noticeable increase in butanol production in trials including selenium and molybdenum, 2.5 times that of the control flask with a concentration of 0,1 g/L.

Moreover, while the combination *of C. carboxidivorans* and *M. sueciensis* did not lead to a substantial increase in alcohol production, it notably enhanced chain elongation, as evidenced by higher concentrations of butyrate and caproate compared to the control flasks.

Overall, these findings demonstrate the positive impact of trace elements, particularly selenium and molybdenum, on alcohol production and chain elongation in anaerobic gas fermentation. Future research should focus on exploring the specific pathways and enzymatic reactions influenced by trace elements, as well as investigating additional trace element combinations to maximize their potential in industrial applications.

Lower pH

Recent research indicates that the pH of fermentation environments significantly influences the process of chain elongation and the production of alcohols in mixed microbial cultures. In some scientific research, the impact of fermentation pH on the production of higher alcohols using mixed cultures was investigated (Ganigué et al., 2016). The study reveals that a lower fermentation pH, particularly around 4.75, significantly enhances the production of alcohols, with the maximum concentrations of butanol and hexanol achieved being 1.1 g/L and 0.6 g/L (Ganigué et al., 2016). However, maintaining the pH around this lower range is critical as further lowering the pH could detrimentally affect the chain elongation process. In our experimental set up, the fermentation conducted at a pH of 5.5 aimed to explore the potential influence of lower pH levels on the product spectrum. Lower pH values result in higher concentrations of hydronium ions in the solution, leading to increased conductivity. The primary objective of this experiment was to assess whether *M. sueciensis* could grow at a pH of 5.5

The selection of a pH of 4.5 for this experiment was strategic, considering its proximity to the pKa of acetate, which represents the equilibrium point between acetate and undissociated acetic acid. However, comparison between the initial and final stages of the experiment revealed minimal variation in the concentrations of acetate, butyrate, caproate, ethanol, butanol, and hexane.

Further investigation is needed to explore the potential effects of lower pH levels, as no significant differences were observed within the tested range. It is important to note that alcohol transformation is thermodynamically favored under pH conditions closer to the pKa of acetate, which is pH 4.5. Therefore, future experiments should consider exploring pH levels below 4.5 to comprehensively evaluate their impact on fermentation outcomes.

In summary, while initial trials did not show substantial differences in product concentrations at pH 5.5, there remains a need for additional experimentation, particularly at lower pH levels, to fully elucidate the effects of pH on fermentation processes and optimize conditions for enhanced product yields. (Zheng et al., 2020, January 13).

Salt trials & electroflasks

Observations in the trickle-bed reactor revealed a notable correlation between pH adjustments using sodium hydroxide (NaOH) and increased electrical conductivity, indicative of heightened salt concentration. This phenomenon suggested enhanced biofilm formation and improved gas exchange, encouraging a closer investigation on a smaller scale.

While the control trial exhibited notable chain elongation, trials with KCl showed a remarkable improvement in alcohol production, evidenced by a 6% increase in ethanol production, as depicted in figures 41 and 42. However, when a combination of NaCl and KCl was employed, the efficacy of chain elongation did not match that of the control trial. Although alcohol production reached 4% ethanol concentration, it did not attain the levels achieved with KCl alone. Potential explanations for this variance may involve differences in microbial activity, substrate preferences, or interactions between chloride ions in the mixed salt solution. Further investigation is necessary to clarify these factors.

Overall, experiments with salt highlighted the positive impact of adding KCl on alcohol production, showing a potential role for salts in optimizing reactor conditions for better alcohol synthesis. These findings highlight the importance of salt composition in modulating fermentation outcomes and justify continued exploration to optimize reactor conditions and maximize alcohol production efficiency.

Using electroflasks is a new way to improve fermentation (Fuchs et al., 2023). One big benefit of electroflasks is that they can change the electrical environment in the fermentation process. This helps control how microbes work. By adjusting the voltage and how the electrodes are set up, electroflasks give a flexible way to make fermentations better and get more out of it. Different set up of electroflasks were tried before. For this experiment, a membrane-fitted electroflask was used. The membrane serves to facilitate selective ion transport and separation between the anode and cathode compartments, crucial for maintaining electrochemical environments during fermentation.

The cathode material chosen for this setup is plain carbon cloth. Carbon cloth offers a high surface area for microbial attachment, providing an ideal substrate for biofilm formation and efficient electron transfer to support microbial growth in electrochemical systems. This promotes enhanced bioreactor performance and productivity.

On the other hand, the anode material selected is a stainless steel electrode E316L (Nirosta V2A). Stainless steel electrodes are renowned for their corrosion resistance and excellent electrical conductivity, making them well-suited for anodic reactions in electrochemical bioreactors. The use of stainless steel electrodes ensures long-term stability and reliability in harsh fermentation environments.

To integrate the electrodes into the electroflask system, they were introduced through a drilled hole in the rubber cap of the electroflask. This setup allows for precise positioning of the electrodes within the fermentation vessel, ensuring optimal electrochemical performance and efficient utilization of electrical energy for enhanced fermentation outcomes.

5.2 Trickle bed reactor

Several paper highlighted the benefits of continuous syngas fermentation, demonstrating its potential for producing higher alcohol concentrations efficiently (Batlle-Vilanova et al., 2017) (Liu et al., 2013). The study described in "Continuous syngas fermentation for the production of ethanol, n-propanol and n-butanol" shows the benefits granted by continuous fermentation systems in comparison to batch processes (Liu et al., 2013). Key advantages include achieving significant ethanol, n-propanol, and n-butanol concentrations using a continuous system with cell recycle, leading to 8 g/L ethanol, 6 g/L propanol, and 1 g/L butanol. These findings underscore the effectiveness of continuous fermentation processes over batch processes, particularly in terms of achieving higher product concentrations.

In our experiment, we used trickle bed reactors (TBRs) as the primary setup for both traditional gas fermentation (reactors FRI, FRII, and FRIII) and electro-fermentation (reactors Elena and Zorro). Trickle bed reactors offer several advantages that make them suitable for our experimental objectives.

Research has shown that trickle bed reactors provide excellent mass transfer capabilities, ensuring efficient contact between the microbial culture and the substrate (Liu et al., 2013).

This promotes better substrate utilization and metabolite production, crucial for both gas fermentation and electro-fermentation processes.

Reactors FR1 and FR3 exhibited a significant increase in the production of acetate, butyrate, and caproate, indicating successful chain elongation processes. However, alcohol production remained consistently low throughout the experiment duration. Figures 50, 51, and 52 illustrate a noticeable rise in concentrations of butyric acid and caproic acid across all three columns (FR1, FR2, and FR3), highlighting the occurrence of chain elongation across diverse reactor setups.

Interestingly, ethanol and butanol production remained minimal across most trials, except for FR2, where a relatively high concentration of butanol was observed prior to a medium swap. Following the swap, the butanol concentration returned to near-zero levels. The reason behind this phenomenon remains unclear, but it is noteworthy that FR2 exhibited the highest ethanol concentration among all continuous trials, peaking at 3.4 g/L. This result differs from the ethanol concentration reported in the paper mentioned above, where a concentration of 8 g/L was achieved. This discrepancy may occur from variations in experimental conditions, such as differences in reactor design, operational parameters, or biological factors influencing product yields.

Electro-fermentation

Some researches described that electro-fermentation, demonstrates notable advantages over traditional gas fermentation techniques (Zhang et al., 2023) (Fuchs et al., 2023) (Choi et al., 2014).

The study on "Highly selective butanol production by manipulating electron flow via cathodic electro-fermentation" (Choi et al., 2014) highlights the potential of electro-fermentation in enhancing butanol selectivity and production. Electro-fermentation, using cathodic electrons to influence the NADH/NAD+ ratio, proved effective in shifting metabolic pathways towards butanol production, achieving a concentration of 13.14 g/L with high selectivity (90.44%). This contrasts with traditional fermentation, which lacks the advantage of electron manipulation, resulting in lower butanol yields. The combination of cathodic electro-fermentation and methyl

viologen significantly optimized the electron flow, showcasing a promising approach for increasing butanol production efficiency and selectivity.

In the experiment for electro-fermentation, two reactors, Elena and Zorro were set up. The idea was to see if applying electricity could improve chain elongation and alcohol production compared to traditional gas fermentation in reactors FRI, FRII, and FRIII. This setup allowed to directly compare the effects of electro-fermentation to standard syngas trickle bed reactors.
The cathode of the Zorro reactor was made from the electrically conductive polymer polylactide coextruded with black carbon to obtain electric conductivity. To exclude the possibility that chain extension is associated with the degradation of polylactide, we constructed additional experiments involving Elena, utilizing non-biodegradable polypropylene supplemented with black carbon as a cathode as mentioned in 2.1. This adjustment was intended to compare the results of Elena with Zorro using a new cathode and making sure if the results can be reproduced again.
Regarding the Zorro reactor, significant chain elongation was observed, particularly evident starting from day 80, with high concentrations of caproate and butyrate. Electricity had a positive influence on chain elongation, with peak concentrations of caproate reaching almost 3 g/L and butyrate reaching 15 g/L by this date. Alcohol production was also noticeable, peaking at 0,4 g/L of butanol.

After a medium swap after day 80, acetate content increased sharply, and chain elongation continued, although not as prominently as before the swap. Interestingly, no obvious biofilm formation occurred in the Zorro reactor, and the reason for this remains unclear. However, this also serves as an indication that polylactide is either not degraded or undergoes minimal degradation as otherwise a biofilm would be seen. Additionally, the electrical conductivity decreased after 80 days, likely due to the inability to form a biofilm.

Elena served as a control experiment compared to Zorro, with modifications to promote biofilm formation. Although a medium swap incorporating trace elements Ni, Se, and W was conducted after 108 days to assess potential improvements, significant changes were not observed. Similar to Zorro, acetate concentration increased after the swap, and successful alcohol production was noticeable, with a peak butanol concentration of 0,2 g/L achieved.

After 157 days, the gassing composition was changed from H_2/CO_2 to $H_2/CO_2/CO$ to potentially enhance alcohol production and chain elongation. While a slight increase in caproate and butanol concentrations was discernible from this date, further observation of CO's effects is needed for accurate and comprehensive results.

These results suggest that while traditional gas fermentation processes in reactors FRI, FRII, and FRIII successfully promoted chain elongation, they were less effective in stimulating alcohol production. Conversely, electro-fermentation in reactors Elena and Zorro showed promising potential in enhancing ethanol production.

Overall, our findings suggest that electricity positively influences chain elongation and alcohol production, leading to higher concentrations of caproate, ethanol, and butanol compared to similar experiments. Further optimization and refinement of experimental parameters may enhance the efficiency and productivity of our system for potential applications in biofuel production or bioremediation processes and further investigation is needed to understand the underlying mechanisms driving these outcomes and to optimize electro-fermentation processes for improved alcohol synthesis and chain elongation efficiency.

6 Conclusion and Future Objectives

In conclusion, trickle bed reactor systems have shown promising results with respect to chain elongation especially with the help of *M. sueciensis*. Electro-fermentation techniques demonstrated improved alcohol production. However more detailed research will be needed to understand how it works and how to further improve the process. *C. carboxidivorans*'s ability to positively affect alcohol production suggests it could be important for industrial use.

Trials involving variations in pH levels revealed that, within the tested range, no significant differences were observed. Nevertheless, it was established that alcohol transformation is thermodynamically favorable below the pKs of acetate which is pH 4.5. To comprehensively assess the impact of lower pH levels, additional experimentation is necessary, extending the investigation to values below pH 4.5.

Additionally, experiments with salt showed that adding KCl had a positive effect on alcohol production. These findings signify the potential role of salts in optimizing reactor conditions for improved alcohol synthesis.

In the pursuit of further objectives, it is crucial to acknowledge the potential challenges associated with increasing chain length, as this may lead to higher toxicity levels. To address this concern, future research should explore strategies to mitigate toxicity while maximizing chain elongation.

Moreover, trying out different combinations of strains to improve productivity is worth looking into. Mixing different strains in trickle bed reactor systems might open up new possibilities for making alcohol production more efficiently.

Moreover, the application of electro-fermentation in trickle bed reactors stands out as a promising avenue for increasing productivity. Integrating electrochemical processes into the reactor design may offer unique advantages, and further exploration is needed to fully understand the implications and potential benefits of this approach in the context of alcohol synthesis. Thus, future research should focus on refining operational parameters, mitigating toxicity concerns, and exploring innovative approaches such as electro-fermentation to advance the field of trickle bed reactor technologies.

References

Alhayek, A., K.H. Hirsch, A. (2023). Bacterial metalloproteases as promising drug targets for antivirulence agents. Annual Reports in Medicinal Chemistry, Volume 60, p. 107-134

de Souza, Y. P. A., & Rosado, A. S. (2019). Opening the black box of thermophilic autotrophic bacterial diversity. In Microbial Diversity in the Genomic Era (pp. 333-343). Academic Press.

Arends, J. B., & Verstraete, W. (2012). 100 years of microbial electricity production: three concepts for the future. Microbial biotechnology, 5(3), 333-346.

Bajracharya, S., Krige, A., Matsakas, L., Rova, U., & Christakopoulos, P. (2022). Advances in cathode designs and reactor configurations of microbial electrosynthesis systems to facilitate gas electro-fermentation. Bioresource Technology, 354, 127178.

Batlle-Vilanova, P., Ganigué, R., Ramió-Pujol, S., Bañeras, L., Jiménez, G., Hidalgo, M., ... & Puig, S. (2017). Microbial electrosynthesis of butyrate from carbon dioxide: Production and extraction. Bioelectrochemistry, 117, 57-64.

BesTECH: Bio-Electric Syngas Technology for the Production of Biomass Derived BioFuels and Platform Chemicals. (n. D.). https://www.best-research.eu/en/competence_areas/all_projects/view/677

Choi, O., Kim, T., Woo, H. M., & Um, Y. (2014). Electricity-driven metabolic shift through direct electron uptake by electroactive heterotroph Clostridium pasteurianum. Scientific reports, 4(1), 6961.

Diallo, M., Kengen, S. W., & López-Contreras, A. M. (2021). Sporulation in solventogenic and acetogenic clostridia. Applied Microbiology and Biotechnology, 105(9), 3533-3557.

Edel, M., Philipp, L. A., Lapp, J., Reiner, J., & Gescher, J. (2022). Electron transfer of extremophiles in bioelectrochemical systems. Extremophiles, 26(3), 31.

European Commission: REPowerEU - affordable, secure and sustainable energy for Europe: URL: https://commission.europa.eu/strategy-and-policy/priorities-2019-2024/european-green-deal/repowereu-affordable-secure-and-sustainable-energy-europe_en (2024)

Fuchs, W., Rachbauer, L., Rittmann, S. K. M., Bochmann, G., Ribitsch, D., & Steger, F. (2023). Eight Up-Coming Biotech Tools to Combat Climate Crisis. Microorganisms, 11(6), 1514.

Ganigue, R., Sanchez-Paredes, P., Baneras, L., & Colprim, J. (2016). Low fermentation pH is a trigger to alcohol production, but a killer to chain elongation. Frontiers in microbiology, 7, 702.

Holden, J. F. (2009). Extremophiles: hot environments. 127-146.

Kallscheuer, N., Polen, T., Bott, M., & Marienhagen, J. (2017). Reversal of β-oxidative pathways for the microbial production of chemicals and polymer building blocks. Metabolic engineering, 42, 33-42.

Lin, Z., Cong, W., & Zhang, J. A. (2023). Biobutanol Production from Acetone–Butanol–Ethanol Fermentation: Developments and Prospects. Fermentation, 9(9), 847.

Liu, K., Atiyeh, H. K., Stevenson, B. S., Tanner, R. S., Wilkins, M. R., & Huhnke, R. L. (2014). Continuous syngas fermentation for the production of ethanol, n-propanol and n-butanol. Bioresource technology, 151, 69-77.

Mannaa, M., Han, G., Seo, Y. S., & Park, I. (2021). Evolution of food fermentation processes and the use of multi-omics in deciphering the roles of the microbiota. Foods, 10(11), 2861.

Mann, M., Effert, D., Kottenhahn, P., Hüser, A., Philipps, G., Jennewein, S., & Büchs, J. (2022). Impact of different trace elements on metabolic routes during heterotrophic growth of C. ljungdahlii investigated through online measurement of the carbon dioxide transfer rate. Biotechnology Progress, 38(4), e3263.

Manna, D., Chowdhury, R., Calay, R. K., & Mustafa, M. Y. (2024). Experimental Insights into the Fermentation of Pyro-Syngas to Ethanol in a Semi-Batch and Continuous Stirred Bioreactor with Mathematical Modelling and Optimization. Energies, 17(3), 562.

Ellacuriaga, M., Gil, M. V., & Gómez, X. (2023). Syngas Fermentation: Cleaning of Syngas as a Critical Stage in Fermentation Performance. Fermentation, 9(10), 898.

Mohan, S. V., VARJANI, S., & PANDEY, A. (2018). Microbial electrochemical technology: sustainable platform for fuels, chemicals and remediation. Elsevier.

National Geographic Society. (2022). Renewable Ressources https://education.nationalgeographic.org/resource/renewable-resources/

Nimbalkar, P. R., Khedkar, M. A., Parulekar, R. S., Chandgude, V. K., Sonawane, K. D., Chavan, P. V., & Bankar, S. B. (2018). Role of trace elements as cofactor: an efficient strategy toward enhanced biobutanol production. ACS sustainable chemistry & engineering, 6(7), 9304-9313.

Pant, D., Singh, A., Van Bogaert, G., Olsen, S. I., Nigam, P. S., Diels, L., & Vanbroekhoven, K. (2012). Bioelectrochemical systems (BES) for sustainable energy production and product recovery from organic wastes and industrial wastewaters. Rsc Advances, 2(4), 1248-1263.

Ragsdale, S. W., & Pierce, E. (2008). Acetogenesis and the Wood–Ljungdahl pathway of CO2 fixation. Biochimica et Biophysica Acta (BBA)-Proteins and Proteomics, 1784(12), 1873-1898.

Scarborough, M. J., Myers, K. S., Donohue, T. J., & Noguera, D. R. (2020). Medium-Chain Fatty Acid Synthesis by “Candidatus Weimeria bifida” gen. nov., sp. nov., and “Candidatus Pseudoramibacter fermentans” sp. nov. Applied and Environmental Microbiology, 86(3), e02242-19.

Steger, F., Ergal, İ., Daubek, A., Loibl, N., Rachbauer, L., Fuchs, W., ... & Bochmann, G. (2022). Trickle-bed bioreactors for Acetogenic H2/CO2 conversion. Frontiers in Energy Research, 10, 842284.

Stoll, I. K., Boukis, N., & Sauer, J. (2020). Syngas fermentation to alcohols: reactor technology and application perspective. Chemie Ingenieur Technik, 92(1-2), 125-136.

Sydow, A., Krieg, T., Mayer, F., Schrader, J., & Holtmann, D. (2014). Electroactive bacteria—molecular mechanisms and genetic tools. Applied microbiology and biotechnology, 98, 8481-8495.

Tarasava, K., Lee, S. H., Chen, J., Köpke, M., Jewett, M. C., & Gonzalez, R. (2022). Reverse β-oxidation pathways for efficient chemical production. *Journal of industrial microbiology & biotechnology*, *49*(2), kuac003.

Zhao, J., Zhang, C., Sun, C., Li, W., Zhang, S., Li, S., & Zhang, D. (2018). Electron transfer mechanism of biocathode in a bioelectrochemical system coupled with chemical absorption for NO removal. Bioresource technology, 254, 16-22.

Zhang, Y., Li, J., Yong, Y. C., Fang, Z., Yan, H., Li, J., & Meng, J. (2023). Highly selective butanol production by manipulating electron flow via cathodic electro-fermentation. Bioresource Technology, 374, 128770.

Zheng, T., Li, J., Ji, Y., Zhang, W., Fang, Y., Xin, F., ... & Jiang, M. (2020). Progress and prospects of bioelectrochemical systems: electron transfer and its applications in the microbial metabolism. Frontiers in Bioengineering and Biotechnology, 8, 10.

Zhu, Y. (2007). Immobilized cell fermentation for production of chemicals and fuels. Bioprocessing for value-added products from renewable resources, 373-396.

List of Figures

7 List of Tables